



National Library
of Canada

Bibliothèque nationale
du Canada

Canadian Theses Service

Service des thèses canadiennes

Ottawa, Canada
K1A 0N4

NOTICE

The quality of this microform is heavily dependent upon the quality of the original thesis submitted for microfilming. Every effort has been made to ensure the highest quality of reproduction possible.

If pages are missing, contact the university which granted the degree.

Some pages may have indistinct print especially if the original pages were typed with a poor typewriter ribbon or if the university sent us an inferior photocopy.

Previously copyrighted materials (journal articles, published tests, etc.) are not filmed.

Reproduction in full or in part of this microform is governed by the Canadian Copyright Act, R.S.C. 1970, c. C-30.

AVIS

La qualité de cette microforme dépend grandement de la qualité de la thèse soumise au microfilmage. Nous avons tout fait pour assurer une qualité supérieure de reproduction.

S'il manque des pages, veuillez communiquer avec l'université qui a conféré le grade.

La qualité d'impression de certaines pages peut laisser à désirer, surtout si les pages originales ont été dactylographiées à l'aide d'un ruban usé ou si l'université nous a fait parvenir une photocopie de qualité inférieure.

Les documents qui font déjà l'objet d'un droit d'auteur (articles de revue, tests publiés, etc.) ne sont pas microfilmés.

La reproduction, même partielle, de cette microforme est soumise à la Loi canadienne sur le droit d'auteur, SRC 1970, c. C-30.

THE UNIVERSITY OF ALBERTA

THE TRANSPORT OF INFRARED RADIATION THROUGH TISSUE

By

© RICHARD J. CRILLY

A THESIS

SUBMITTED TO THE FACULTY OF GRADUATE STUDIES AND RESEARCH
IN PARTIAL FULFILLMENT OF THE REQUIREMENTS FOR THE DEGREE OF

MASTER OF SCIENCE

IN

BIOPHYSICS

DEPARTMENT OF PHYSICS

EDMONTON, ALBERTA

FALL 1987

Permission has been granted to the National Library of Canada to microfilm this thesis and to lend or sell copies of the film.

The author (copyright owner) has reserved other publication rights, and neither the thesis nor extensive extracts from it may be printed or otherwise reproduced without his/her written permission.

L'autorisation a été accordée à la Bibliothèque nationale du Canada de microfilmer cette thèse et de prêter ou de vendre des exemplaires du film.

L'auteur (titulaire du droit d'auteur) se réserve les autres droits de publication; ni la thèse ni de longs extraits de celle-ci ne doivent être imprimés ou autrement reproduits sans son autorisation écrite.

ISBN 0-315-40924-X

THE UNIVERSITY OF ALBERTA

RELEASE FORM

NAME OF AUTHOR: RICHARD J. CRILLY

TITLE OF THESIS: THE TRANSPORT OF INFRARED

RADIATION IN BIOLOGICAL TISSUE

DEGREE: MASTER OF SCIENCE

YEAR THIS DEGREE GRANTED: 1987

Permission is hereby granted to THE UNIVERSITY OF ALBERTA LIBRARY to reproduce single copies of this thesis and to lend or sell such copies for private, scholarly or scientific research purposes only. The author reserves other publication rights, and neither the thesis nor extensive extracts from it may be printed or otherwise reproduced without the author's written permission.

Richard J. Crilly
(Student's Signature)

429 LAKEVIEW DR.
BELLE RIVER ONT.
(Student's Permanent Address)

Date: October 14, 1987

THE UNIVERSITY OF ALBERTA

FACULTY OF GRADUATE STUDIES AND RESEARCH

The undersigned certify that they have read, and recommend to the Faculty of Graduate Studies and Research for acceptance, a thesis entitled:

The Transport of Infrared Radiation in Biological Tissue

submitted by Richard J. Crilly in partial fulfillment of the requirements for the degree of Master of Science.

St. M. kin

(Supervisor)

J. Scamiger

J. Battista

J. F. ...

Frank H. Wezha

Date: Oct 14, 1987

DEDICATION

(This work is dedicated to Holly, who lent me patience when I had none.

Abstract

Recent advancements in the technical application of infrared light to biological tissue for medical purposes has made necessary the investigation of the actual light-tissue interaction. The spectral transmission response of a number of tissues is examined at different tissue thicknesses with the purpose of finding the basic coefficients needed to model the light-tissue interaction using transport theory. On the basis of this model it is hoped that the optimum application of these new medical modalities can be predicted and applied.

This work is an experimental determination of the scatter coefficient and mean free path based on a solution of the transport theory which presupposes a large degree of forward scattering. The scatter phase function and absorption coefficient are also considered but due to limitations of the experimental procedure the results are interpreted in a more qualitative manner. This determination is carried out for a number of wavelengths between 600 and 1100 nm. using a monochromatic light source, an S-1 phototube and collimators in 'near' narrow beam geometry. The tissues examined are human muscle, lactating gland, blood, and adipose tissue and porcine testes and brain tissue.

As the scatter phase function is greatly accentuated in the forward direction 'true' narrow beam geometry (removal of scattered radiation via collimation) was not accomplished with the equipment used. As a result a means of analysis is developed that allows for scattered radiation in the transmitted beam by the introduction of the 'scatter number'. This scatter number, which can be used in cases where the collimation allows a very small angle of transmitted detection, gives some qualitative insight into the degree of forward scattering found in each of the tissues. This particular form of analysis has the potential of providing the means of deriving the absorption and scatter coefficients separately instead of in their composite sum (the attenuation coefficient) as is normally done by the application of Beer's Law.

ACKNOWLEDGEMENT

I would like to acknowledge the help and support of the staff at the Cross Cancer Institute with a special thanks to Eric, Finn, Frank, and Lawrence, in the shop who always had a practical solution. I would also like to thank my supervisors for the patience given to my enthusiastic 'bull in a china shop' approach to the problems encountered in this work. Finally I would like to thank Dr. Brian Wilson, and Stephen Flock of the Hamilton Regional Cancer Center for their expertise and assistance given in the course of 'trying to understand'.

Table of Contents

Chapter		Page
1.	Background	1
	Objectives.....	1
	Scientific Experience.....	4
	Medical Needs and Applications.....	6
	Diaphanography.....	6
	Photodynamic Therapy.....	10
	Surgical Lasers.....	11
2.	Experimental Setup and Preliminary Testing..	14
	Experimental Objectives.....	14
	Equipment.....	16
	Light Source	16
	Monochromator	17
	Collimation Assembly	20
	Sample Holder	20
	Detector	26
	Amplifying and Noise Reduction System	26
	Sample Preparation	28
	In Vivo vs In Vitro	29
3.	Experiment I: Transmission Spectra	33
4.	Experiment II: Transmission Analysis.....	41
	Background Theory.....	41
	Zero Thickness Extrapolation.....	48
	Mathematical Model: Theory.....	55

Table of Contents

Chapter	Page
	Mathematical Model: Analysis..... 58
	Absorption Coefficient..... 59
	Scatter Coefficient..... 60
	Scatter Number 60
5	Conclusions and Comments..... 70
	Experimental Observations70
	Experimental Models..... 71
	Practical Application of Results..... 74
	Bibliography78
	Appendix I: Derivation of Diffusion Approximation... 84
	Appendix II: Diffusion Approximation - Summary of Past Results..... 87

List of Figures

Figure		Page
1.	Definition of Depth by Degree of Diffusion	3
2.	Absorption Coefficient vs Wavelength of Common Absorbing Chemicals in Tissue (100-1200 nm)	5
3.	Tissue Heating Effects	6
4.	Basic Diaphanography System	9
5.	Experimental Set Up	15
6.	Transmission Ratio vs Wavelength defining the Resolution of the KIPP monochromator (1.02 μm)	18
7.	Transmittance vs Wavelength for the Kodak 88A Gelatine Filter	19
8.	Transmission Ratio vs Wavelength defining the Resolution of the SPEX monochromator (0.57 μm)	21
9.	Transmission Ratio vs Wavelength defining the Resolution of the SPEX monochromator (1.01 μm)	22
10.	Collimator and Mounting Assembly (Side View)	23
11.	Rear Collimator Assembly (Magnified View)	24
12.	Mounting Shutter	25
13.	Relative Response vs Wavelength of the S-1 Phototube	27
14.	Transmission Ratio vs Temperature for Porcine Adipose Tissue	30
15.	Transmission vs Wavelength (Human Lactating Tissue)	36
16.	Transmission vs Wavelength (Whole Human Blood)	36

List of Figures

Figure		Page
17.	Transmission vs Wavelength (Human Skin Tissue)	37.
18.	Transmission vs Wavelength (Human Adipose Tissue)	37
19.	Transmission vs Wavelength (Human Breast Tumor)	38
20.	Transmission vs Wavelength (Porcine Brain Tissue)	38
21.	Transmission vs Wavelength (Porcine Muscle Tissue)	39
22.	Transmission vs Wavelength (Porcine Testicular Tissue)	39
23.	Transmission vs Wavelength (Human Adipose Tissue) High Wavelength Resolution - Comparison Study	40
24.	Definition of Depth by Degree of Diffusion	44
25.	Ln (1/Transmission Ratio) vs Sample Thickness Whole Human Blood	46
26.	Ln (1/Transmission Ratio) vs Sample Thickness Porcine Brain Tissue	48
27.	Defining Angle of Collimation	48
28.	Apparent Mean Free Path vs Sample Thickness Whole Human Blood	51
29.	Apparent Mean Free Path vs Sample Thickness Porcine Brain Tissue	51
30.	Mean Free Path vs Wavelength Zero Extrapolation Method - Porcine Brain	52
31.	Mean Free Path vs Wavelength Zero Extrapolation Method	53
32.	Scatter Factor vs Wavelength Zero Extrapolation Method	54
33.	Defining d_{Scat}	56
34.	Absorption Coefficient vs Wavelength (Human Adipose Tissue)	61

List of Figures

Figure		Page
35	Absorption Coefficient vs Wavelength (Whole Human Blood)	61
36	Scatter Coefficient vs Wavelength (Human Adipose Tissue)	62
37	Scatter Coefficient vs Wavelength (Whole Human Blood)	62
38	Scatter Coefficient vs Wavelength (Porcine Brain Tissue)	63
39	Scatter Coefficient vs Wavelength (Human Lactating Tissue)	63
40	Scatter Coefficient vs Wavelength (Human Muscle Tissue)	64
41	Scatter Coefficient vs Wavelength (Porcine Testicular Tissue)	64
42	Scatter Coefficient vs Wavelength (All Tissues)	65
43	Scatter Number vs Wavelength (Human Adipose Tissue)	66
44	Scatter Number vs Wavelength (Whole Human Blood)	66
45	Scatter Number vs Wavelength (Porcine Brain Tissue)	67
46	Scatter Number vs Wavelength (Human Lactating Tissue)	67
47	Scatter Number vs Wavelength (Human Muscle Tissue)	68
48	Scatter Number vs Wavelength (Porcine Testicular Tissue)	68
49	Scatter Number vs Wavelength (All Tissues)	69
50	Mean Free Path vs Wavelength Mathematical Model	77

List of Figures

Figure		Page
51.	Penetration Depth Spectrum Kidney and Liver	88
52	Penetration Depth Spectrum Human Brain	89

CHAPTER ONE BACKGROUND

OBJECTIVES

Technical advancement in electronics and optics has opened the way for the use of non-ionizing radiation in medicine. The advent of lasers and optical fibers allow much more flexibility in the application of high intensity low energy photon beams. Computers, and improved solid state detectors allow for better control and analysis of the often complicated procedures and results. While all the 'tools' are in position for use, the basic understanding of the light tissue interaction is still a concern to the medical physicist.

The physicist's goal is to develop a model with which reliable predictions can be made concerning the results of these new medical procedures. In deciding on what model to use there are two basic options open to him. The first, electromagnetic theory, involves treating the radiation as a wave moving through electric and magnetic fields defined by boundary conditions describing the medium. The second, transport theory, considers light to be made up of particles, (photons), that interact with the individual 'targets' that make up the material.

Electromagnetic theory is presently used medically for the planning of hyperthermia treatments. At these wavelengths the areas of interest, such as tumor volumes, are close enough to the microwave source so that the 'near field solution' describes the situation. This means the solution of the problem is potentially dependent on the interaction between the wave polarity and the medium's geometry. Because the method is dependent on whether the electric field vector is perpendicular or parallel to the direction of propagation the results can be mathematically complex in all but the simplest of cases.

Mathematically the description of photons of any energy moving through any medium is described by transport theory as long as certain conditions are met (Wolf (1975), Fante (1981)). Of these conditions those that pertain to the situation involving living tissue are ; 1) the mean free path is much larger than the size of inhomogeneities in

the transport medium, 2) changes in the electrical permittivity are small at boundaries, and 3) the radiation remains nearly transverse. Assuming that these conditions are met, transport theory ignores some of the problems encountered in wave mechanics to give a simplified view of the phenomena. In the particular experimental situation encountered in this work the transport equation has the form;

$$\hat{\Omega} \cdot \nabla I = -\mu_0 I + \frac{\mu_s}{4\pi} \int S(\hat{\Omega}', \hat{\Omega}) I(\hat{\Omega}') d\hat{\Omega}' \quad (1)$$

where: I is the specific intensity of the photons,

$\hat{\Omega}$ is a unit vector defining the direction of flight of the photon,

μ_0 is the linear attenuation coefficient [cm^{-1}],

μ_s is the linear scattering coefficient [cm^{-1}]

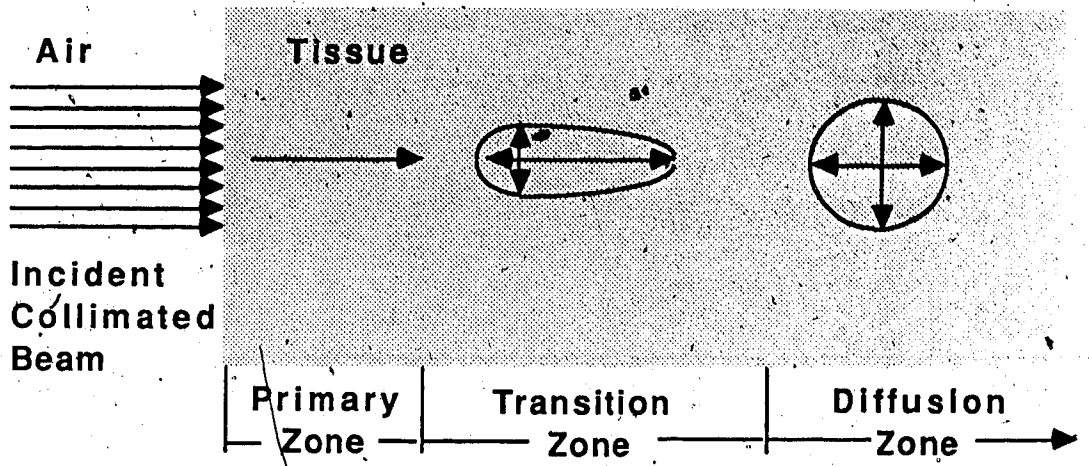
such that $\mu_0 = \mu_a + \mu_s$,

μ_a is the linear capture (or absorption) coefficient [cm^{-1}],

and $S(\hat{\Omega}; \hat{\Omega}')$ is the scatter phase function (also called the angular scattering probability function).

The equation has been presented here to give the reader some concept of terms used in the rest of the introduction, a more in depth look at these concepts can be found on page 41.

Within transport theory there are a number of solutions and approximations that apply to very specific situations and are significantly simpler than the general case. With this simplicity in mind past works attempted to use these approximations to obtain the basic parameters involved with radiative transport. The most common of these approximations are Beer's law and the diffusion approximation. The first pertains to situations where scatter can be ignored while the second refers to the diffusion zone where diffuse scattered radiation is predominant (see figure 1). The figure shows the development of scattered radiation as the thickness of the transport medium increases. In cases where there is no scatter ($\mu_s=0$) the primary zone extends throughout the tissue.



The length of the arrows represent the relative fraction of photon flux in the direction indicated

Figure 1

The basic goal of this work is two fold. The first is to examine the transmission properties of various tissues to see if there are any unusual properties at any specific wavelengths that may be exploited for medical purposes. The second purpose of this study is to try to ascertain experimentally the nature, and if possible, the value, of the coefficients and functions that describe the tissue dependent aspect of the transport solution. In particular, the initial goal of this project was to find the average distance between interaction events, the mean free path. As the project advanced it became apparent that the situation was more complex than originally thought and allowances had to be made in the theory used to analyze the situation. These changes in themselves allowed other coefficients related to transport theory to be either measured or speculated on. These other factors include the scatter coefficient, the absorption coefficient and the angular scatter distribution function (better known in radiative transfer problems as the scatter phase function). (See Dunderstadt (1977))

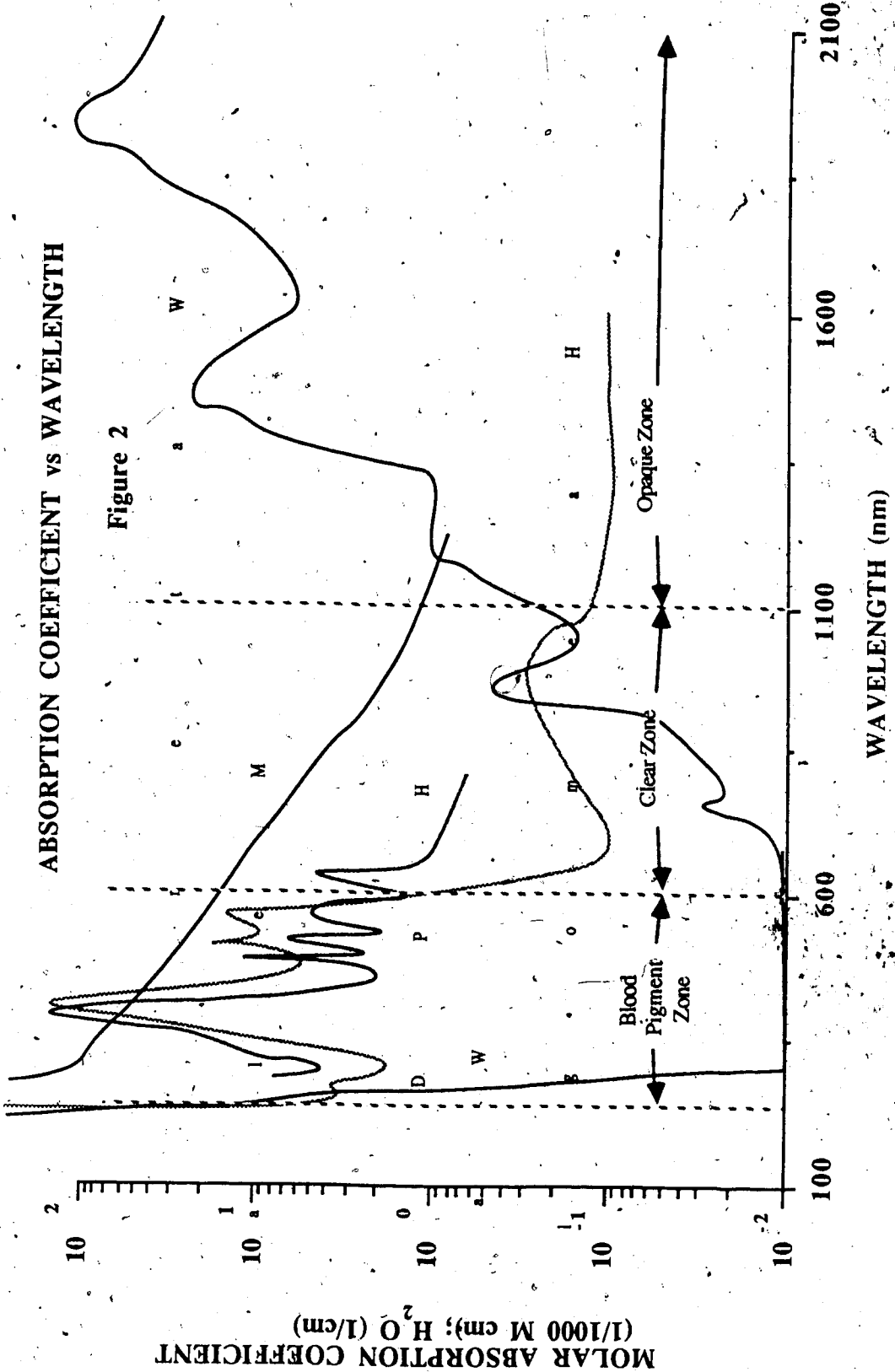
SCIENTIFIC EXPERIENCE

The goals of this research are not in themselves new practical methods for the application of infrared radiation to medicine. The results of these tests are meant to supply the required insight needed to develop infrared technology for practical application. In order to better understand how the intermediate goals of this research fit with respect to the overall application of infrared radiation to medicine a review of what is known and how it is applied is in order. With this background, the necessity of the work compiled in this thesis will become obvious.

The first and most obvious aspect of the light tissue interaction is the ability of any particular wavelength of light to be transmitted through the tissue. Figure 2 (Polanyi (1978)) shows the molar absorption coefficient at body temperature for the more important absorbing compounds found in mammalian tissue. The absorption properties of these compounds define three distinct wavelength ranges of particular interaction type: the blood-pigment zone, the clear zone, and the opaque zone. The blood-pigment zone with wavelengths from 230 to 600 nm encompasses those wavelengths where light does not interact with water and yet is readily absorbed by hemoglobin and melanin. The clear zone, from 600 to 1100 nm, is where the main form of tissue interaction is that of scattering, thus allowing deep penetration of the radiation through the tissue. The final range from 1100 nm up is called the opaque zone because of the strong absorption of water at these wavelengths. Since water is present in all living tissue, absorption is confined to the immediate surface of the tissue.

ABSORPTION COEFFICIENT VS WAVELENGTH

Figure 2



The absorption of light by tissue usually results in heating of the tissue. The degree of heating depends on the intensity of the light source, the time of exposure, and the tissue's ability to dissipate thermal energy. As the optical properties are dependent on the structure of the tissue, changes in the tissue due to heating can change the optical properties. This change in tissue structure has been noted by Boulois (1986), and Wilson (1986) and is summarized in the following table (Hetzel (1986)).

Temperature °C	Effects on Tissue
30 - 60	Welding (in small structures) Hyperthermia
60 - 65	Coagulation
65 - 90	Protein Denaturation
90 - 100	Drying
>100	Vaporization Carbonization (Ablation)

Figure 3

While the work presented in this study is obtained at body temperature, this does not exclude its importance in areas of the field where high intensity beams are used to obtain such effects as ablation or coagulation. In most high intensity cases the penetration depth of laser effects is decided when the tissue is still at body temperature. The depth of the radiation effects can be approximated knowing the initial penetration of light at body temperature.

MEDICAL NEEDS AND APPLICATIONS

The importance of infrared radiation in medicine can be seen in the growth of its applications in recent years. In order to understand what avenues are most important in the study of the light-tissue interaction a summary of the most prominent of these infrared applications is given.

Diaphanography

One of the first uses for non-ionizing radiation was put forward by Cutter in 1929. (Cutter (1929)) Dr. Cutter used a strong visible light source against one side of a patient's breast and searched for abnormalities by observing the transmitted light. Using this crude method, Cutter was capable of differentiating transparent (cysts and abscesses) and opaque abnormalities (carcinomas and hematomas). While this method of transillumination showed some initial promise, techniques such as x-ray mammography proved superior and by the 1940's most investigators had abandoned it.

Interest revived in the late 1970's with the application of infrared film allowing more use of the optimal clear zone. With this improvement, the technique took on a new name, diaphanography. Present methods use an infrared sensitive video camera to pick up the image transmitted through the breast. The set up of a diaphanography system is shown in figure 3. The source of light incident on the breast alternates between two wavelengths, one in the blood-pigment zone and the other in the clear zone. The signal transmitted through the breast is digitized and shown as a combination of grey levels and pseudo-colour. The grey tone, which is the sum of the transmission at both wavelengths, is meant to show up blood vessels, vascularization and fibrosis. The pseudo-colour, which is defined by the ratio of the transmission of the two wavelengths, is meant to show subtle differences in the more optically similar tissue types. This ability to see small differences is dependent on the tissues under examination having a reasonable difference in their attenuation coefficients in at least one of the selected wavelengths. This aspect of the technique is most commonly used in the identification of cysts.

While technology has greatly improved the effectiveness of diaphanography the inherent problem of degradation of the resultant image by scattered light remains. The deeper the volume of interest is in the subject, the greater the deterioration of the image due to scatter originating in the intervening tissue. Presently depths of about one to two cm can be imaged with some degree of diagnostic value. Because of these poor images, diaphanography has never been considered as a primary form of breast screening. Its major use is as a secondary method of diagnosis or a primary method only when conditions preclude the use of mammography. The technique is being evaluated presently at the Cross Cancer Institute. (Castor (1986))

In its present form, infrared imaging is extremely limited in its applications. Mechanical improvements, such as breast compression, may greatly improve the method. Unfortunately this is not the ultimate limitation; the actual interaction of light and tissue is poorly understood. The measurements of the fundamental properties of this interaction are essential to any advancement in the field. Only when these fundamental principles are understood can a true analysis of the method and its limitations be ascertained.

Basic Diaphanography System

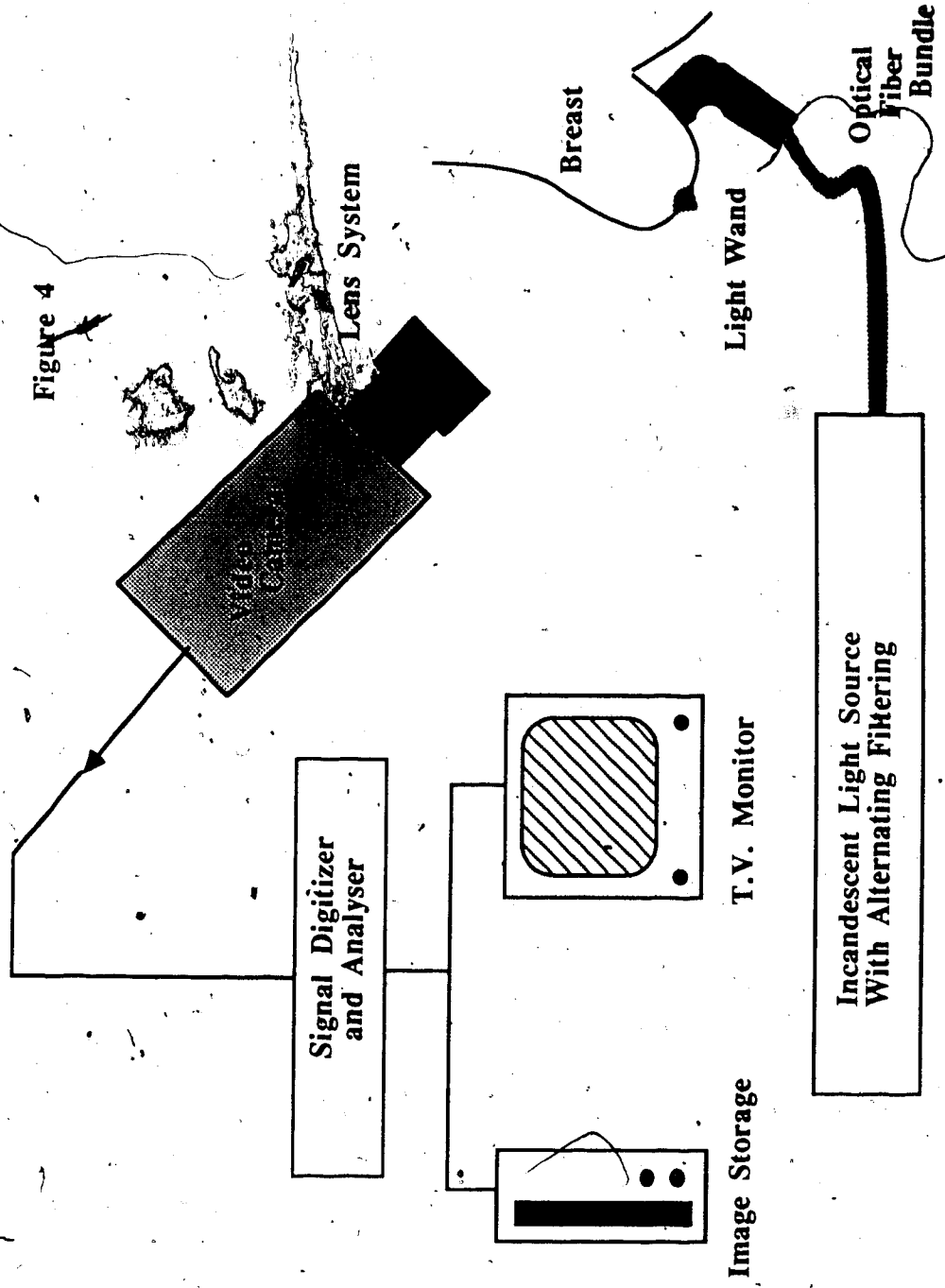


Figure 4

Photodynamic Therapy

There is a certain class of drugs that has been found to be inert inside living tissue unless activated by light of a specific frequency. Given that a number of these drugs such as haematoporphrin derivative (HPD) are tumor specific, the application to oncology is obvious. This procedure is also being investigated at the Cross Cancer Institute.

This photochemical reaction results in oxygen in the cell being converted to its singlet excited state, which in turn oxidizes organic molecules and kills the cell. As the drug is a photocatalyst it does not lessen in concentration due to the interaction and thus provides a stable reagent. The only real problem is to find out how much photosensitizing chemical is concentrated in the tumor and deliver the required amount of light to the drug.

Since HPD has an activation peak on the edge of the clear zone (633 nm) the application of light to the tumor volume should be a straight forward procedure, providing the nature of light transport is understood. (Wilson (1986-1), Profio (1981))

The problem of mapping the concentration of HPD is simplified by the fact that it fluoresces when irradiated with UV light. This fluorescence has even been suggested as a means of detecting very superficial tumors (van der Putten (1983), Profio (1984), Katsuo (1984)). Thus an optical fiber used to probe into the tumor can inject the UV light and then act as a detector to measure the concentration-dependent light intensity. As the fluorescence occurs in the blood-pigment range of wavelengths in highly vascularized tumors only very localized measurements are possible. The local volume size for which the concentration measurement is valid is once again dependent on a good understanding of the light's mean free path in various tissues.

New drugs use wavelengths further into the clear zone thus increasing the light penetration depth. While much optical work has been done at 633 nm, these new drugs indicate the need for an extended experimental base. In order to facilitate the potential for all forms of photosensitive drugs the optical properties within the entire clear zone must be explored. Such investigations constitute part of this work.

Surgical Lasers

Lasers with their excellent mechanical coupling to optical fibers have added a new flexibility to the application of light to medicine. The development of lasers in medicine over the last five years can be gauged by the appearance of three new scientific journals devoted to biomedical lasers as well as a number of excellent text books (e.g. Goldman-Ed.(1984), and Wolbarsht-Ed.(1971)). Any attempt to summarize all their uses in this thesis would be redundant, instead an outline of the boundary conditions that regulate their application is given. These boundary conditions include the wavelength treatment zones, the intensity, and the time of exposure.

The first wavelength zone to be considered is the blood-pigment region. At these wavelengths the laser offers the ability to selectively apply thermal effects to tissue with high concentrations of blood or melanin. The relatively unhindered movement of light through water and thin layers of semipellucid tissue allows such procedures as the 'welding' of damaged retina through the vitreous humour and the coagulation of microcapillaries in port wine stains.

The application of lasers that work in the blood-pigment frequencies at higher intensities results in a surgical scalpel with the ability to coagulate blood vessels at depth from the incision. The extent of this thermal reaction is largely contingent on the exact wavelength of the laser, the tissue being irradiated, and the duration of the exposure. Lower scalpel intensities allow the thermal heating effects to develop at greater depths before surface optics change due to carbonization or ablation and stop the transport of radiation beyond the surface. This is of great advantage when the surgeon wants to produce hyperthermia and coagulation in the area around a tumor extraction. Unfortunately this property of the beam produces scar tissue that may counter the cosmetic or physiological functions of the tissue.

In the opaque zone, the lasing of tissue is completely superficial since the main absorber is the most common component of living tissue, water. Given sufficient intensity, the water of the cells is turned to vapor almost instantly causing the cell to literally explode. Thermal effects are thus kept to the immediate area of irradiation resulting in small precise incisions with minimal scarring. Unfortunately because of this exploding aspect, when excising tumors, the resulting plume of lased material may contain viable cancer cells that can be reabsorbed by the body to form metastases (Polanyi (1978)). Still outside the area of oncology the main laser used in surgery to date has been in the opaque zone (the CO₂ laser) in spite of the fact that no optical fiber system is presently available at these wavelengths and the laser must be directed by way of mirrors mounted in a hinged mechanical arm.

The above mentioned treatment zones must be augmented by an additional range called the non-thermal zone. This covers a relatively new generation of ultra-violet medical lasers (excimer lasers) whose energy is great enough to cause photoablation (Boulinois (1986)). It is supposed that photoablation occurs when the bonds of organic molecules disassociate by the absorption of a single photon. This phenomena coupled with good beam control results in very straight shallow cuts with minuscule thermal effects. Typically microscopic slices prepared of transverse incision cross sections show cell walls cut in two with the adjacent cell unaffected. While the advantages of this laser for cosmetic and microsurgery are apparent, the full potential of this modality can only be attained when a good understanding of the interaction mechanism is achieved.

The history of medical physics in radiation oncology is one where the physicists were confronted with a developed application and asked to support it. This is the exact opposite of the traditional scientific approach of starting with simple experiments and models and slowly building towards the more complex situation. In the face of such pressure physicists were forced to develop semi-empirical methods until a good scientific

model could be perfected. Now that better methods and understanding are available a good deal of energy must be expended in updating the initial 'stop gap' procedures. Much of this extra effort could have been avoided if the physicists had known of the need in advance and performed the basic experiments used to develop the fundamental theory. The field of infrared interaction with tissue is dangerously close to the same situation faced by the early medical radiation physicists. History may once again repeat itself at a different wavelength!

In summary, it can be seen that although infrared light is already used in medicine to a high degree, the understanding of the basic mechanisms of interaction is primitive. Because of the high clinical potential of infrared radiation, a full understanding of its properties must be attained in the near future. This treatise is one of the first steps in this direction.

CHAPTER TWO EXPERIMENTAL SET UP AND PRELIMINARY TESTING

EXPERIMENTAL OBJECTIVES

In order to model the transport of light through tissue accurately the constants and functions μ_0 , μ_s , μ_a and $S(\Omega', \Omega)$ must be found. Due to the wide range of values these factors can attain their experimental determination has proven to be difficult. Indeed within the entire field some of these variables have not been measured using an accepted experimental method. While the main goal of the experiment described in this thesis was to find the mean free path ($\delta_0 = 1/\mu_0$) this is not the work's only focus. The experimental methods used when dealing with organic tissue for the purpose of optical experiments are for the most part specific and new. While the reasoning behind experiments described here may seem obvious, they are the result of many trials performed to find what conditions are needed to maintain consistency in results.

The main objective of the experiment was to measure the ratio of the photon energy fluence with, and without a tissue sample in the beam. This ratio, called the transmission ratio (T), is understood to be equal to the ratio of the related specific intensities based on the idea that the photon energy fluence (Ψ) measured by the detector is related to the specific intensity (I) by;

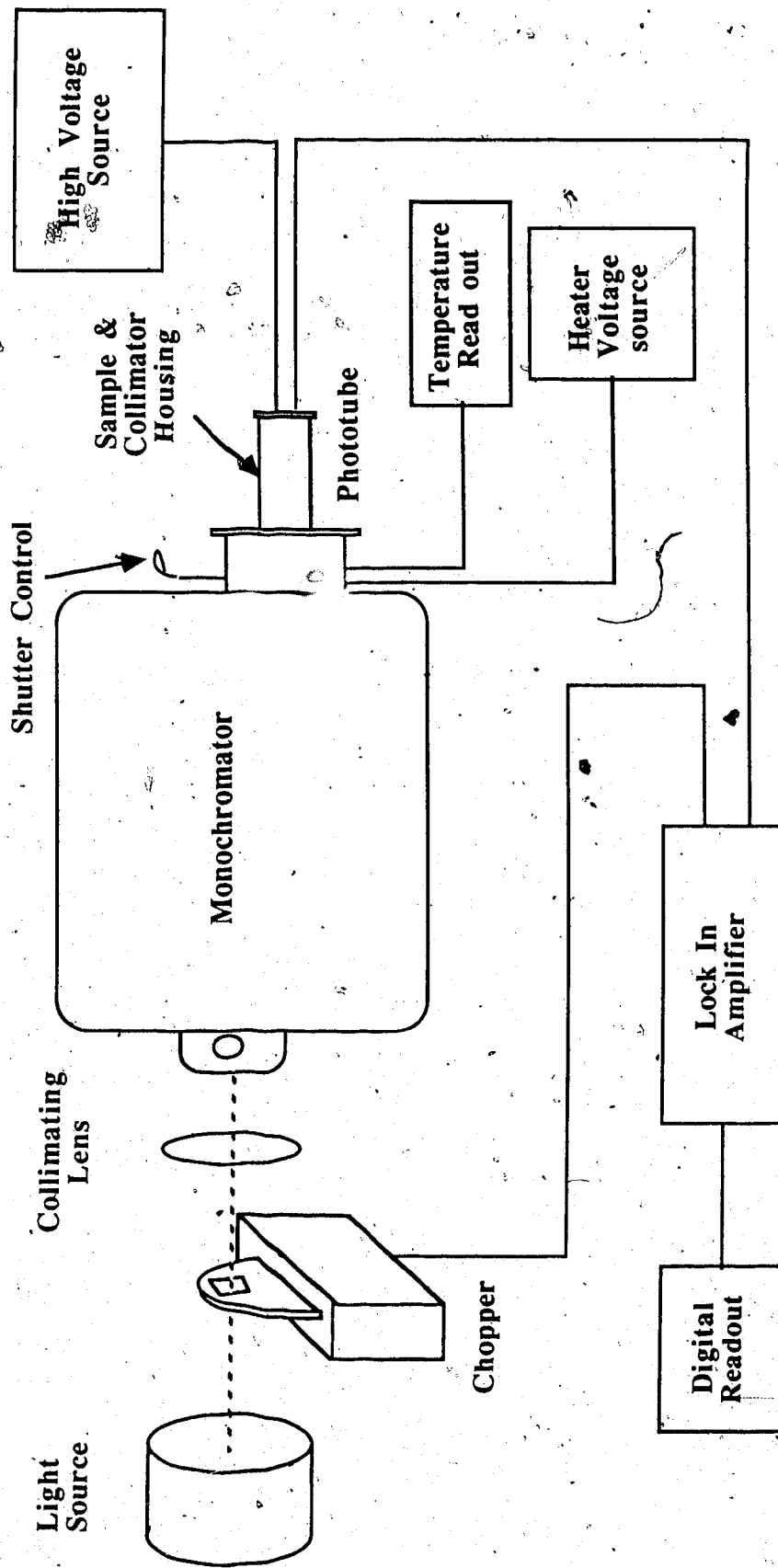
$$\Psi = \int_A I \, dA = I \int_A dA \quad (2)$$

where A is the cross sectional area of the beam seen by the detector.

The transmission ratio was obtained using the experimental layout illustrated in figure 5. Eicher, Knof and Lenz (1977) used a simpler form of this setup for their work. An alternative experimental method is given by Norris and Butler (1961) but this system does not allow for post sample collimation and is meant to give an absorption spectrum only. At the time this experiment was being performed a similar one was being carried out

Experimental Set Up

Figure 5



by Stephen Flock at Ontario Cancer Foundation in Hamilton, for further details see Flock (1987).

A collimated polychromatic light source passed through a monochromator which allows the operator to select a beam of quasi-monochromatic radiation. This selected light is passed through the sample assembly on to a phototube where its energy fluence is measured with and without the sample in place.

EQUIPMENT

Light Source

There were two kinds of light sources used in accordance with the type of monochromator used. A 50 watt (12 volt) tungsten filament light was powered by a low noise voltage regulator when the double prism monochromator (brand name-KIPP) was in use. The grating monochromator (brand name-SPEX), with improved wavelength resolution, dispersed the incident light to a greater degree necessitating the use of a more intense light source. The beam was collimated by a double convex lens before reaching the monochromator. Only when dealing with 'thick' (1.5 mm) samples of blood at short wavelengths did this source prove insufficient.

For the SPEX monochromator it was found that a 1000 watt xenon arc lamp was needed in order to achieve the necessary intensity. The placement of the lamp in the system was the same as for the filament source, but the lamp was so bright it had to be shielded to make the situation bearable for the personnel involved. Collimation was provided by an f/2.4 parabolic mirror (39 cm focal length) situated behind the lamp coupled with an f/1.7 double convex lens (17.3 cm focal length). All horizontally mounted arc lamps have an inherent dark spot in the center of their beam. Because of this dark spot the collimated light source was offset slightly from the optical axis of the SPEX monochromator.

Monochromator

The KIPP is a double prism monochromator which uses two flint prisms with a refraction angle of 54 degrees and an arrangement of mirrors to break down the collimated polychromatic light into a quasi-monochromatic form. As the wavelength resolution is dependent on the change in refractive index with wavelength, and this is not a linear dependence, the resolution is not constant for all wavelengths. The wavelength resolution was measured using the mercury line at 1014 nm. The full width at half maximum (FWHM) was 30 nm (see figure 6). At shorter wavelengths the KIPP was unable to resolve the mercury couplet (577 - 579 nm) but as the beam spans the same angle for both wavelength ranges it can be calculated from the calibration graph of the monochromator as 9 nm.

The SPEX is a single grating monochromator that depends on the reflective diffraction properties of a grating to spread out the spectrum of the polychromatic light. This is in accordance to the grating equation (Hecht (1976));

$$a (\sin \theta_m - \sin \theta_i) = m\lambda \quad (3)$$

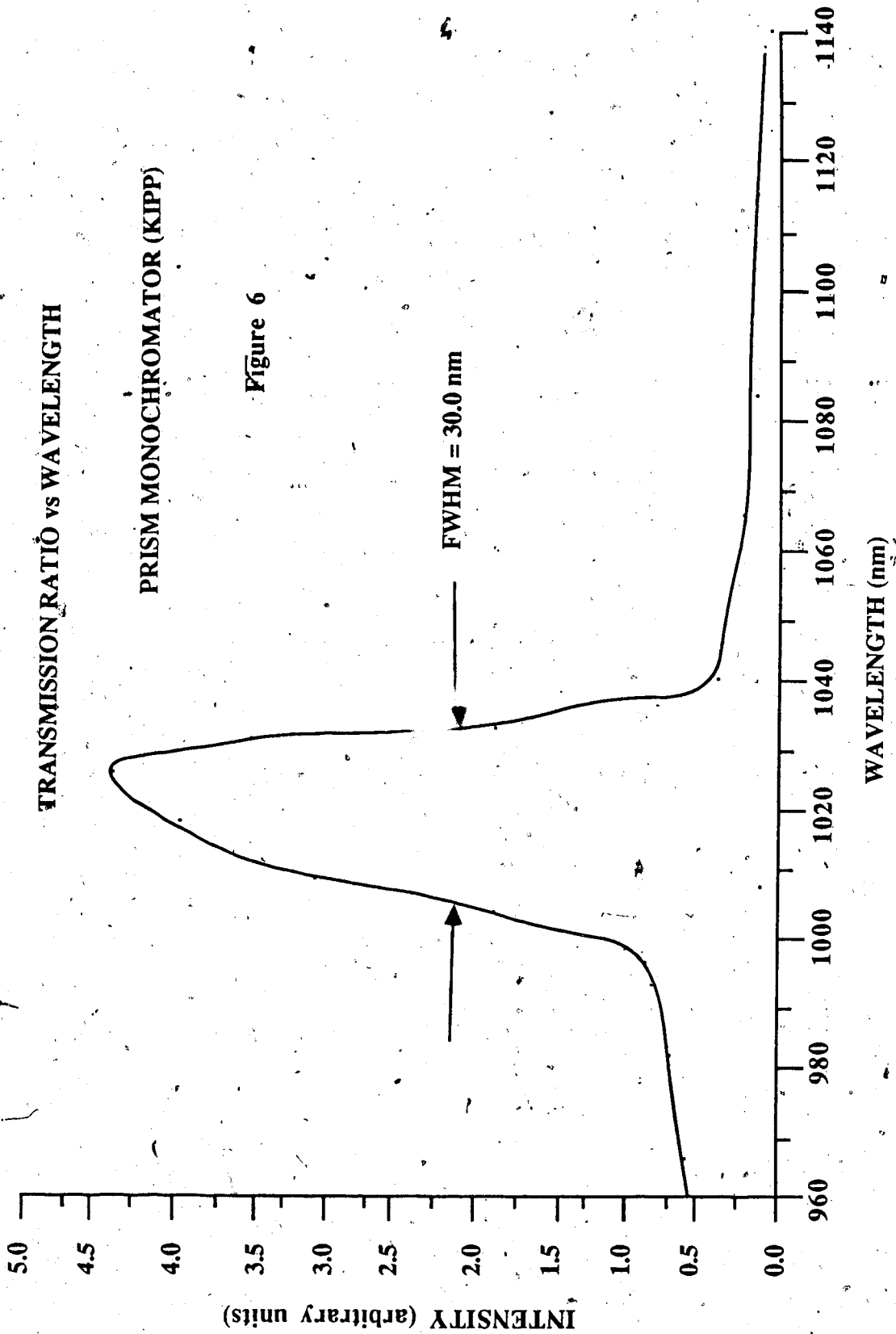
where a = the inverse of the grating density

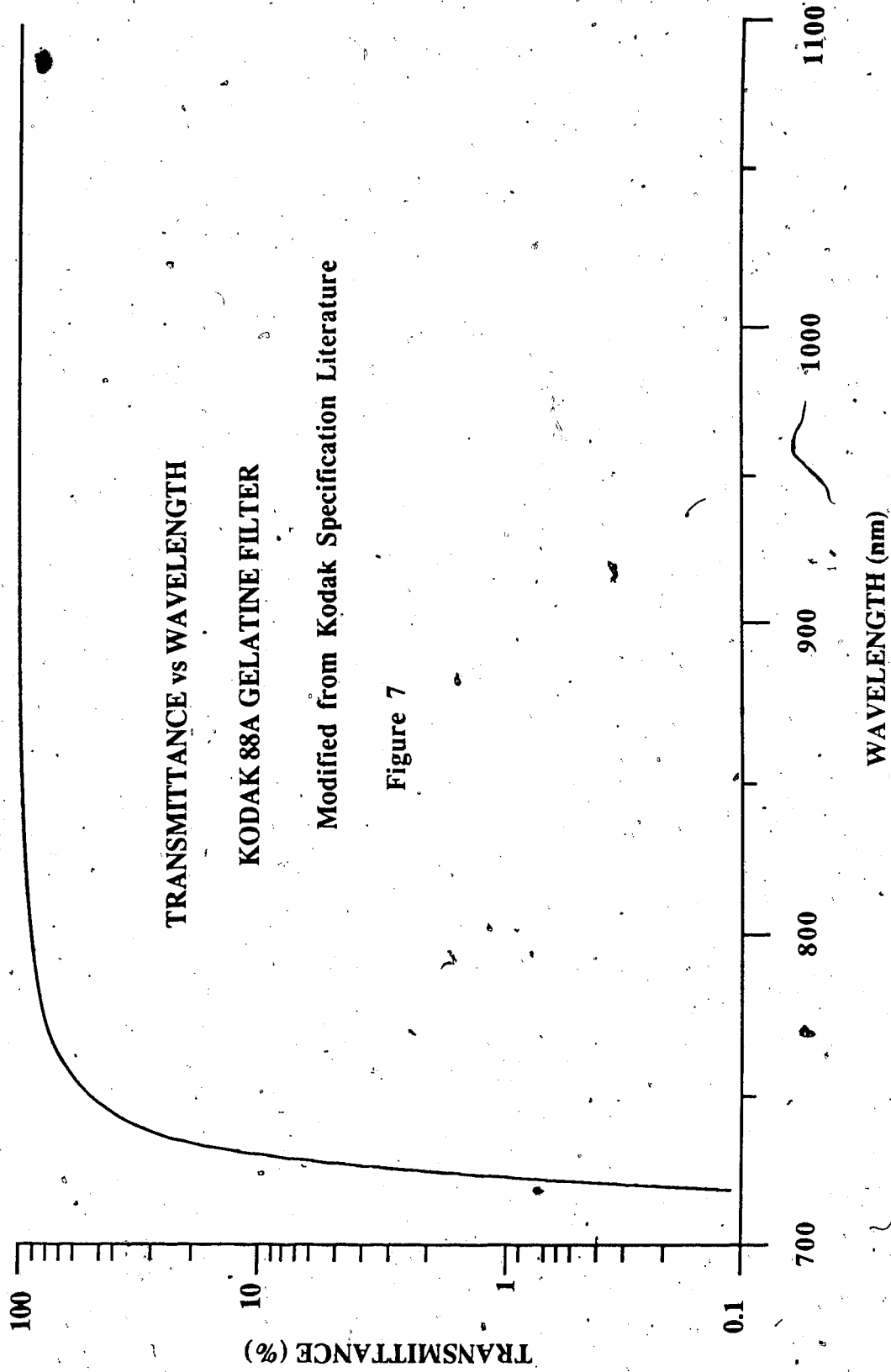
θ_m = the angle of the refracted beam of order m

θ_i = the angle of the incident beam

λ = the wavelength of the beam of interest

From the above equation it can be seen that given a wavelength of λ_a of order n that there will be an overlap with light of wavelength $\lambda_b = \lambda_a/2$ of order $2n$ providing λ_b exists in the incident beam. In the experiment involving the SPEX monochromator this is indeed the case. This problem was resolved by putting a KODAK 88A gelatine filter over the exit port for wavelengths greater than 800 nm. The 'high pass' response curve for the filter can be seen in figure 7.





The SPEX monochromator has a wavelength resolution FWHM of 1 nm to define the 1014 nm mercury line and a FWHM of 0.7 nm to define the 577 nm mercury couplet (see figure 8 & 9). As this is better than an order of magnitude than the KIPP, the SPEX was used to look for structure in the tissue spectra.

Collimation Assembly

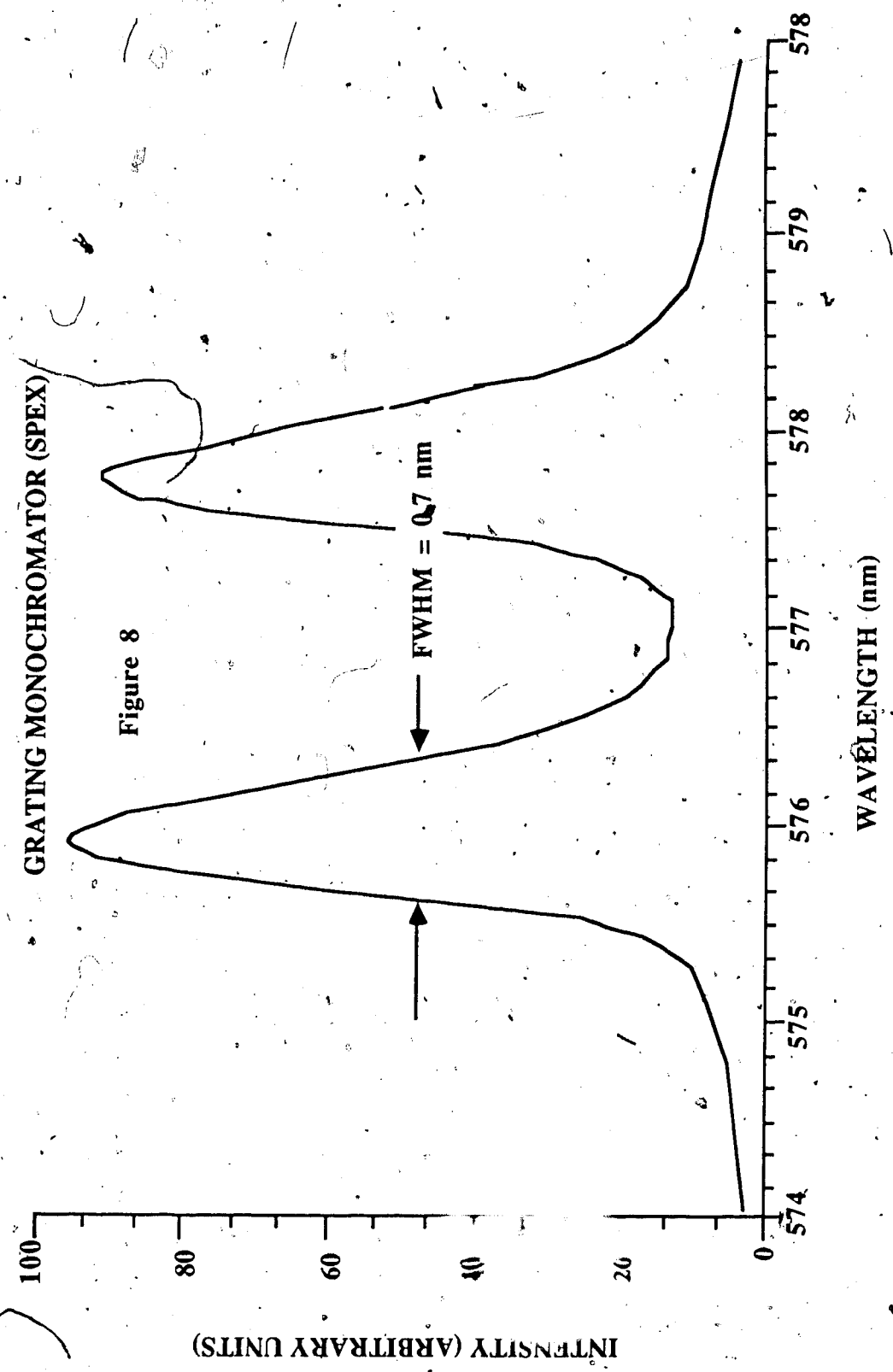
Collimation of the beam was of two parts. The pre-sample collimation attempted to condition the beam into a parallel form as prescribed by narrow beam geometry. The post-tissue collimation was intended to eliminate as much of the scattered light as possible, leaving only unscattered incident light in the transmitted beam. The size of the holes used in the collimator was ultimately dictated by the minimum intensity that the phototube could detect at its least sensitive point in the wavelength range of interest (see figure 10).

The sample shutter was placed close to the exit port to allow for the smallest area of tissue to be irradiated by the most intense beam possible. This meant that the pre-tissue collimation of the beam was done before the beam entered the monochromator via the lens and aperture system. Given this set up, the KIPP monochromator has an exit beam with a dispersion angle of 3.7 degrees before the post-tissue collimator (see figure 11).

Sample Holder

The sample was mounted on a shutter that allowed the beam to pass either through a mounted tissue sample or unimpeded through the collimator assembly (see figure 12). This allows the two factors of the ratio to be measured within a short time period. This aspect of the experimental design is necessary to overcome the problem of the inherent drift in the intensity found in all light sources.

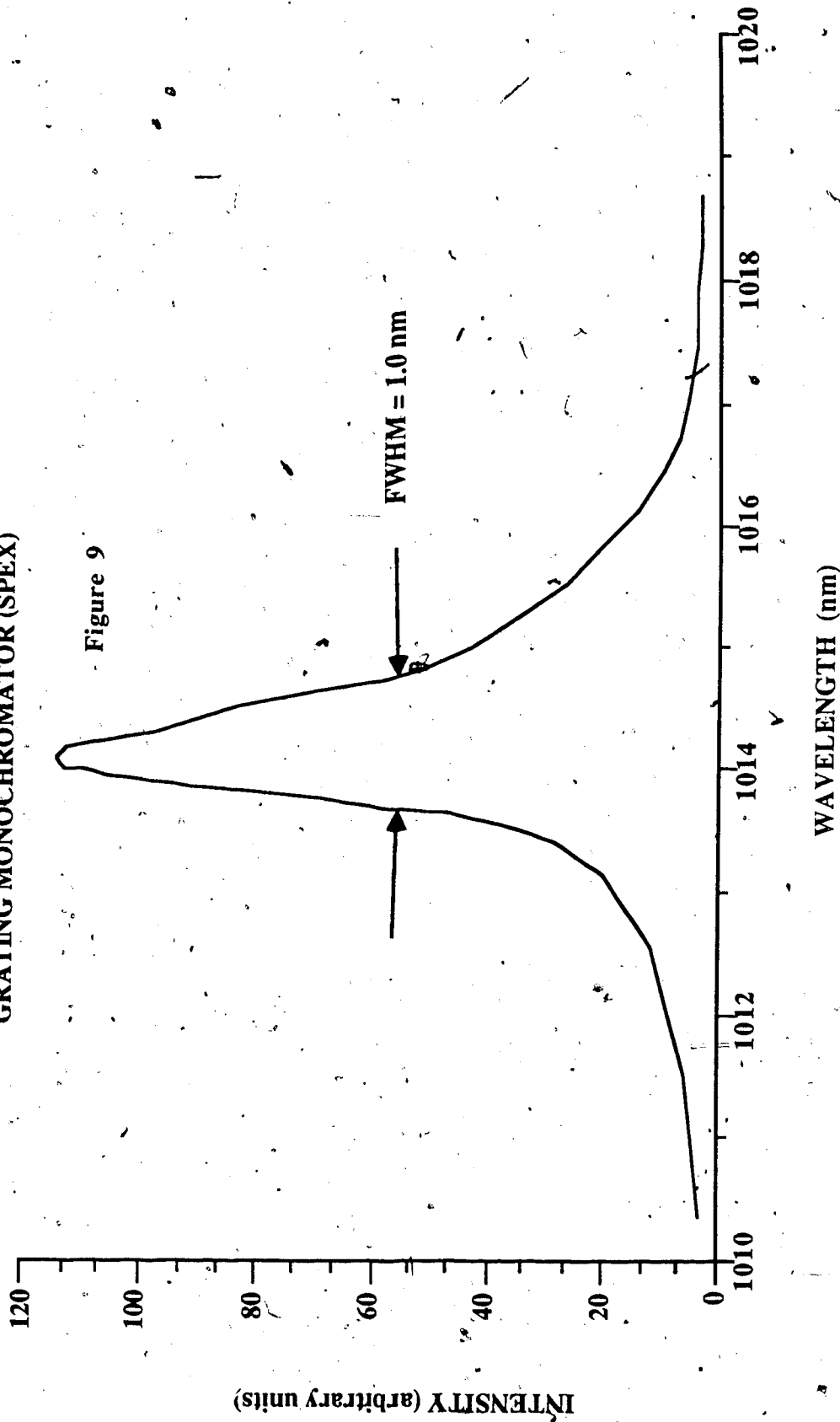
INTENSITY vs WAVELENGTH
GRATING MONOCHROMATOR (SPEX)



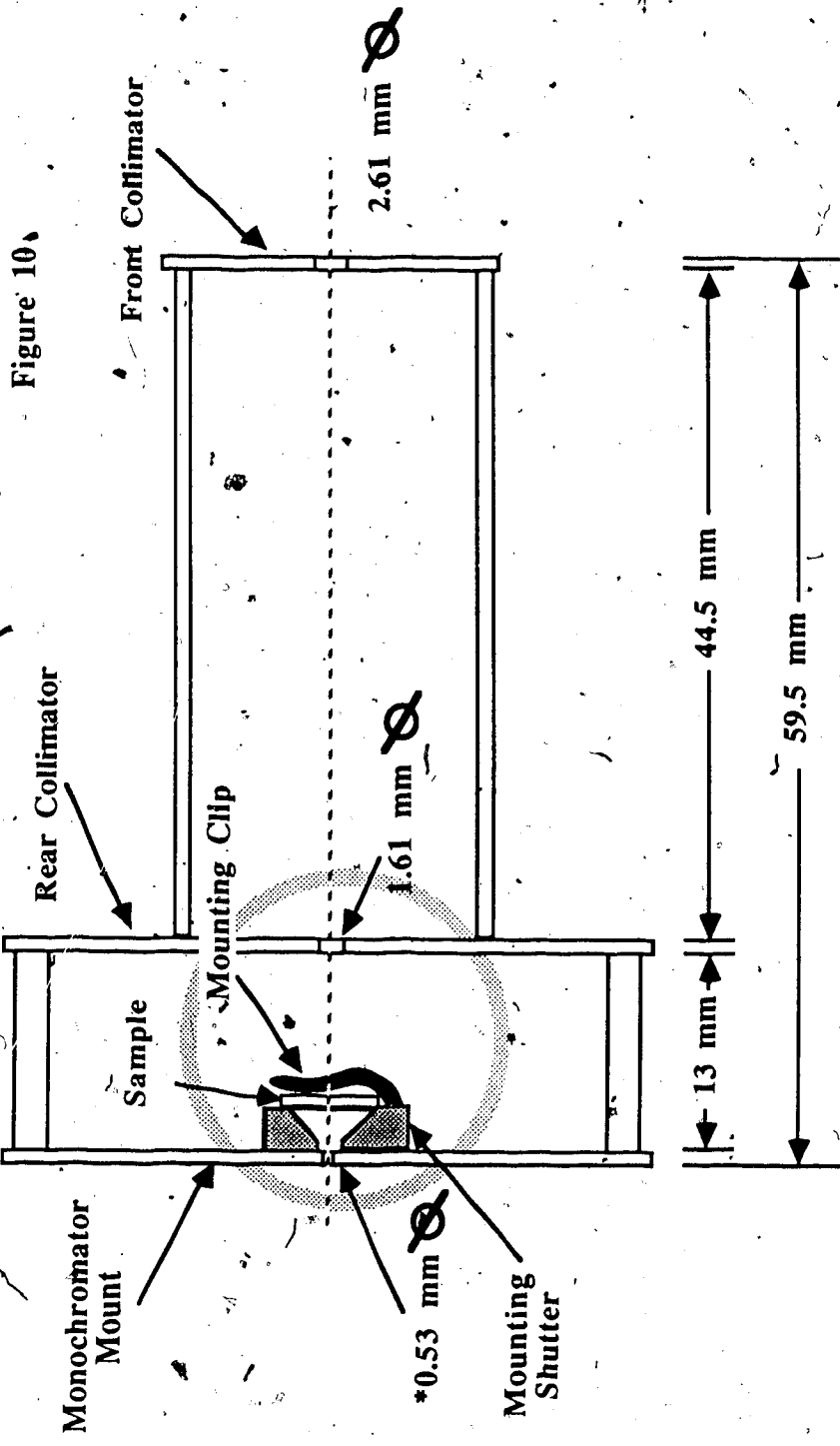
INTENSITY (ARBITRARY UNITS)

WAVELENGTH (nm)

INTENSITY vs WAVELENGTH
GRATING MONOCHROMATOR (SPEX)



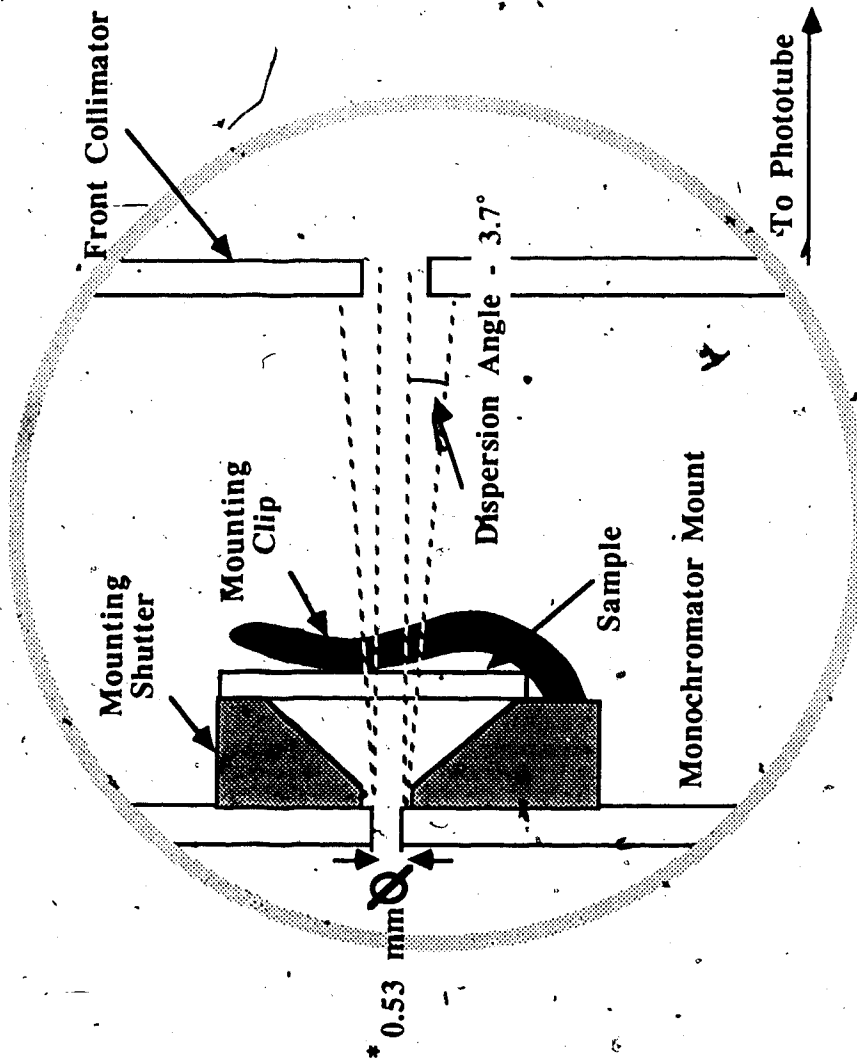
Collimator & Mounting Assembly - Side View



*1.6 mm \varnothing for blood and adipose tissue

Rear Collimator Assembly
Magnified View

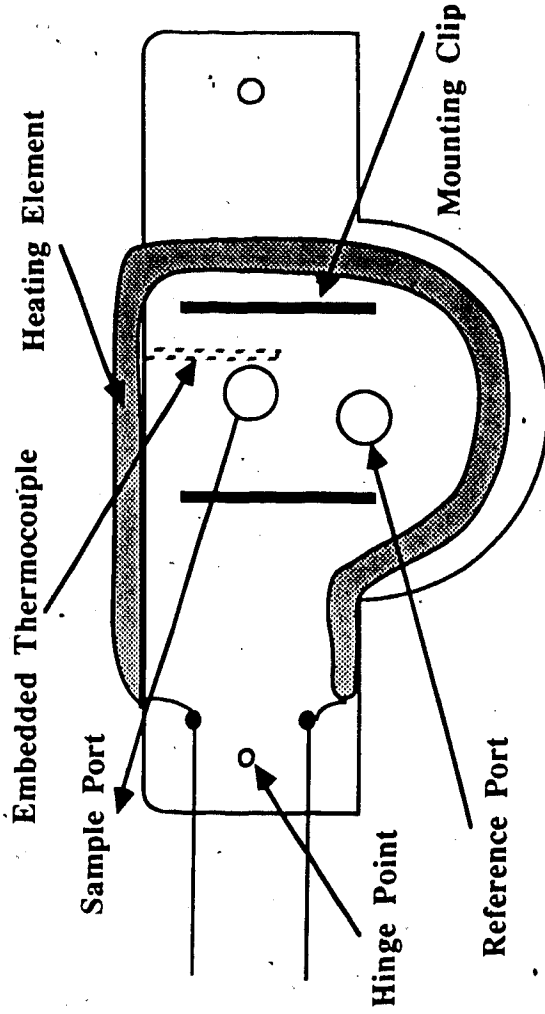
Figure 11



*1.6 mm \varnothing for blood and adipose tissue

Mounting Shutter

Figure 12

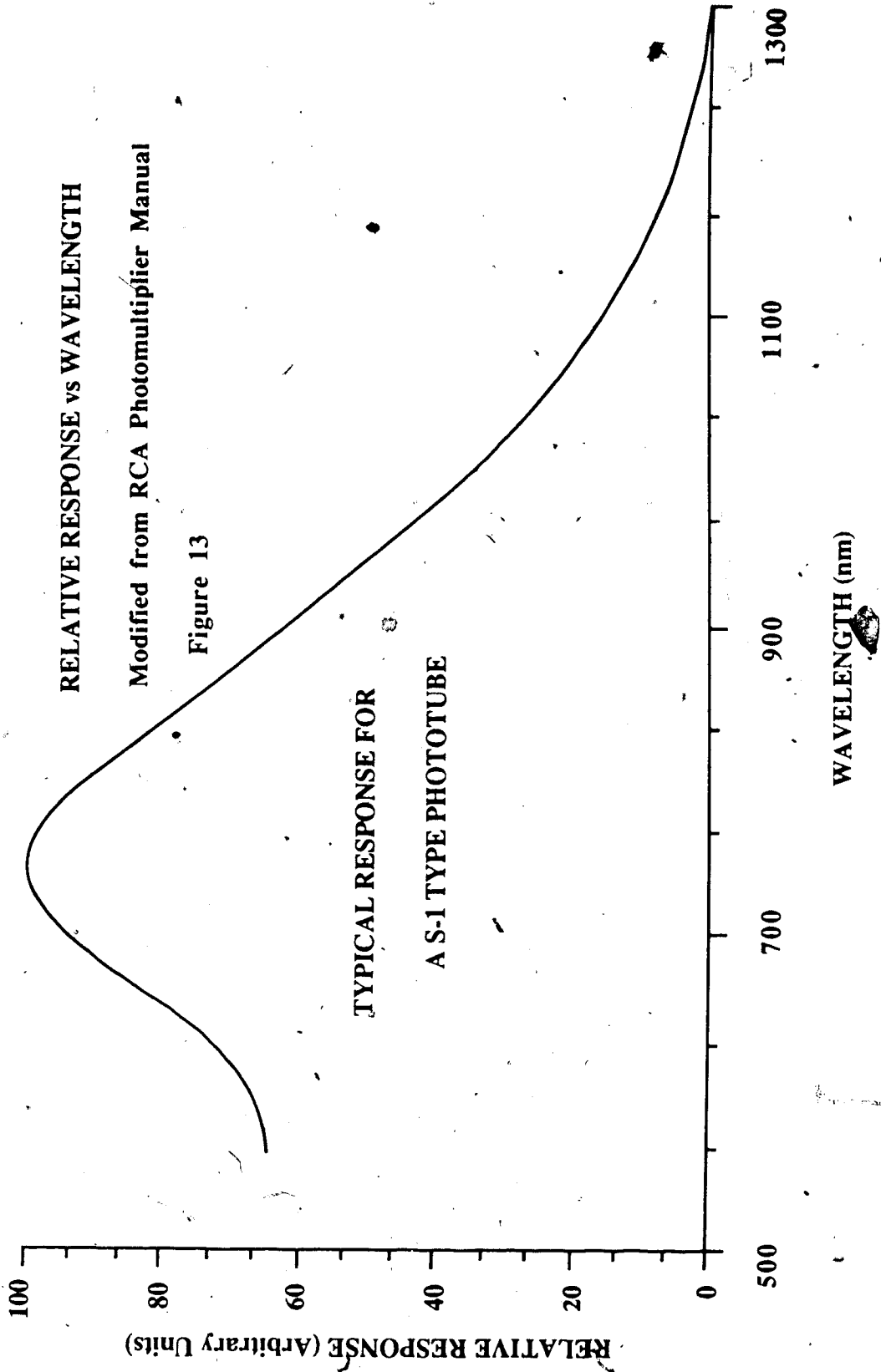


Detector

The detector was an S-1 response phototube working at 1200 volts delivered by a regulated voltage source. The wavelength sensitivity of the phototube was the ultimate limiting factor in the experiment's design. The response curve for a typical S-1 tube can be seen in figure 13. At the time of the experiment the phototube proved to be the most sensitive detection device available. Given the advancements in solid state technology any future experiments should consider photodiodes during experimental design.

Amplifying and Noise Reduction System

The chopper was used to convert the constant intensity light source into one whose intensity alternates with a well defined frequency. The lock-in amplifier then only accepts that part of the signal that has the correct frequency as defined by the chopper. Thus by tracking the frequency of the chopper, the band width of the lock-in amplifier can be set as narrow as possible, and minimize the amount of noise received. The amplifier also has an internal gating mechanism tied to the chopper frequency to allow the input signal to disregard part of the input signal by means of a phase shift. This aspect of the amplifier was not used for this experiment and accordingly the phase adjustment was set to get maximum signal. It should be noted that this procedure also automatically eliminates any background signal in the sample holder due to a light leak or black body radiation.



SAMPLE PREPARATION

Human tissue samples were collected within a few hours of resection from patients undergoing surgery involving either biopsy or amputation. Porcine samples were collected fresh from healthy sacrificed specimens. These samples were then submerged in a tissue embedding medium (O.C.T.) and frozen. Ideally the tissues should be frozen as quickly as possible in liquid nitrogen to prevent the formation of large ice crystals. In order to have the samples frozen fresh, the use of liquid nitrogen was not always possible, particularly when working on the periphery of a busy surgical ward.

The experimental results hinged on the idea that the tissue samples retain their physical structure as closely as possible to the *in vivo* situation. This condition was the limiting factor on how thin the microtome could cut the frozen sections. While it is true that microtomes are used regularly to cut tissue to 5 μm thicknesses, this is done for qualitative analysis of the tissue's cell structure and make up. The lower limit of thickness at which acceptable samples could be cut for the purposes of this experiment is very much dependent on the tissue type, but usually was in the range of 100 μm .

It should be noted that fatty tissue freezes at much lower temperatures than other tissues. For this reason the cutting of these tissues was done at lower microtome refrigerator settings. Typically the settings were -20C for normal tissues and -35C for fatty tissues.

Samples were mounted between two microscope glass cover slips approximately 150 microns thick, the exact thickness being measured by a micrometer and taken into account in the final measurement.

Copper spacers were placed around the sample to assure thickness value and uniformity. The thickness of the actual tissue sample was cut just slightly larger (5 μm) than the copper spacer to be sure the sample was in direct contact with the glass slides.

The tissues were saturated with electrolyte balanced solution to help avoid any air bubbles that might be present. The electrolyte solution mimics the intracellular fluids avoiding osmotic pressures and flows that would change the tissue structure.

The final step in preparation was to seal the glass slides in place with a synthetic resin and allow them to cure for about half an hour in a cool place. Once cured the sample thickness was measured with a micrometer. The glass thickness was subtracted from the measured value and the result recorded as the actual sample thickness.

Once the tissue samples were ready they were examined under a microscope to identify those areas that kept their optical integrity intact. The requirements of a valid sample were that the tissue structure was not torn, and that there were no air bubbles or foreign tissues structures in the sample. This requirement of a single tissue type was obviously impossible when looking at the spectral response of a highly vascularized tumor and therefore no measurement of attenuation coefficients was attempted.

Blood presents its own problems in mounting. The samples must be extracted with heparin to stop clotting. The amount of heparin used is small and as it is the body's own anti-coagulant it was deemed not to affect the results. The blood also settles over time requiring that the sample be agitated or replaced periodically during testing.

IN VIVO VS IN VITRO

Of major concern in this type of experiment is that the tissue samples retain as many of their *in vivo* characteristics as possible. In order to apply the results of the experiment to living tissue any differences between the two situations must be taken into account.

The most obvious difference between the two situations is that of tissue temperature. A 1.5 mm sample of porcine adipose tissue had its transmission ratio measured for a number of different temperatures with a 1000 nm light beam. The results are plotted on figure 14. The result was judged to be due to actual changes in the optical

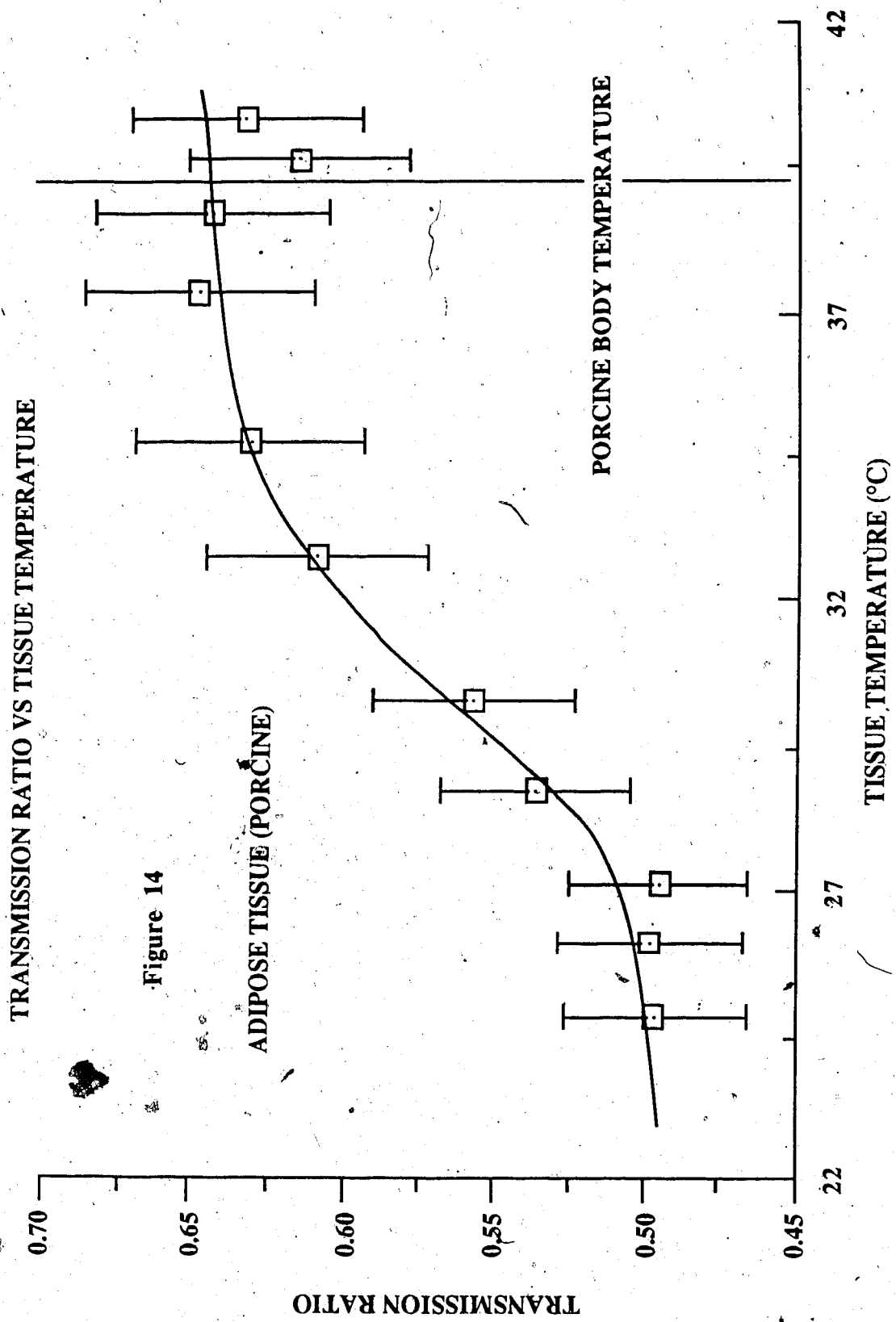


Figure 14

43

properties of the tissue. The possibility that the optical change was due entirely to thermal expansion was ruled out for two reasons: first, the density change over this temperature interval for water is less than 0.3 %, an amount far too small to affect the observed change in optical properties; the second was that the dimension of the sample mounting with least resistance to pressure was that parallel to the beam, thus changes in the actual thickness of the sample would not change the optical thickness.

These results showed that the sample holder needed to be heated as the optical properties of the tissues were dependent on temperature. This was accomplished by securing a wound nickel chromium heating element to the shutter with silicone. The element was connected to a variable voltage source. A thermocouple was implanted near the shutter hole to monitor the temperature of the shutter. Detector readings were started as soon as the tissue was stabilized at its normal body temperature (37°C for human tissue, 39°C for porcine tissue).

The reflection and absorption influences of the glass mounting and electrolyte solution was checked using a mounted sample of the solution. Testing showed the sample to have a transmission ratio of 97% uniformly for all wavelengths measured. Measurements of the transmission ratio of tissue are corrected accordingly.

B. Wilson (1985) points out that at 630 nm the absorption coefficient for whole blood is at most a few percent of the overall attenuation coefficient. This point of view is supported by Doiron (1984) in his experiments with cat brain at 633 nm. This suggests that at the majority of the wavelengths looked at in this experiment blood absorption is not important.

At the wavelength intervals where blood absorption is a problem the oxygen levels of the blood under examination must be taken into account. The oxygen concentrations are an issue because of the relative amount of absorption of hemoglobin (Hb) and oxyhemoglobin (HbO_2). As a sample ages the HbO_2 breaks down to Hb and O_2 resulting

in a difference in the spectrum below 600 nm. This change is small and may affect only the lower wavelengths considered when looking at blood.

CHAPTER THREE EXPERIMENT I: TRANSMISSION SPECTRA

Of prime interest in this study is any spectral dependent 'peculiarities' that may be exploited for practical medical purposes (e.g. tumor identification and/or treatment). Of these, tissue specific 'windows' and/or 'stops' in the spectral response offer some of the greatest potential for imaging and treatment using infrared light. To explore the existence of such properties, the transmission spectrum of several tissues were investigated using the KIPP monochromator as described in the section on experimental set up.

In cases where human tissue samples were difficult to obtain, porcine tissue was substituted. Porcine tissue was chosen as it is from an omnivorous mammal with approximately the same heart to body-size ratio as man. These species traits give rise to a great biological similarity of tissues at the cellular level that has been utilized in a wide range of research areas. (Bustad (1966)) The tissues selected for examination were porcine brain, human adipose, human skin, dense human breast tumor, human lactating gland and porcine testicular tissue.

The actual use of infrared radiation as an imaging mode in thermography is at wavelengths of 7000 to 13000 nm to monitor temperatures from 0 to 65 C. This is well above the 1100 nm maximum wavelength used in this experiment. In this experiment what black body thermal radiation present at the wavelengths under examination was removed by the chopper and lock-in amplifier.

The scattering in this experiment was expected to be due mainly to internal reflection and refraction off small inhomogeneities such as cell walls and nuclei. This being the case, there are a number of such structures which are close to the same size as the wavelengths being investigated. From basic geometric optics it is known that when such a situation develops there is the possibility of resonant frequencies at which reflection and/or transmission are radically changed. If these wavelengths were present it should be

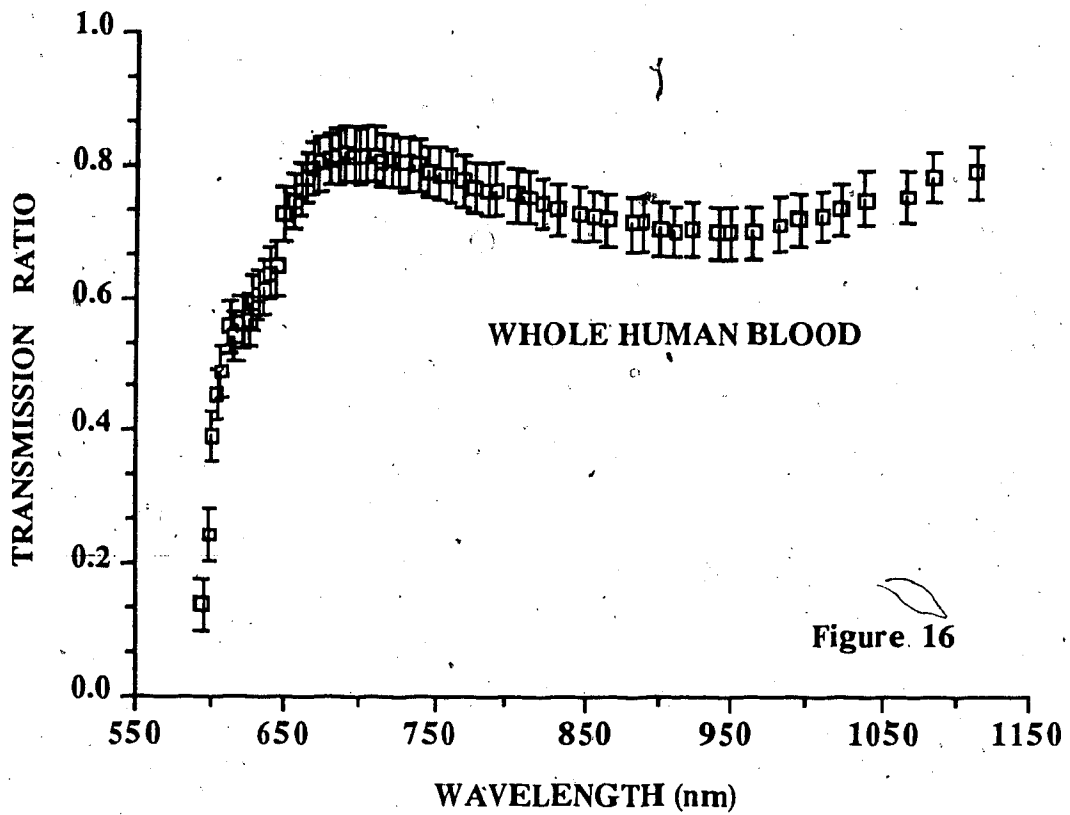
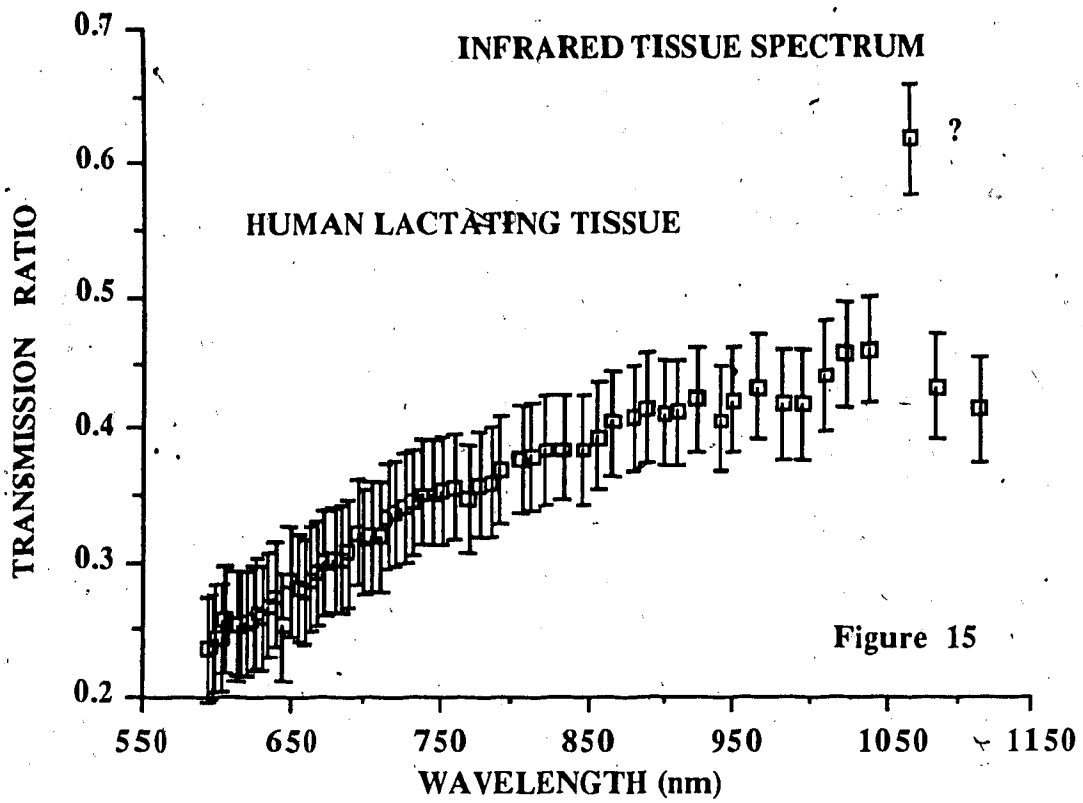
expected that they would show up as changes in the scatter conditions which would lead to changes of the amount of light detected. Such an effect was reported by Wilksch and Jacka (1984) who claimed that the myofibrils of the muscle tissue were acting as a diffraction grating. This, it was claimed, resulted in an enhanced forward scattering of the radiation and an associated anisotropic scattering function. As Wilksch and Jacka worked only at one wavelength it was supposed that given the wavelength dependency of diffraction gratings a spectral analysis would evaluate the validity of this explanation.

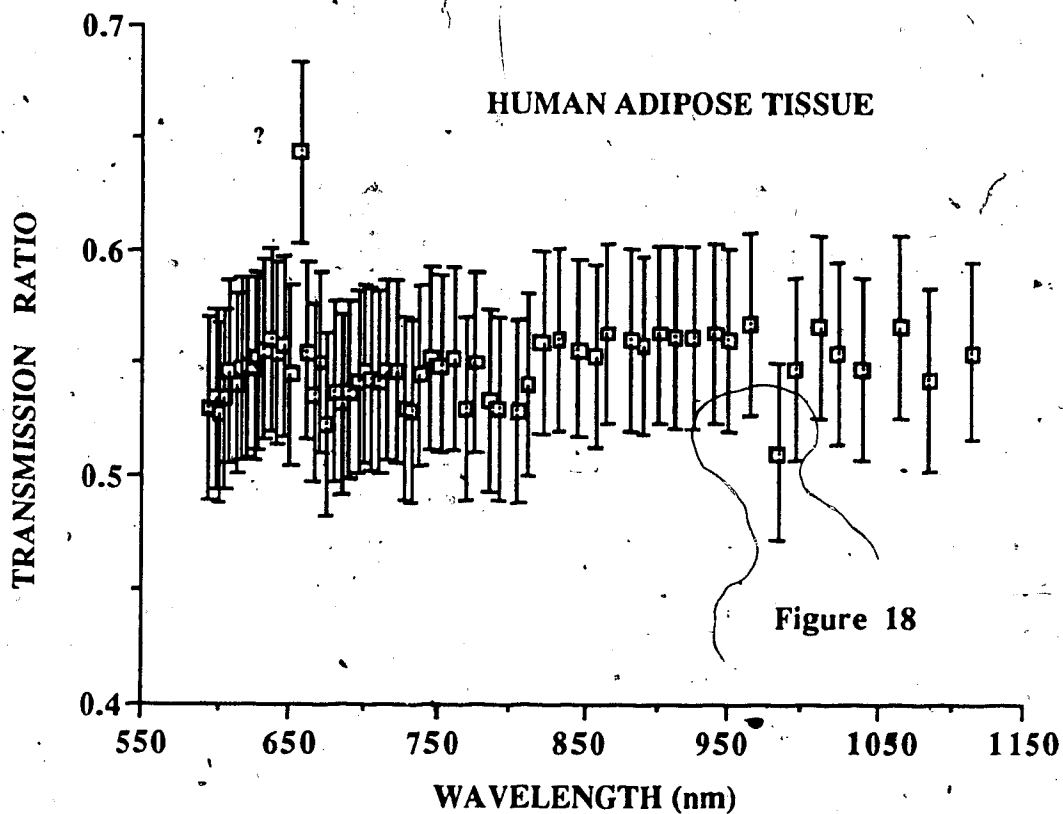
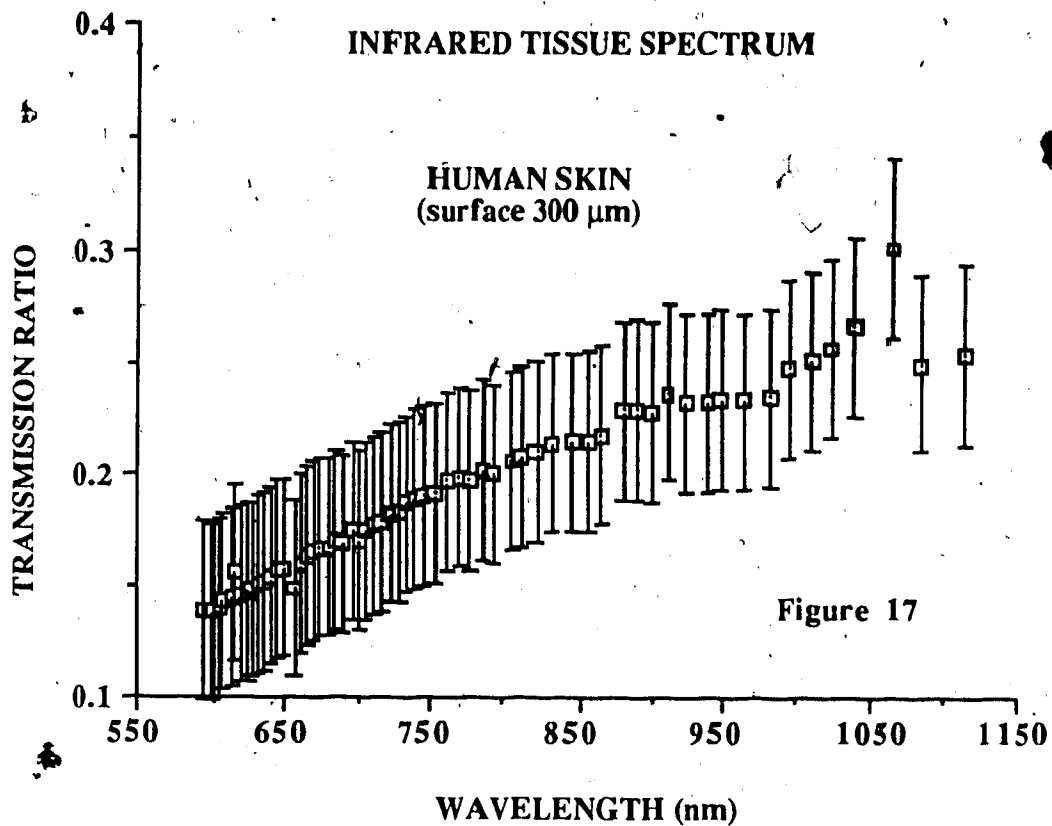
At the time that this experiment was performed the literature (Profio and Doiron (1981)) suggested that the scattering was only slightly anisotropic and thus penetration depths measured in diffusion type situations were only an order of magnitude larger than the mean free path. With this fact in mind an attempt to look for wavelength dependent changes in the scatter function were made by cutting the sample slices to what was thought to be a few mean free path thick ($\sim 300 \mu\text{m}$) for all tissues except blood. Blood samples were prepared to be $150 \mu\text{m}$ thick. The post tissue collimation system was removed giving an angle of collimation to the detector of approximately 28° .

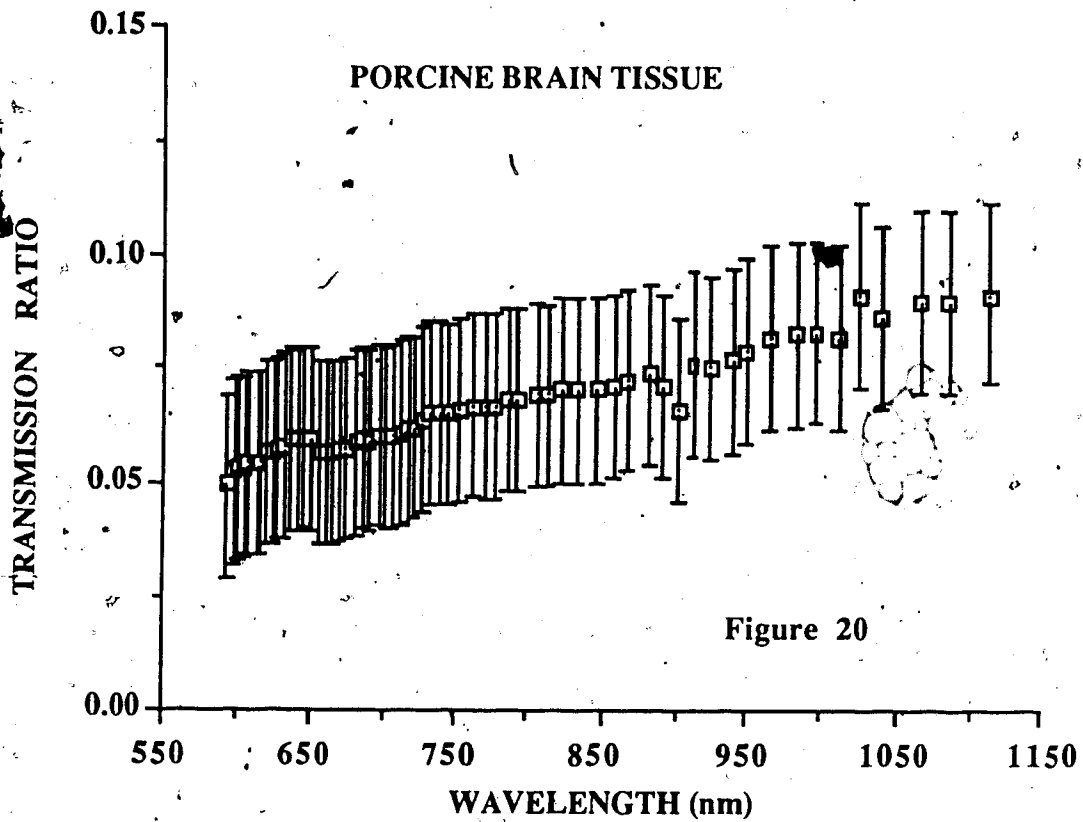
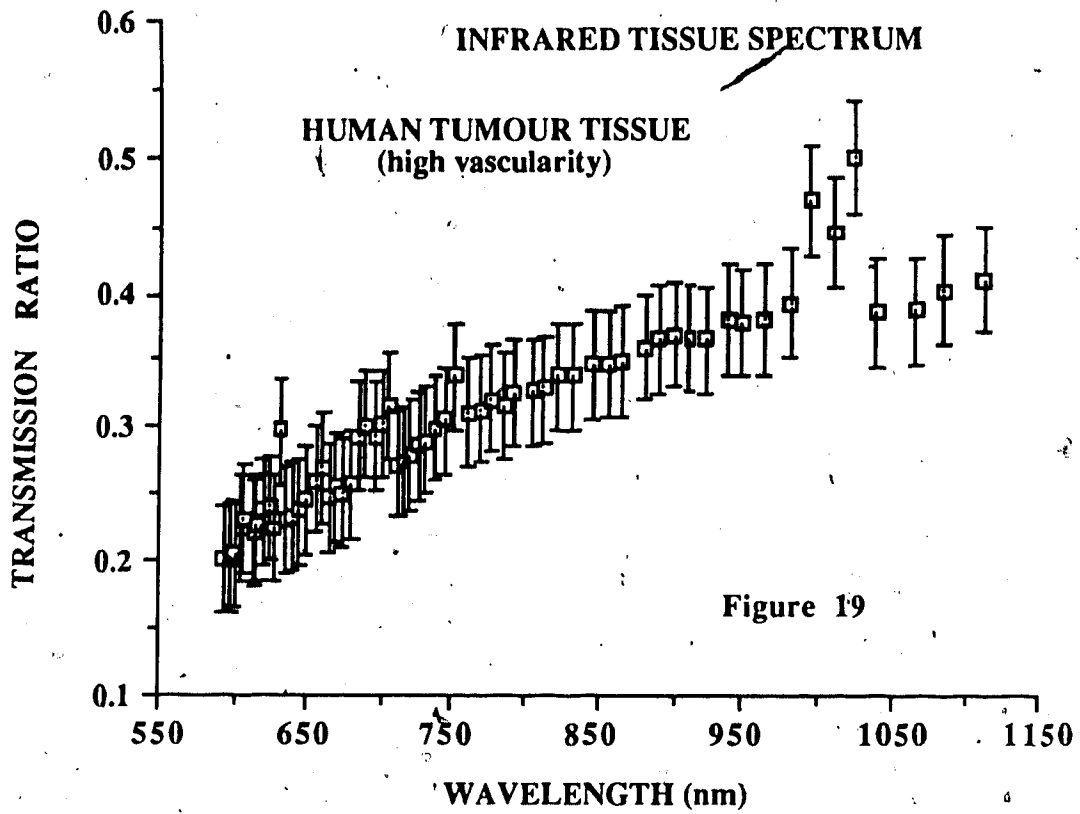
Actual chemical absorption due to water and lipids would be expected but it was suspected that much thicker samples would have to be used to see these effects (Bolin (1984)). The suspicions that the weak chemical absorption would not be visible were confirmed in the results shown in figures 17 through 24. There is a complete lack of feature in the spectrum between 600 and 950 nm. This lack of feature is also reported in similar experiments for bovine muscle (Preuss (1982)), human adipose tissue, human glandular tissue, human breast tissue (Ertefia (1985), Shalev(1985)), porcine brain, rabbit muscle and human blood. (Wilson (1985)) Note that points marked with a "?" were found not to be reproducible when additional scans were made. All tissues with the exception of adipose tissue and blood display an apparent increase in transparency as wavelength increases. This agrees with observations made on human skull, human chest wall, human abdominal wall, and human scrotum made by Wan (1981).

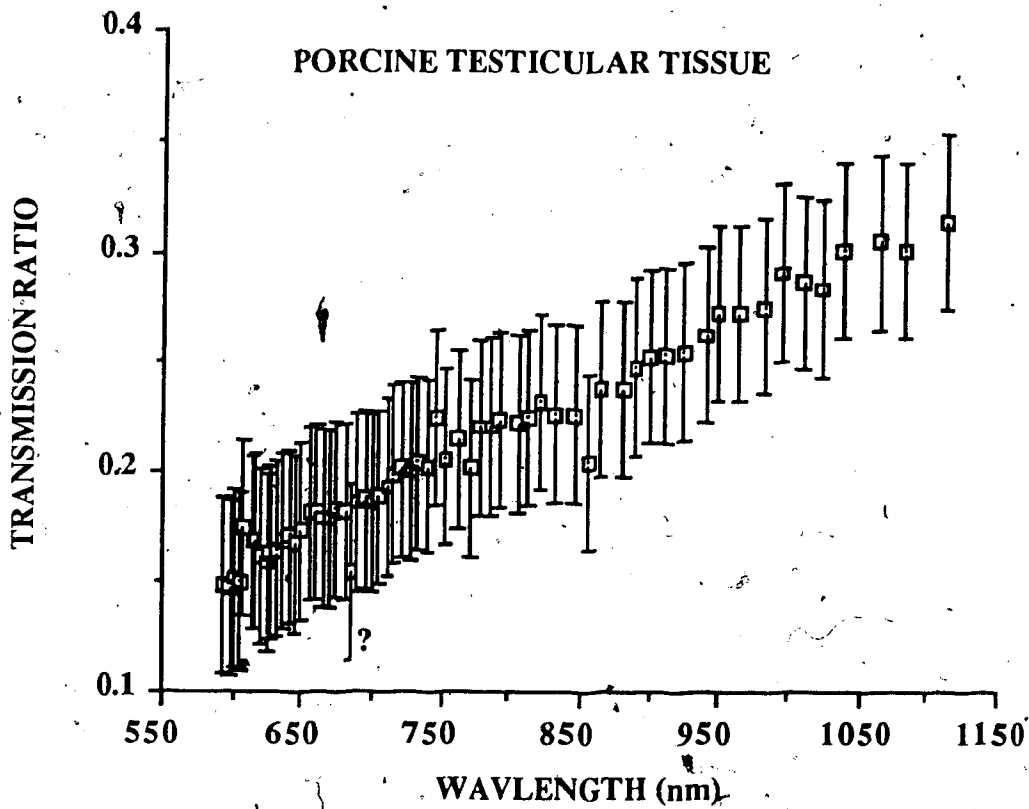
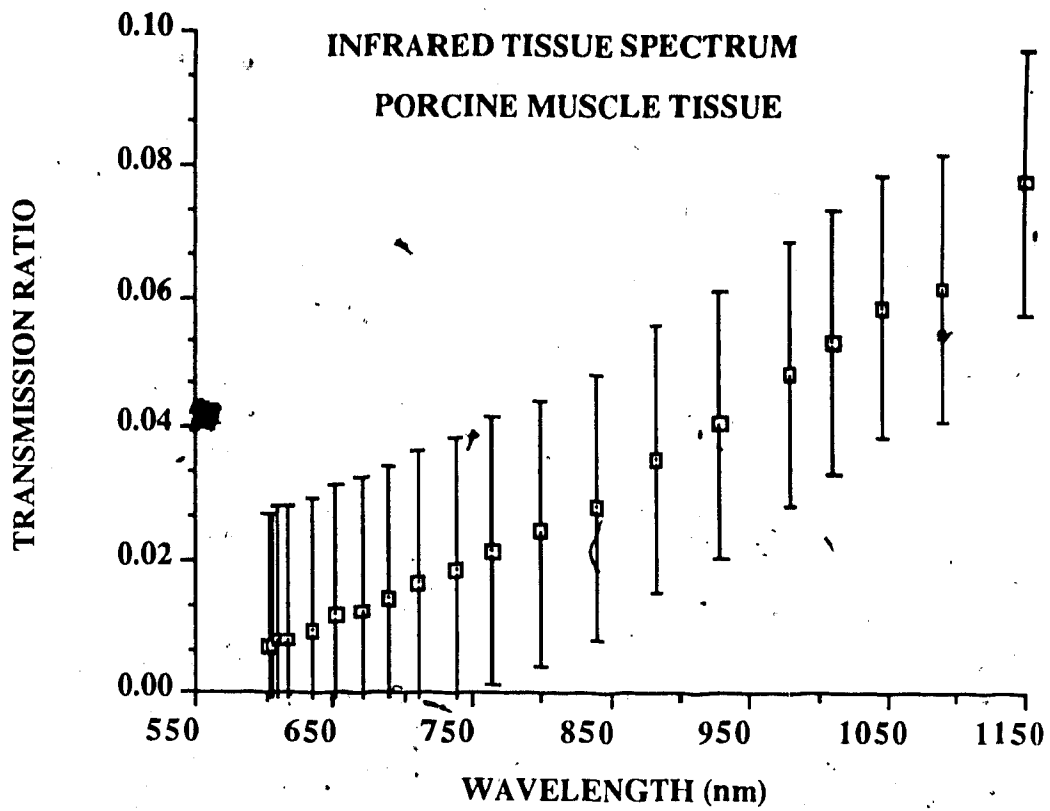
The strong absorption of red and near red light in blood is readily evident but the much weaker absorption due to water around 970 nm is not readily apparent.

On the basis that the effects were too small to be seen at the wavelength resolution given by the KIPP monochromator, the experiment was repeated using the SPEX monochromator and argon light source. This was strictly a qualitative comparison of the resultant spectral output of the arc lamp light with and without tissue in the beam. Any regions of interest seen on the scan over the 800 to 1200 nm range were re-examined at a slower wavelength scan rate. This comparison was carried out for adipose tissue and blood and, taking into account the slow fluctuation of the lamps actual intensity, no areas of interest appear in either case. An example of the results for the adipose tissue is shown in figure 25. In the actual experiment saturation peaks were investigated separately at a lower sensitivity.









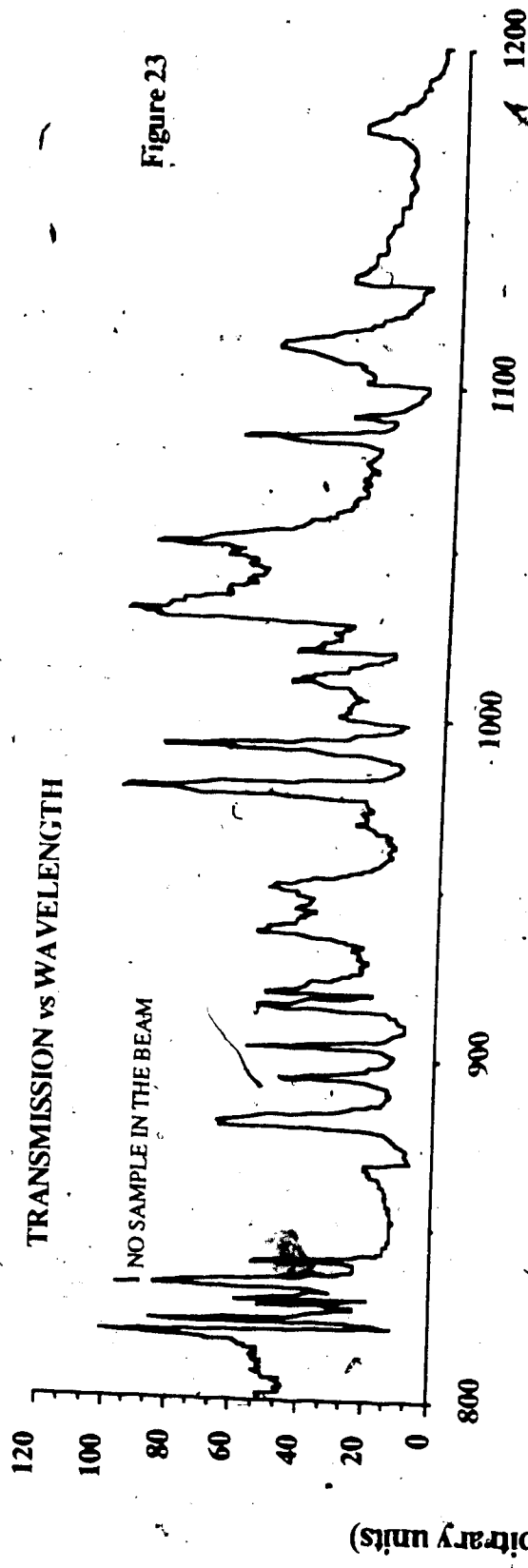
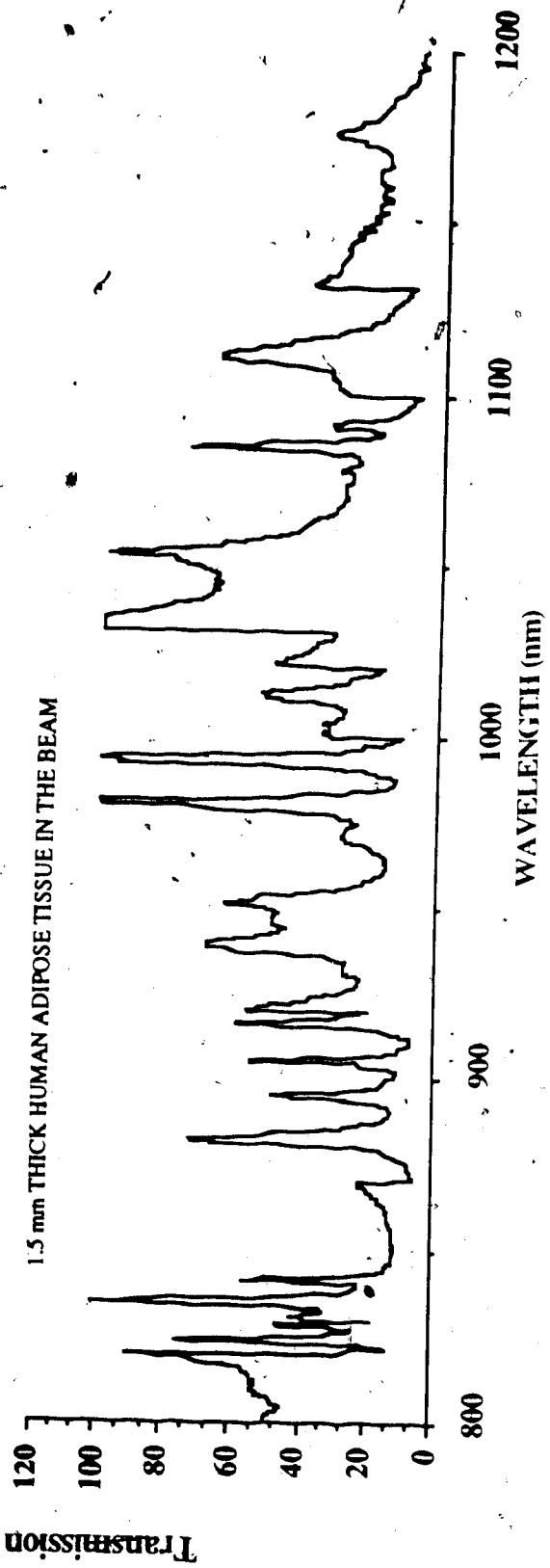


Figure 23



CHAPTER FOUR EXPERIMENT II:

TRANSMISSION ANALYSIS

BACKGROUND THEORY

Transport theory is used in describing everything from the molecular orientation of macromolecules to the diffusion of light through stellar atmospheres. As a result the names and definitions of the related variables are as varied as the subjects it covers. For this reason care should be taken when comparing the derivations and interpretations shown here with those found elsewhere in the literature. For the most part this text will use the notation defined at the initial meeting of the American Association of Physicists in Medicine which was set up to standardize nomenclature in the field of medical physics.

While the concepts used in this work will be summarized here a detailed derivation of the transport equation used in this work please can be found in Dunderstat (1979) pages 19 to 22.

Starting with the most basic definition of the unit vector defining the directions of movement of the particles involved ;

$$\hat{\Omega} = \frac{\mathbf{v}}{|\mathbf{v}|} = \hat{i} \sin \theta \cos \phi + \hat{j} \sin \theta \sin \phi + \hat{k} \cos \theta \quad (4)$$

The photon number density in six-space is;

$$n(\mathbf{x}, E, \hat{\Omega}, t) d^3r = \text{the probability of finding a photon at } \mathbf{x}, \text{ with energy, } E, \text{ and direction of motion } \hat{\Omega}, \text{ at time, } t.$$

In the case of radiative transport through tissue most of the literature deals with the specific intensity ;

$$I_{\nu}(\mathbf{x}, \hat{\Omega}, t) = h\nu c n(\mathbf{x}, \hat{\Omega}, t) \quad (5)$$

here I_{ν} is a distribution in six space for the frequency ν . As such the value of I_{ν} has no macroscopic meaning unless integrated over some angle or volume. (Wolf 1976)

If it is assumed that the light is monochromatic, time independent, with negligible thermal radiation¹, and that all scatter is coherent then the transport equation can be expressed as;

$$\hat{\Omega} \cdot \nabla I = -\mu_0 I + \frac{\mu_s}{4\pi} \int S(\hat{\Omega}', \hat{\Omega}) I(\hat{\Omega}') d\hat{\Omega}' \quad (6)$$

where: μ_0 is the linear attenuation coefficient [cm^{-1}]

μ_s is the linear scattering coefficient [cm^{-1}]

such that $\mu_0 = \mu_a + \mu_s$.

μ_a is the linear capture (or absorption) coefficient [cm^{-1}]

$S(\hat{\Omega}, \hat{\Omega}')$ is the scatter phase function (also called

the angular scattering probability function)

Since all situations involved in this project use quasi-monochromatic light the ν subscript will be dropped on the understanding that all coefficients encountered are to some degree frequency dependent.

In equation (6) if there is no scatter ($\mu_s=0$) then the solution to the transport equation becomes the well known Beer's Law.

$$I = I_0 e^{-\mu_0 t} \quad (7)$$

It should also be noted that ;

$$\frac{1}{4\pi} \int S(\hat{\Omega}, \hat{\Omega}') d\hat{\Omega}' = 1 \quad (8)$$

and as such $S(\hat{\Omega}, \hat{\Omega}')/4\pi$ is a probability density function in the true mathematical sense. As such it's statistical moments have a real physical interpretation. In particular the first moment of $(\hat{\Omega} \cdot \hat{\Omega}')$ is known as the mean cosine (g) where;

¹ In the case of this experiment, the effect of black body radiation was removed by experimental means. It's importance in a more general case would depend on the given situation.

$$g = \frac{1}{4\pi} \int S(\hat{\Omega}, \hat{\Omega}') (\hat{\Omega} \cdot \hat{\Omega}') d\hat{\Omega} \quad (9)$$

One method of dealing with the scatter in a radiative transfer situation is to try to separate the scattered radiation from the primary such that;

$$I(\mathbf{r}) = I_0 e^{-\mu_0 r} + \mathcal{S}(\mathbf{r}) \quad (10)$$

where $\mathcal{S}(\mathbf{r})$ is the component of intensity due to scatter. The exact method of defining the scatter is to now divide it up into first scatter, second scatter, third scatter etc.

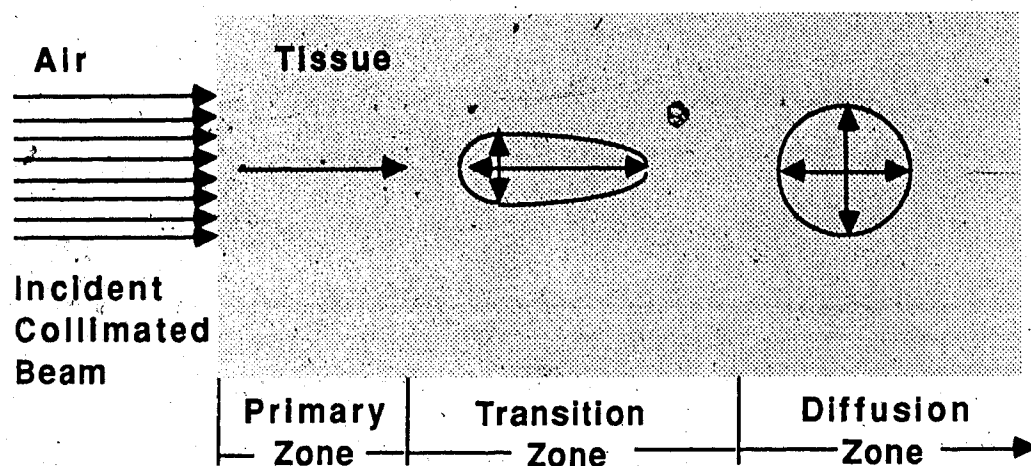
$$\mathcal{S}(\mathbf{r}) = \mathcal{S}_1(\mathbf{r}) + \mathcal{S}_2(\mathbf{r}) + \mathcal{S}_3(\mathbf{r}) + \mathcal{S}_4(\mathbf{r}) + \dots \quad (11)$$

where each scatter component is recursively dependent on the lower scatter components before it in that;

$$\mathcal{S}_{n+1}(\mathbf{x}) = \mu_s \int_0^x \int_{4\pi} \mathcal{S}_n(\mathbf{x}') S(\hat{\Omega}, \hat{\Omega}') d\hat{\Omega}' e^{-\mu_0 \mathbf{x}'} d\mathbf{x}' \quad (12)$$

Unfortunately the number of scatter levels involved combined with the nonexistence of a closed analytic form for the scattering phase function render this route impractical for this case.

The net movement of light through tissue can be divided into three possible zones depending on the tissue thickness. The following diagram summarizes these zones for a highly scattering homogeneous material.



The length of the arrows represent the relative fraction of photon flux in the direction indicated

Figure 24

As the experimental situation encountered in this experiment involves light transmission in the early transition zone, the transmitted beam has components of both the primary and scattered radiation. This circumstance requires a means of analysis that somehow takes both of these components into account in a manageable manner. To do this the experimental data from this and related experiments must be examined carefully to glean necessary information to derive a reasonable model

Several approximations to the exact solution to the transport equation have been formulated in order to describe very specific situations with the most commonly encountered being the diffusion² approximation. This solution depends on the radiation moving in random directions and as such is inapplicable as a useful form of analysis in this case. Nonetheless other experimentalists working in this zone have found that at the wavelengths used in this experiment there is a very high albedo (Flock (1987)), a point supported by work using the Kubella-Munk and related theories (Anderson (1981)).

On viewing the experimental results obtained from this experiment it is tempting to assume that all the transmitted light is unscattered primary beam and simply apply Beer's

² A derivation of the diffusion approximation and summary of some of the experimental results can be found in appendix I and II respectively

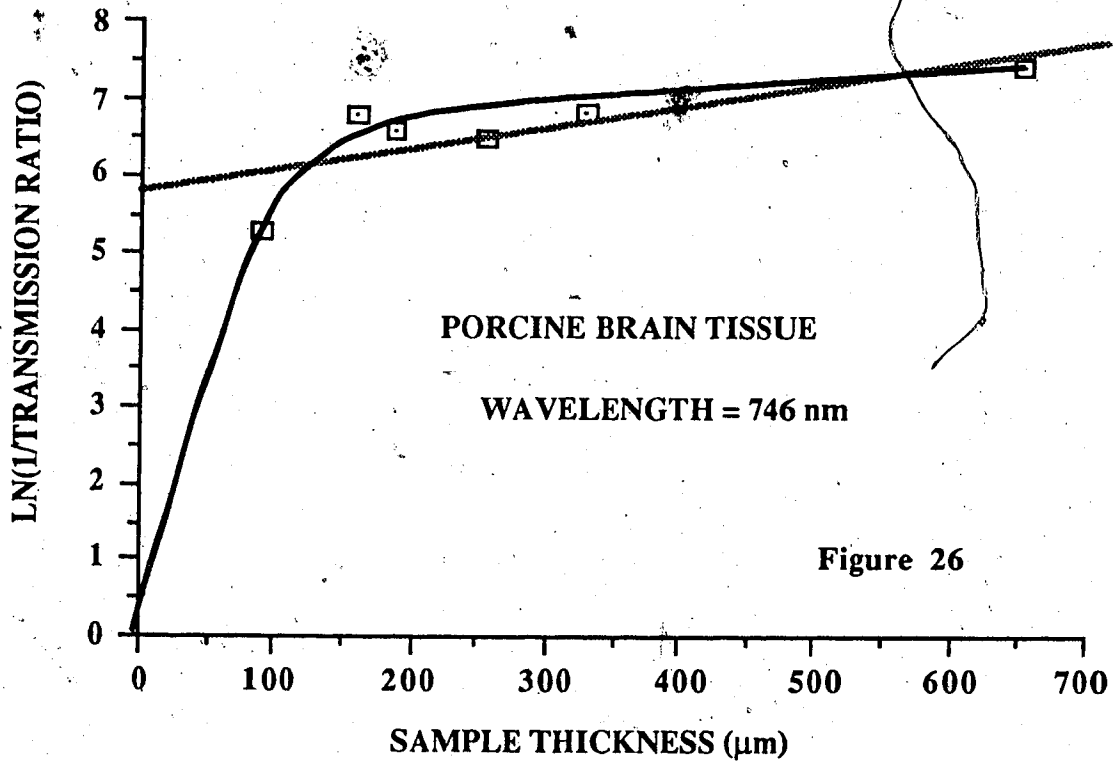
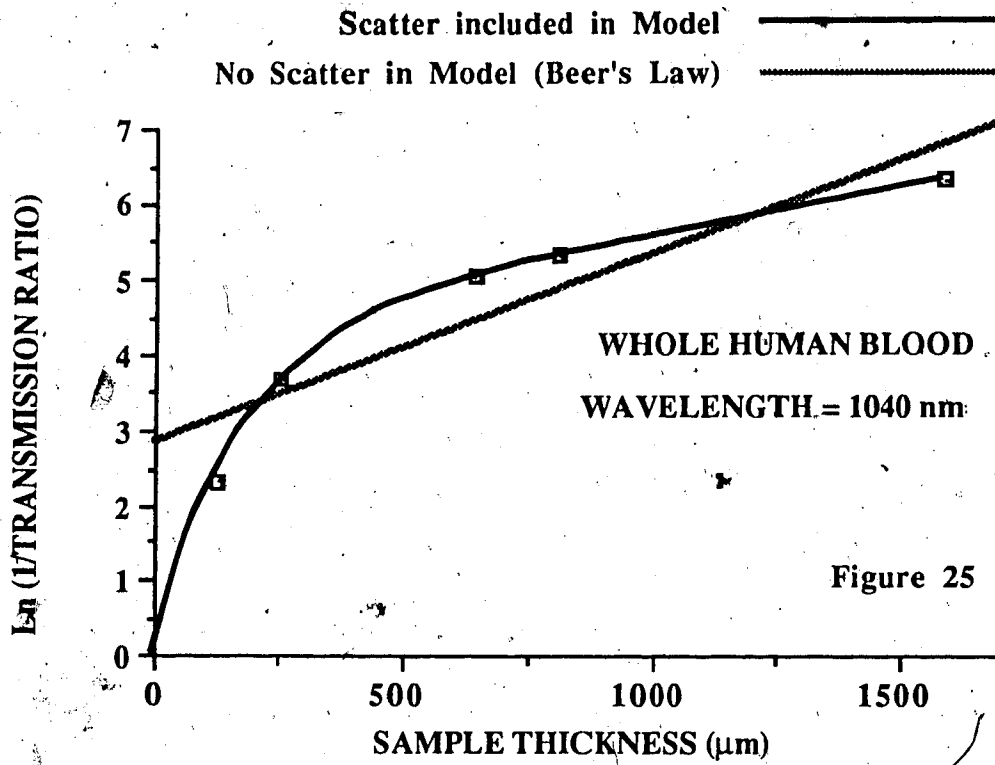
law to what seems to be a straight line graph (see figures 25 & 26). This approach should be viewed with scepticism in that the y-intercept does not pass through the expected zero.

This nonzero intercept of the straight line has two possible explanations. The first possibility is that the glass mounting system causes some systematic reflection of the primary beam. Examination of the data shown in figure 25 suggests that 90% of the signal is being lost by interactions other than the expected light tissue interaction. In the actual experimental procedure the data was corrected to account for reflection based on the transmission measured for a mounted sample of electrolyte solution. This was found to be $\approx 3\%$ for all wavelengths measured, well below that derived using the simple application of Beer's Law.

Stephen Flock in his paper (Flock (1987)) dealing with a similar experiment attributes the higher apparent reflection to the use of 'solid' tissue samples. In these cases he speculates that there would be poor optical coupling at glass-tissue interfaces of the sample holder resulting in much higher reflection than what would be anticipated from a glass-fluid interface. He supports his argument by pointing out that when he uses mounted fluid samples such as an aqueous solution of polystyrene microspheres the resulting plots of $\ln(1/T)$ vs sample thickness display straight line with the intercept going through the origin. When this idea is applied to the data of this experiment there is an apparent contradiction in that the whole blood data (a fluid sample) shows a nonzero intercept in spite of what would be considered good optical coupling.

At this point it should be noted that Flock's fluid samples are made such a way that the mean free path in the fluids are much larger than sample thicknesses involved. The microsphere solution was made so that the mean free path was approximately a millimeter, much larger than the sample thicknesses involved. With the mean free path so large the scatter component of the transmitted beam would be small in comparison to the primary component and Beer's law would be applicable.

Ln (1/TRANSMISSION RATIO) vs SAMPLE THICKNESS



Flock makes use of this condition for optically thin samples by diluting the blood sample to 1 part in 100 to arrive at a mean free path of 344 μm . Experimental results obtained by Zdrojkowski (1969) and Pedersen (1976) indicate mean free paths of 500 μm and 710 μm respectively. If one performs a simple 'back of the envelope' calculation assuming that the mean free path is inversely related to the concentration then the mean free path of whole blood is smaller than 10 μm . This value is much smaller than the sample thickness encountered in either Flock's or this experiment.

This evidence gives credibility to the second possible reason for the non-zero intercept, that being that the application of Beer's law is faulty from the start. A more probable reason for the non-zero intercept is that the basic premise, that the post-sample collimation gets rid all scatter, fails and in fact the transmitted beam is made up of a combination of primary and scattered radiation.

From recent papers (Pedersen (1976), Wilksch (1984), Wilson (1986-2) and, Flock (1987)) it is readily apparent that the scatter phase function is extremely forward peaked. The most recent results obtained by Flock (1987) and Arnfield (personal communication) suggest that the mean cosine (g) for most healthy tissues is greater than 0.97. Adipose tissue is the exception to the rule with a mean cosine of 0.77 (Flock (1987)). Given this extreme degree of forward scattering there is a high probability that the angle of deflection of the scattered radiation will not be enough to move a photon out of the acceptance angle of detection defined by the post sample collimation (see figure 27). In analyzing the data from such a situation, the problem is to determine the relative effects of these two components in order to determine the primary transport coefficients.

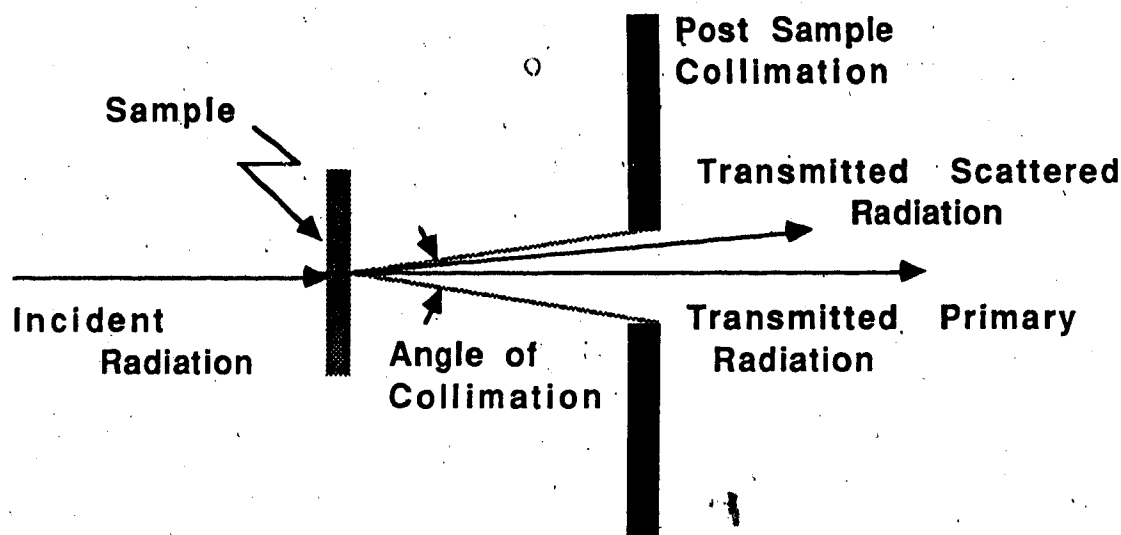


Figure 27

ZERO THICKNESS EXTRAPOLATION

The problem of forward scattered radiation interfering with the 'narrow' collimation reading of a scattered beam is one that until now has not been considered mathematically in the literature. In analyzing the experimental data for presentation (Crilly (Abs.) (1986)) it became clear that such scattered radiation was too big an effect to be ignored. In the absence of a mathematical model to analyze the data, an extrapolation was performed to find the mean free path ($\delta_0 = 1/\mu_0$) at zero tissue thickness. This is much the same procedure as that needed to arrive at "narrow beam" attenuation factors for higher energy medical radiation therapy. (Johns & Cunningham (1983) page 372)

This approach was simplified by transforming the dependent variable into what is called the 'apparent mean free path' (δ_a) such that;

$$\delta_a = \frac{x}{\ln(1/T)} \quad (13)$$

where δ_a is the apparent mean free path length

T is the transmission ratio

x is the sample thickness

The ensuing plot of apparent mean free path vs sample thickness is a nearly straight line as shown in figures 28 and 29.

Applying standard linear regression techniques gives rise to the empirical relationship;

$$\delta_a = \delta_o + f_s x \quad (14)$$

where δ_a is the apparent mean free path [μm]

δ_o is the real or actual mean free path [μm]

f_s is the 'scatter factor'

and x is the sample thickness in μm .

In this empirical relationship the scatter factor has little quantitative meaning as it is a function of the phase function, the collimation angle, and the situation's geometry. In a direct sense it can only be used as a gauge of the increase in the radiation component with depth and must be interpreted carefully in terms of the influencing parameters.

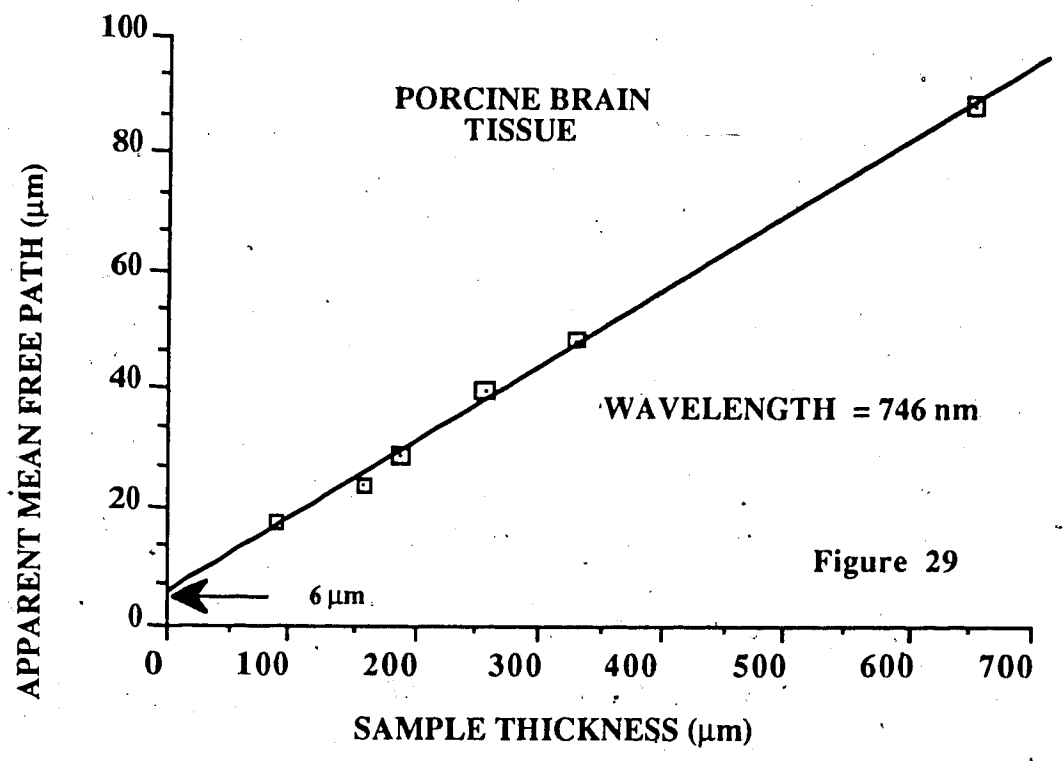
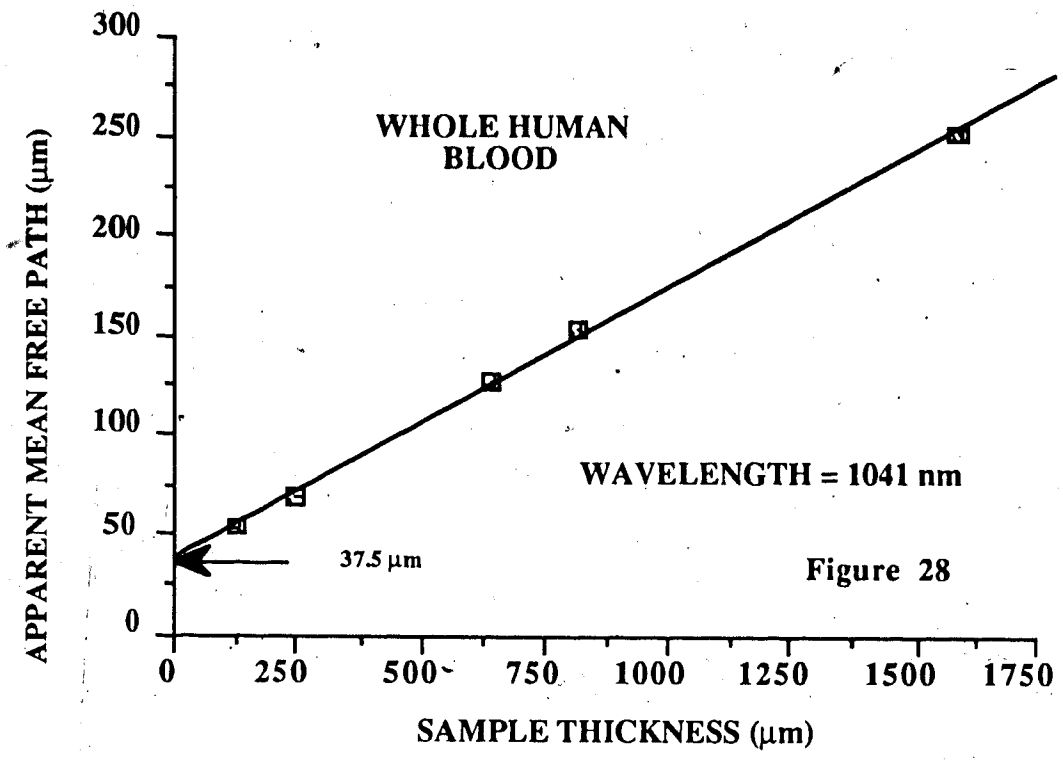
This form of analysis was done for a number of wavelengths to give a mean free path spectrum as shown in figure 30 for porcine brain. The error bars are the 80% confidence levels based on the assumption that the data varied about the straight line in a normal distribution.

The result of applying this analysis to a number of different tissues is shown in figure 31 and 32. It should be noted that for all tissue analyses the true correlation does not fall below 93%.

While this method of analysis does try to take the scatter component into account it has some serious problems in its formulation. As it is entirely empirical, it has no physical basis for its formulation, making quantitative physical interpretation of such things as the scatter factor impossible in a practical sense. The extrapolation assumes that the rate of change of the apparent mean free path is constant with depth for very thin tissue thicknesses of a few mean free path lengths. This situation in view of the complex mathematics that govern the development of the scatter component is highly unlikely. On

the basis of these observations the results of this technique should be viewed with scepticism, though the simplicity of the analysis does allow a means of quick analysis for qualitative comparisons of data.

APPARENT MEAN FREE PATH vs SAMPLE THICKNESS



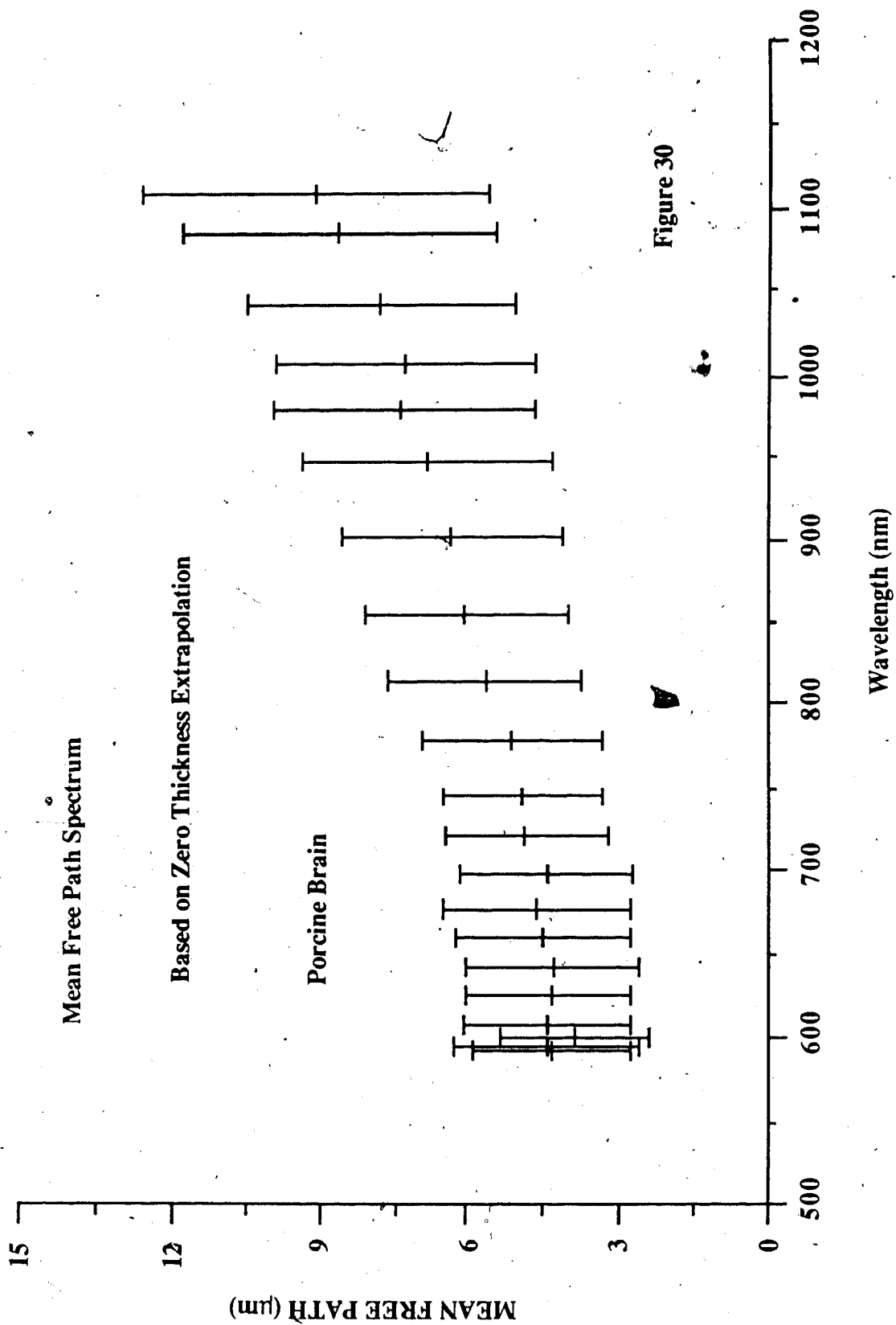


Figure 30

Mean Free Path vs Wavelength Based on Zero Thickness Extrapolation

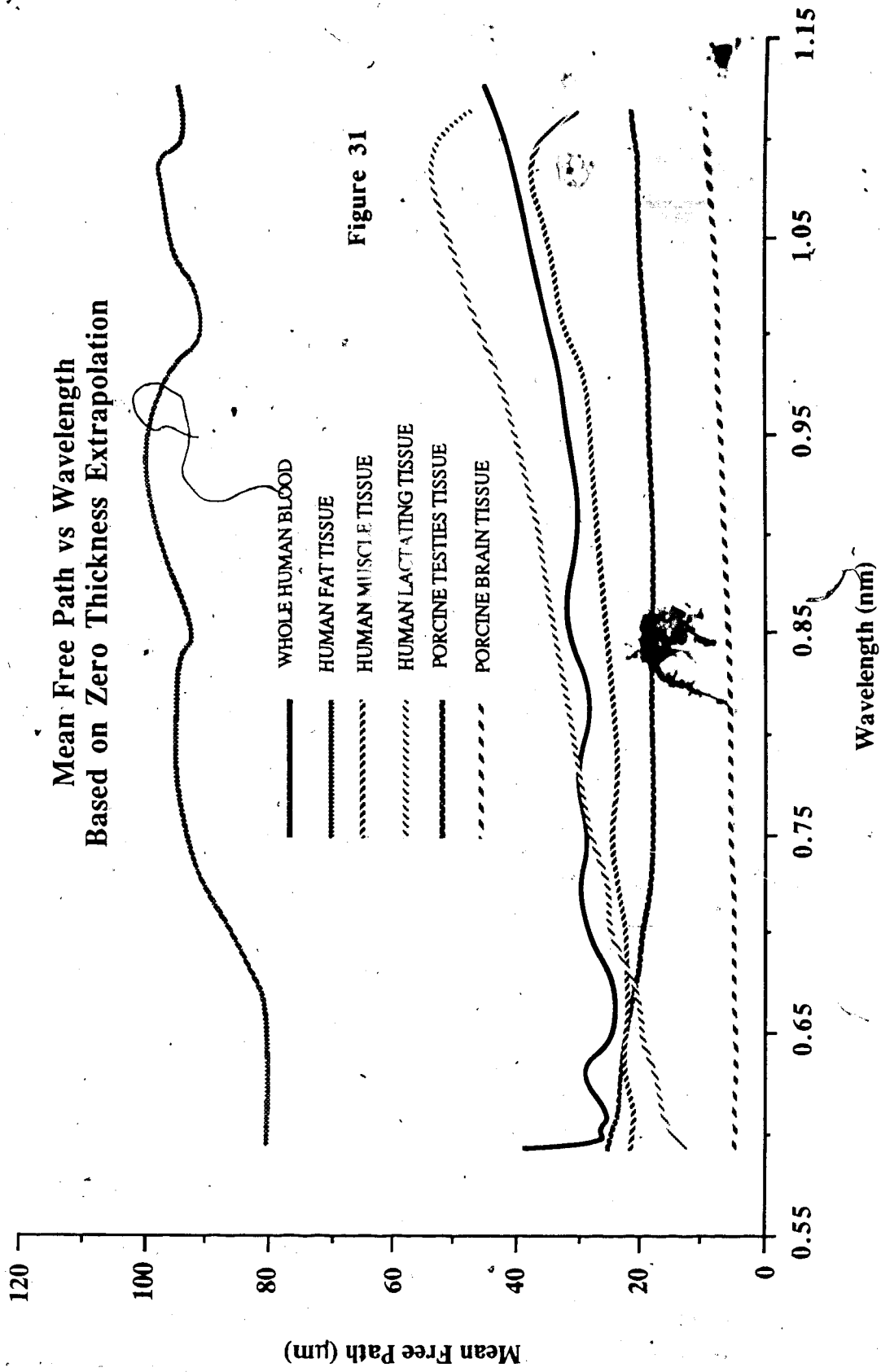


Figure 31

Scatter Factor vs Wavelength Based on Zero Thickness Extrapolation

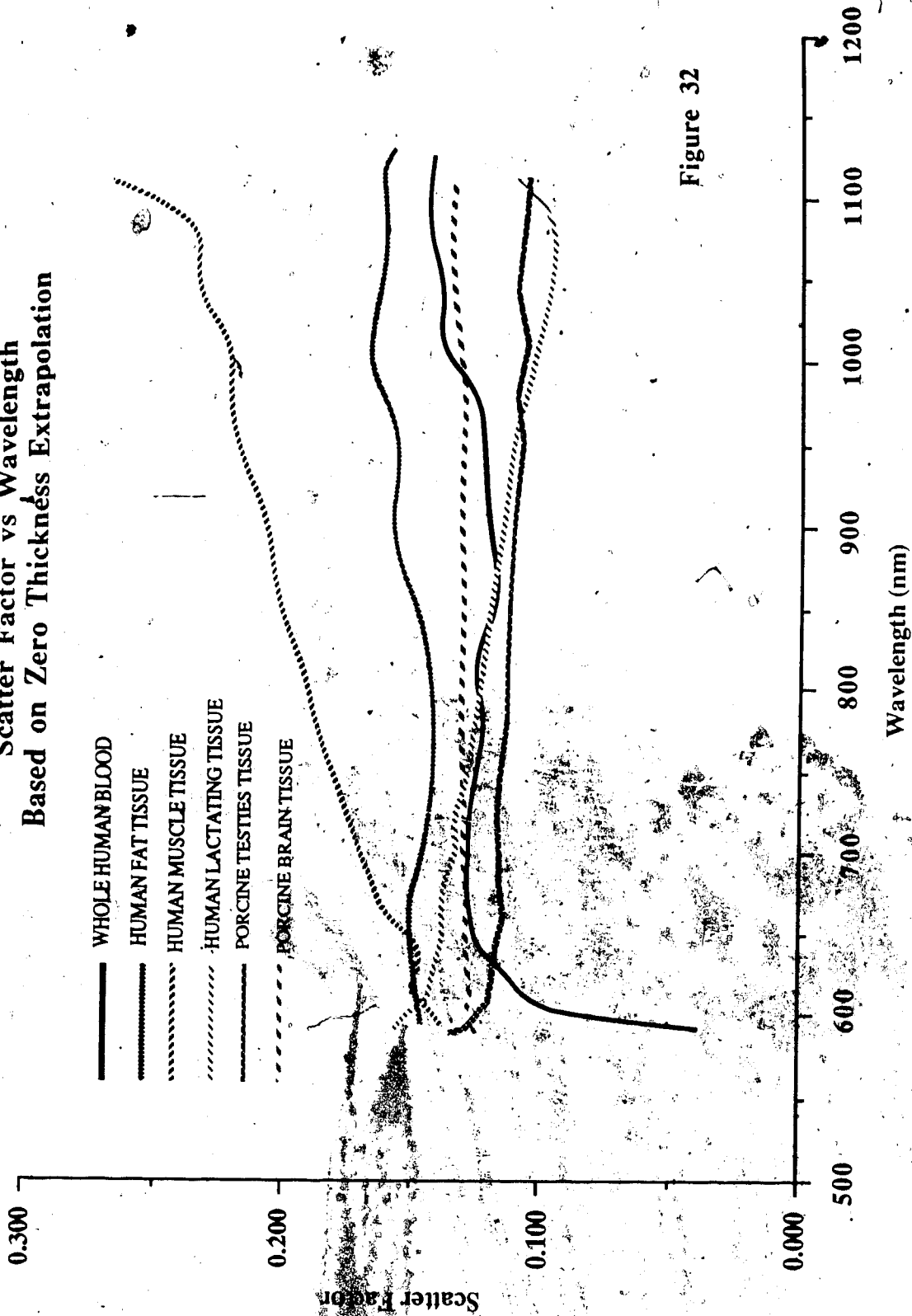


Figure 32

MATHEMATICAL MODEL : THEORY

While the empirical analysis allows some sort of an evaluation of the mean free path independent of scatter it does not allow any physical interpretation of the scatter effects. To alleviate this problem the following mathematical model was developed. In order to take multiple scatter into account scatter consider equation (10);

$$I(x) = I_0 e^{-\mu_0 x} + S(x)$$

where $S(x)$ is the component of intensity due to scatter. Instead of the usual means of defining $S(x)$ in terms of the various levels of scatter a modified form shall be developed which considers the scatter as radiation coming from a source in the tissue itself. From this point of view the scatter term becomes;

$$S(x) = \int_0^x S_0(x') e^{-\mu_{Scat}(x-x')} dx' \quad (15)$$

where $S_0(x)$ is the scatter source term and μ_{Scat} is the attenuation coefficient of the scattered radiation. The problem now is to derive the source term and the scatter attenuation coefficient.

Regarding the scatter attenuation coefficient (μ_{Scat}) it becomes necessary to define something called the scatter number. Consider the following diagram where the angle of collimation (θ_{Col}) is as shown.

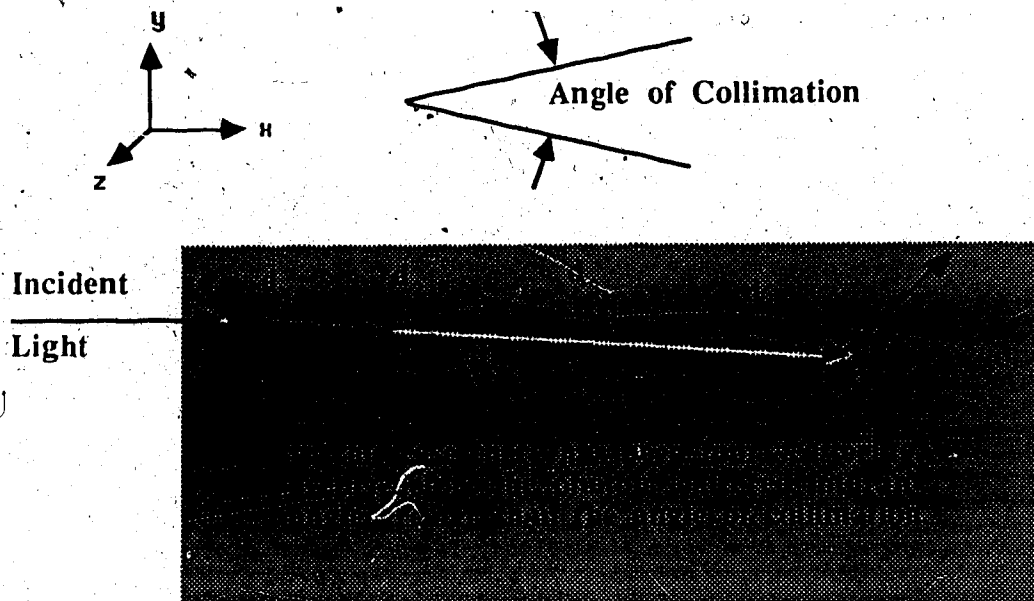


figure 33

If absorption is ignored for the moment and the dark arrows represent the distance between interactions, the total distance the photon covers before its angle of movement is too great to be picked up by the collimator detector system is;

$$d_{\text{Scat}} = \sum_{i=1}^n d_i \quad (16)$$

Now if the angle of collimation is very small the small angle approximation can be invoked to produce;

$$d_{\text{Scat}} \approx x_{\text{Scat}} = \sum_{i=1}^n x_i \quad (17)$$

where d_{Scat} is the distance the photon travels before its angle of direction is greater than half the angle of collimation

and x_i is the x-component of d_i .

In the real world of detectors and sources it is impossible to work with individual photons so the associated statistical analogies are brought into play. Thus the mean

distance a photon travels before it's angle of movement is outside the range of the detector (L_{scat}) is related to the mean free path between scattering events (δ_{Scat}) by:

$$L_{\text{scat}} = \sum_{i=1}^n \delta_{\text{Scat}} = n \delta_{\text{Scat}} = \frac{n}{\mu_s} \quad (18)$$

where n (here after referred as the scatter number) is the average number of scattering events required for the radiation to scatter out of the detector's range. The linear scattering coefficient for scattered radiation leaving the detectable beam is simply the inverse of L_{scat} . As the absorption coefficient is only dependent on pathlength and not the angle of collimation then the total attenuation coefficient for scattered radiation is ;

$$\mu_{\text{Scat}} = \mu_a + \frac{\mu_s}{n} \quad (19)$$

The source term for the scattered radiation can be considered as a line source with a varying intensity given by;

$$S_o(x) = I_o \mu_o \phi_{\text{Col}} e^{-\mu_o x} \quad (20)$$

Where ϕ_{Col} , the forward scatter source function, is that portion of first scattered radiation that remains within the detectable beam such that;

$$\phi_{\text{Col}} = \frac{1}{4\pi} \int_{\theta_{\text{Col}}} S(\hat{\Omega}') d\hat{\Omega}' \quad (21)$$

which has a possible range between 0 and 1.

Performing the integration over the line source results in an equation for the scatter component of the transmission of;

$$S(x) = \frac{I_o \phi_{\text{Col}}}{(n-1)} e^{-\mu_{\text{Scat}} x} \left\{ 1 - e^{-(\mu_o - \mu_{\text{Scat}})x} \right\} \quad (22)$$

If the primary beam is now added to this the transmission ratio can be shown to be;

$$T(x) = \frac{(n-1-\phi_{\text{Col}})}{(n-1)} e^{-\mu_o x} + \frac{\phi_{\text{Col}}}{(n-1)} e^{-\mu_{\text{Scat}} x} \quad (23)$$

It should be noted that this solution presupposes that any radiation leaving the angle of collimation is lost to the experiment. This approximation is valid only if the incident beam is collimated and the sample thickness is much thinner than that required for diffusion zone effects to come into play. In effect this is just an extension of Beer's law where $n=1$.

Work done by Arnfield (unpublished data) involved measuring the ratio of forward to backward scattered radiation at various distances from a collimated light source embedded in tissue. The distance between the end of the source and the point where the ratio is one is considered transition zone. For the tissue examined (R3327-AT rat tumor) the transition zone was found to be 1-2 cm in length. Given the order of magnitude of this value and the fact that the samples are fractions of a millimeter thick, the assumption that reintroduced scattered radiation is negligible can be considered valid.

MATHEMATICAL MODEL : ANALYSIS

While the model presented is from the theoretician's view more accurate it does present a problem when applied to the experimental data involved. The model unfortunately uses four separate coefficients instead of the one as was originally planned for in the application of Beer's Law. Given that there are only five to seven data points this leaves only one to three degrees of freedom for any numerical fit of the equation. In the worst case this would be like defining a slope with only two points, possible, but the associated experimental error could render the results useless. In view of these circumstances it was decided to apply the equation at the other end of extreme from Beer's Law where all first scattered radiation is assumed to stay in the transmitted beam (i.e. $\phi_{Col} = 1$). This would allow a comparison with other work analyzed in the traditional way using Beer's law (Flock (1987)). This should give some idea of the range of values the coefficients of interest should lie in for future work.

The data was analyzed using χ^2 reduction procedures as described in Bevington (1969) to find the scattering coefficient, the absorption coefficient and the scatter number.

The experimental error bars were calculated to the 68% confidence level using the procedure outlined by Rogers (1975). Checks were done to evaluate the local linearity of the fitted parameters with respect to χ^2 with excellent results.

Absorption Coefficient

From other works (Wilson (1986)) it is known that the absorption component of the attenuation coefficient is much smaller than the scatter component. Given the extremely thin tissue samples used in this study it might be expected that the process of absorption plays too small a role to be accurately measured in the experimental procedure. The values derived from the numerical fitting of the experimental results reflected this expectation in all cases except for blood and adipose tissue. The absorption coefficients derived are too small and the error bars too large to reach any real conclusions other than $\mu_a \ll \mu_s$.

The analysis of adipose tissue absorption suggests a significant amount of absorption at a consistent value of about $0.0075 / \mu\text{m}$ for all wavelengths tested (see figure 34). The effect of reflection at the glass tissue boundary was removed from the raw data using measurements made with the sample holder containing only electrolyte balanced solution. This increase in absorption coefficient may be attributable to a slight change in the amount of reflection at the tissue glass interface as the makeup of adipose tissue is mainly lipids instead of solution used to test reflection.

Whole blood showed an increase in absorption in the red part of the spectrum and a small amount of structure at longer wavelengths. This sort of curve was expected as hemoglobin is one of the dominant absorbing compounds at these wavelengths. (see figure 35)

Scatter Coefficient

In the majority of tissues examined the scatter coefficient appears to drop with increasing wavelength. The exception to the rule is once again adipose tissue which seems to have a nearly constant value for all wavelengths.

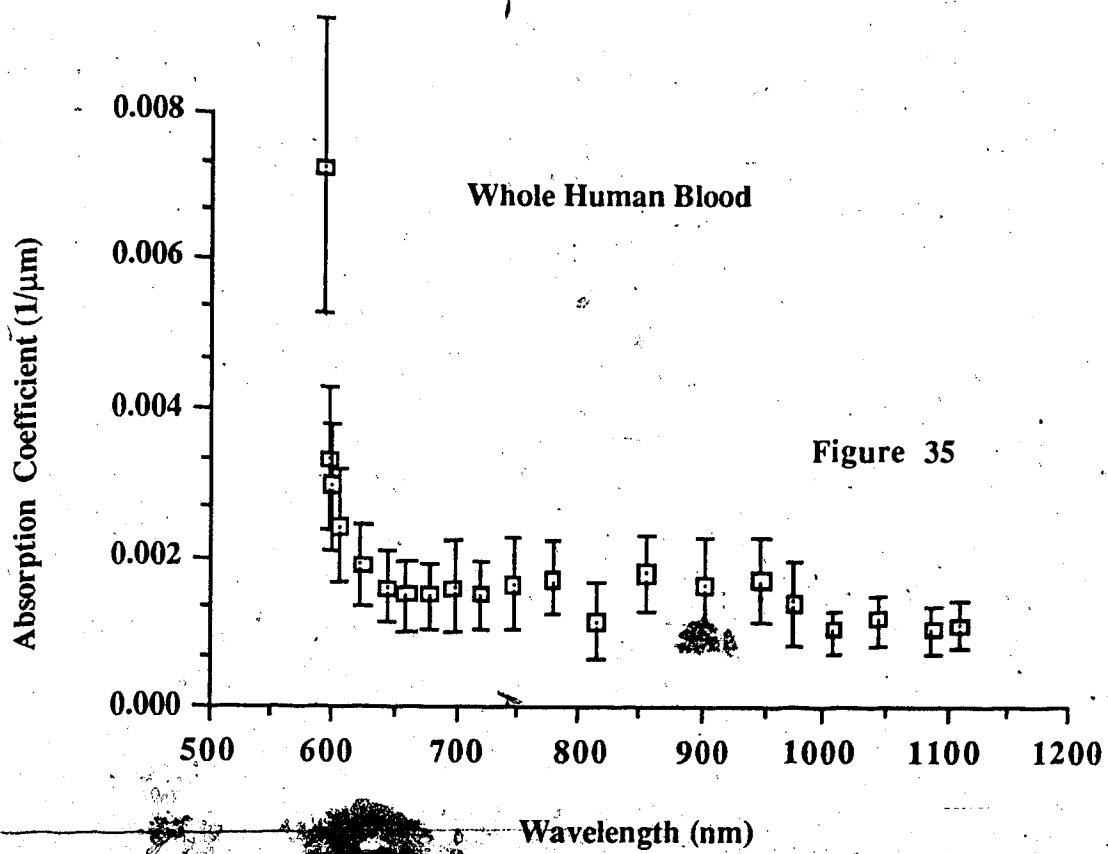
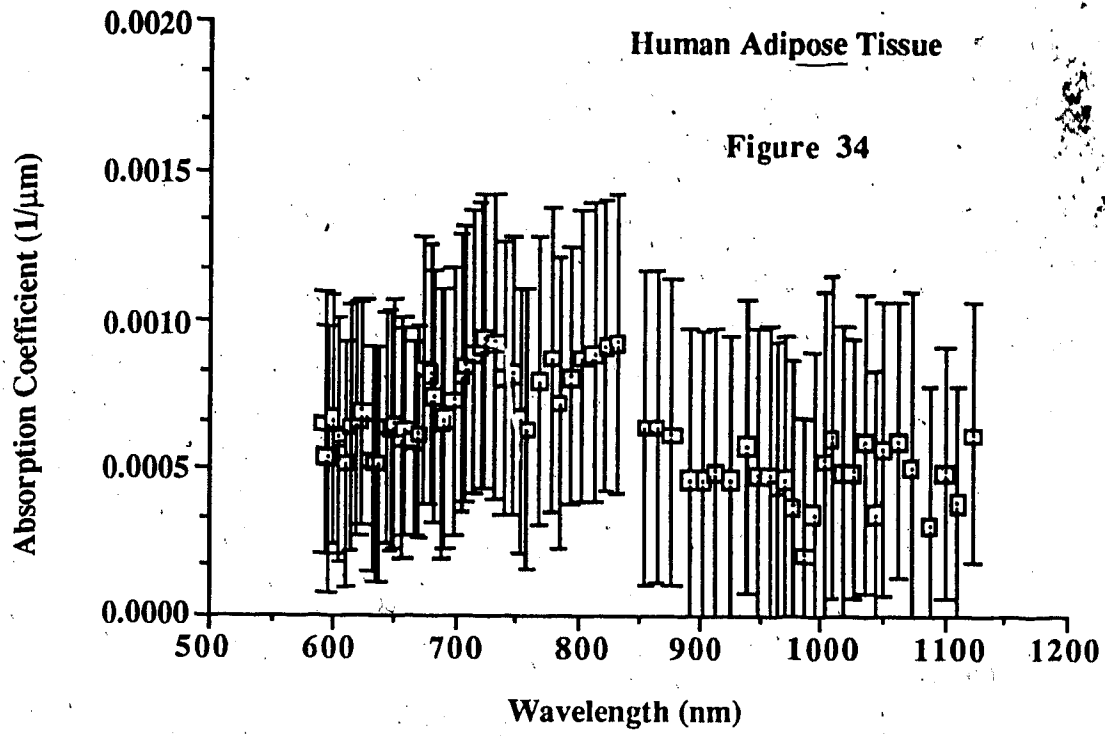
Blood is the only tissue tested that shows possibility of structure in the scatter spectrum in the range from 0.7 to 1.0 μm . Whether this is related to the problems of keeping the blood agitated during the experiment or is a real phenomena would require further testing.

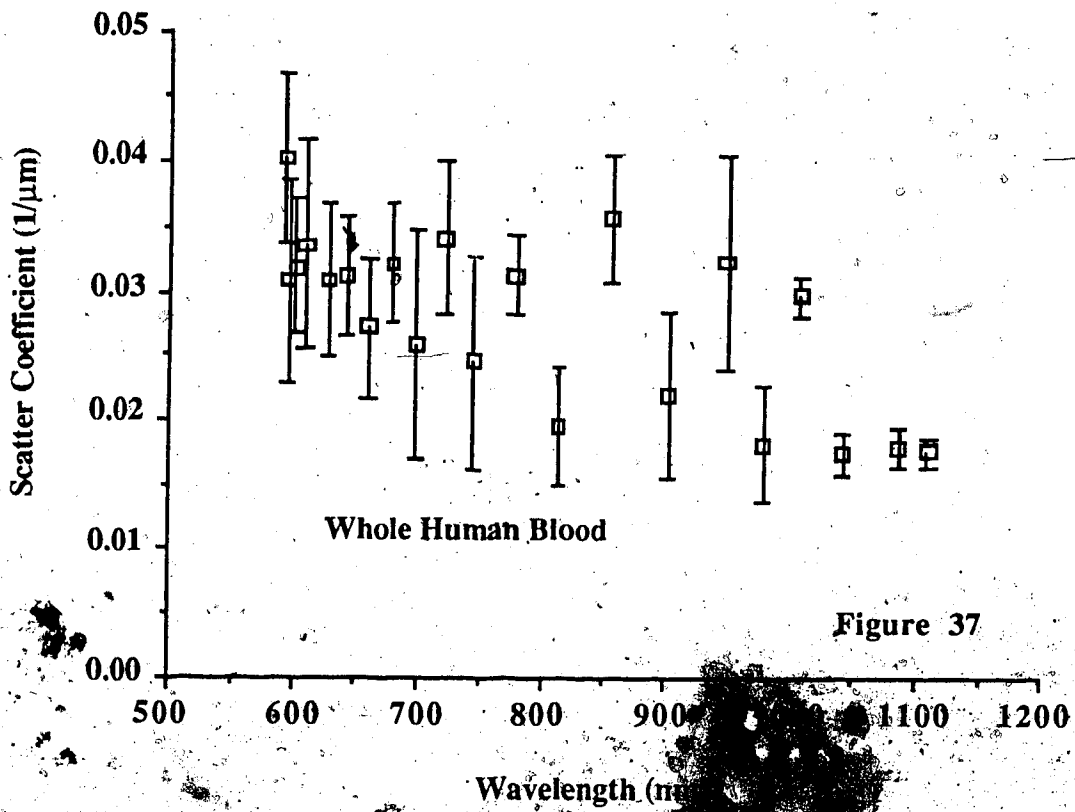
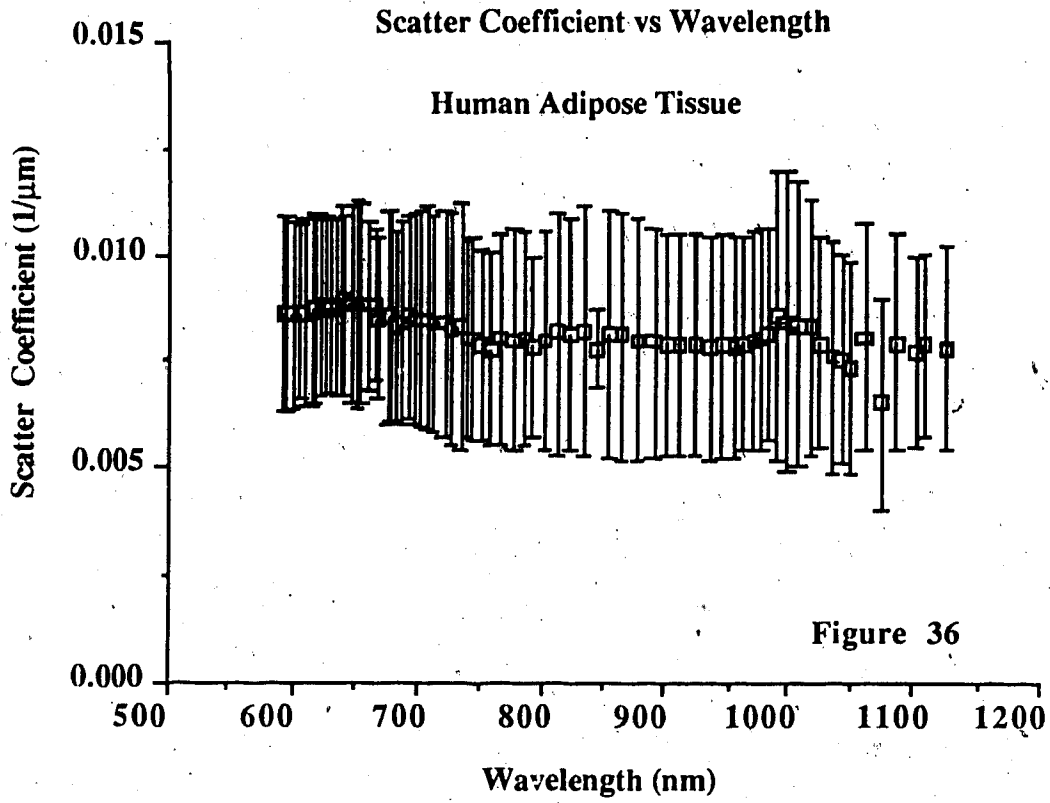
Scatter Number

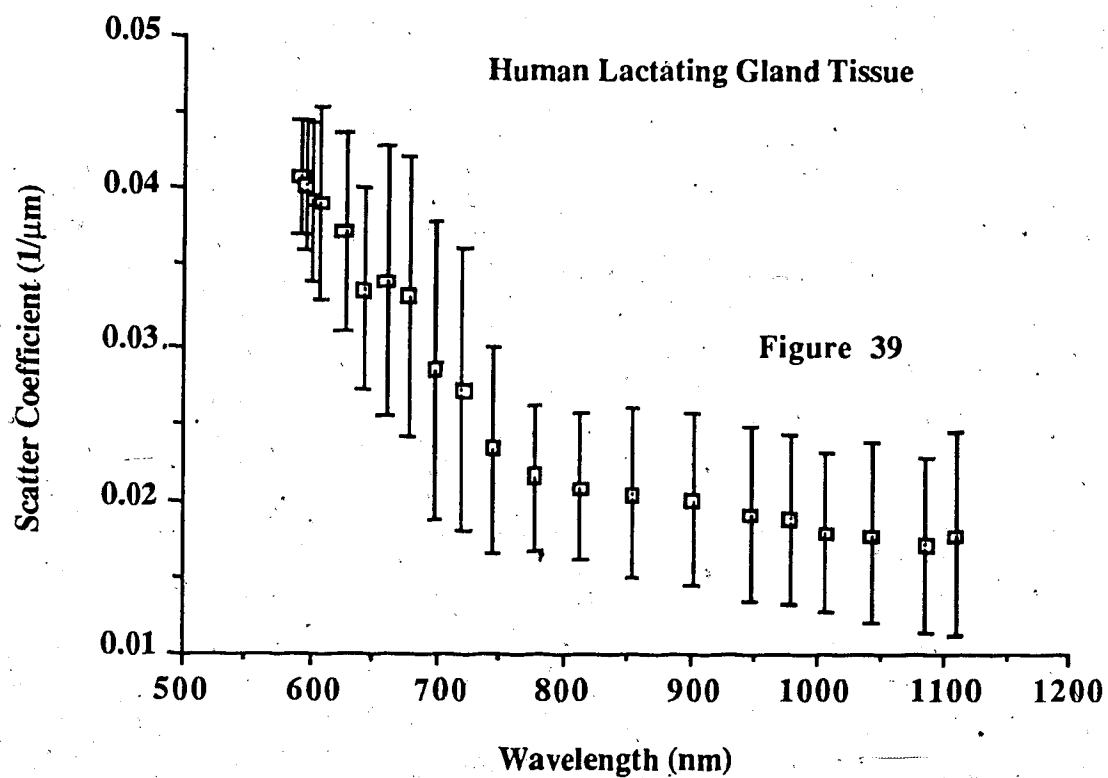
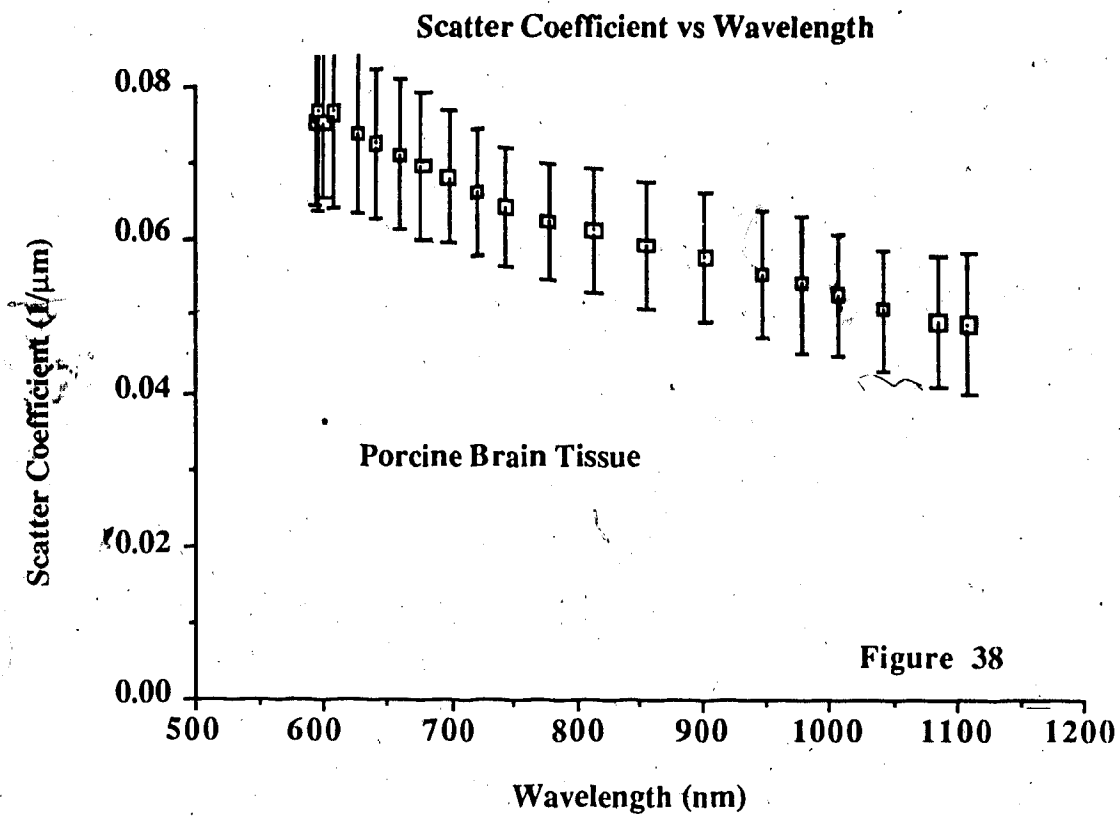
The scatter number doesn't offer any real value from the point of view of providing a reproducible value on which to base differently constructed experiments. The only reasonable interpretation that could be made is that the higher the scatter number the higher the value of the associated mean cosine (g) at that wavelength.

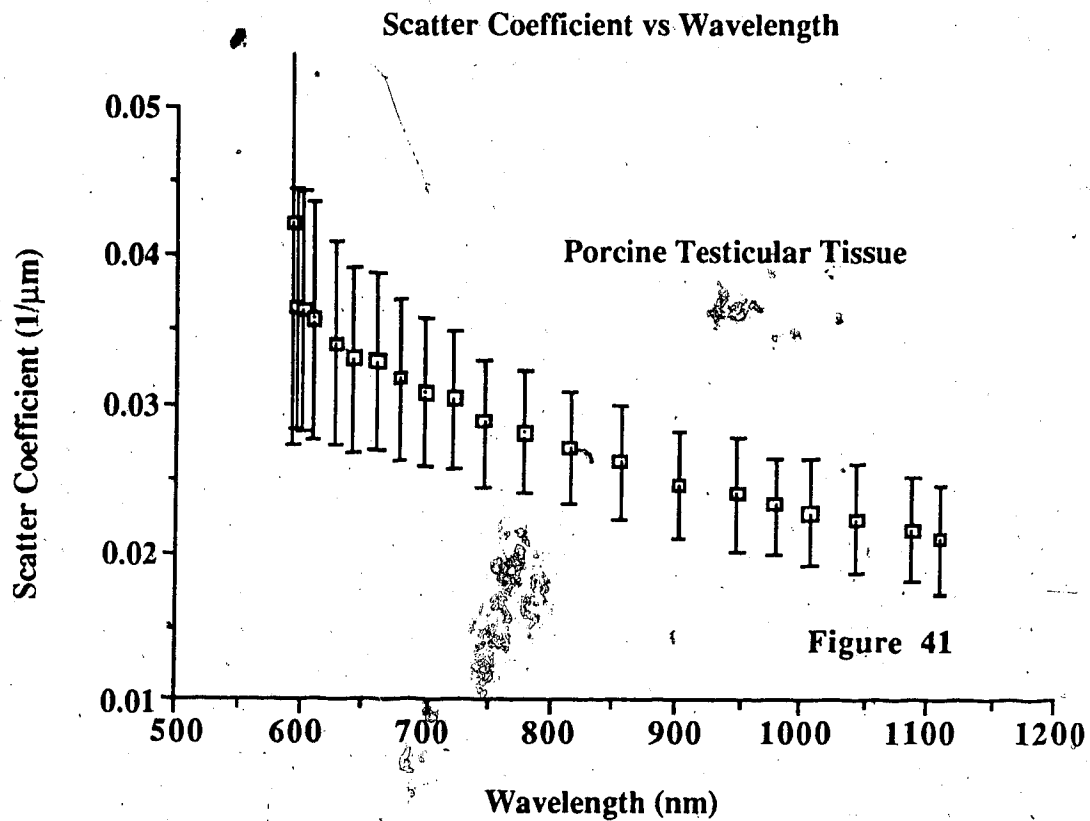
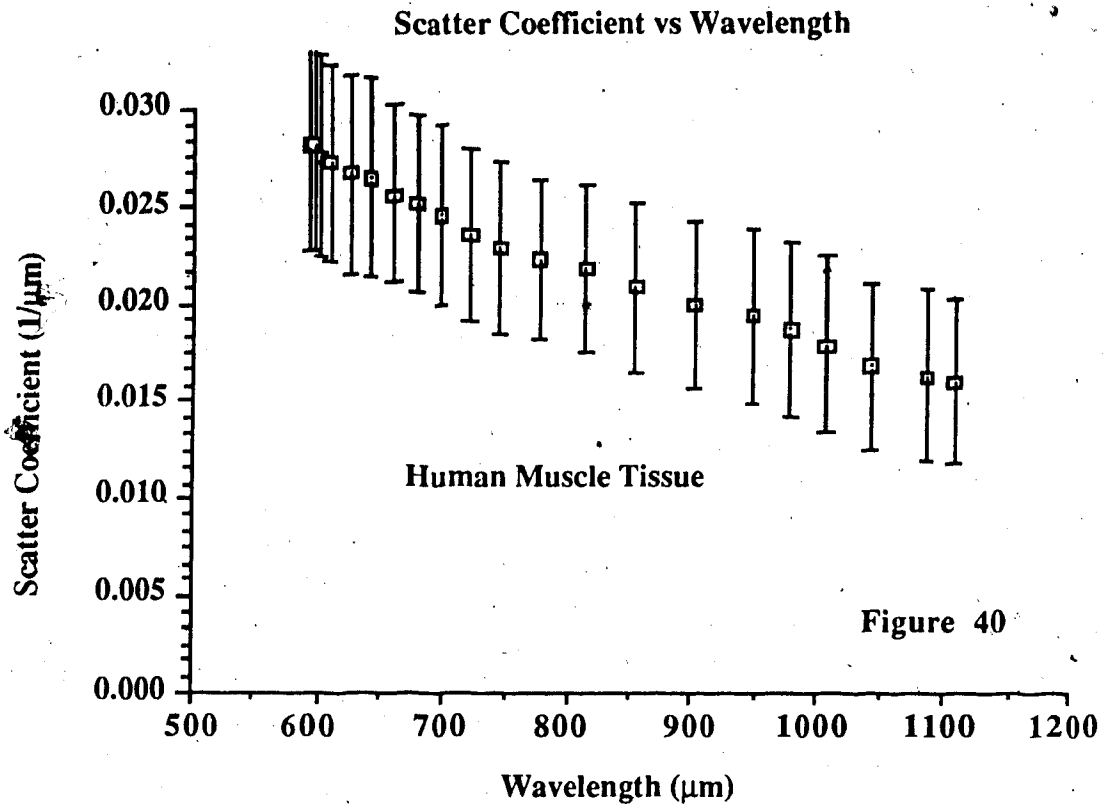
Adipose tissue remains constant for all wavelengths while all other tissues suggest a drop in scatter number with increasing wavelength. Lactating gland tissue shows an increase in scatter number with wavelength but the associated error bars are too large to consider this a valid observation.

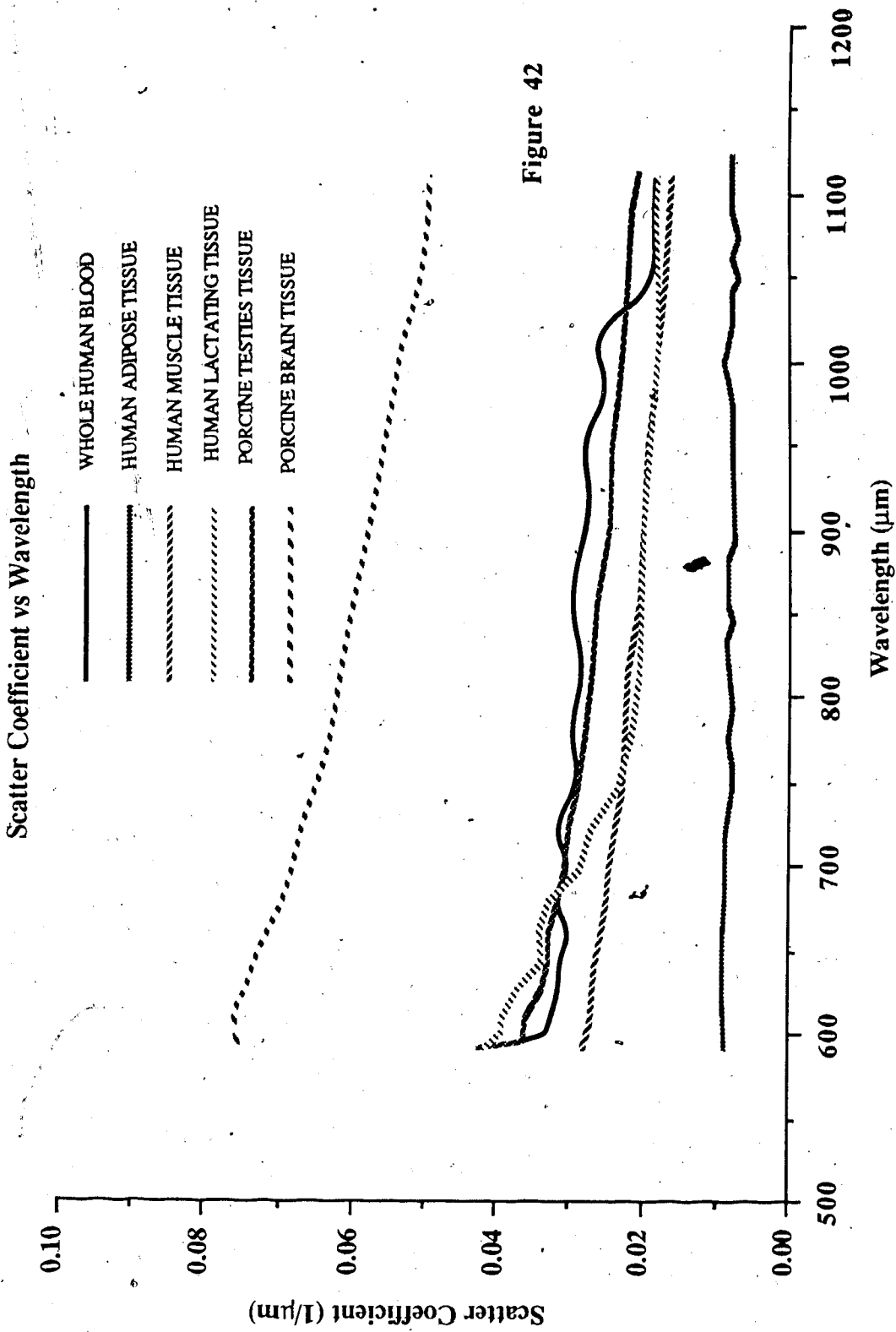
Absorption Coefficient vs Wavelength



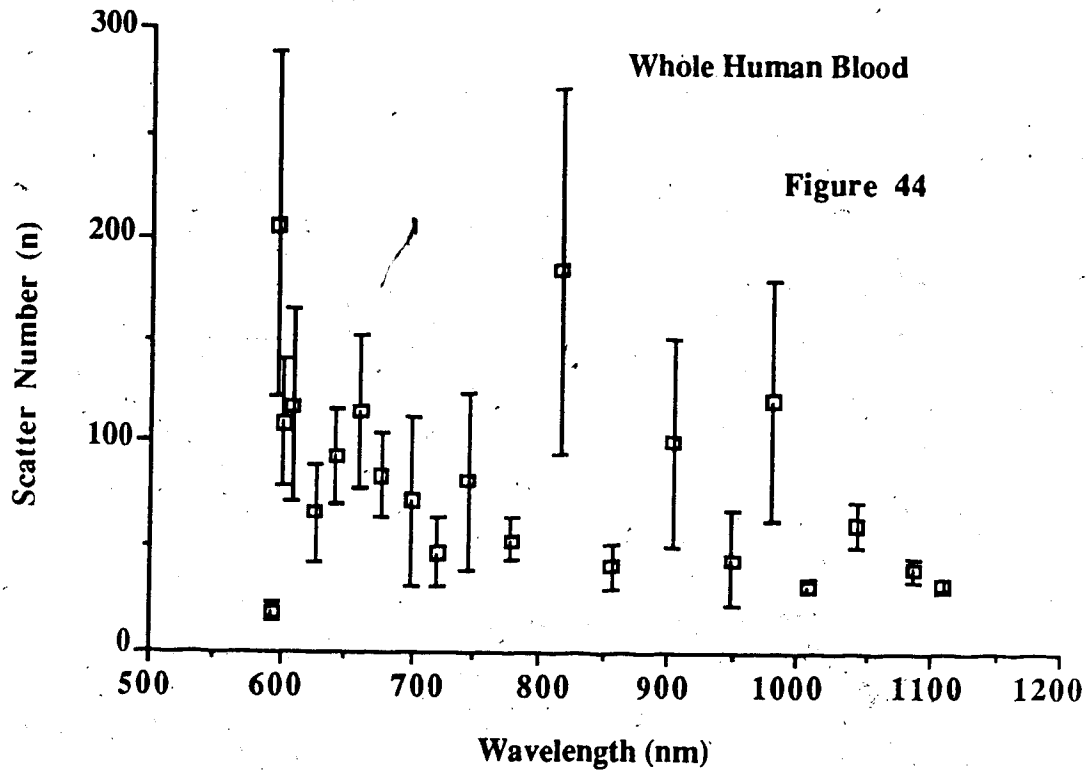
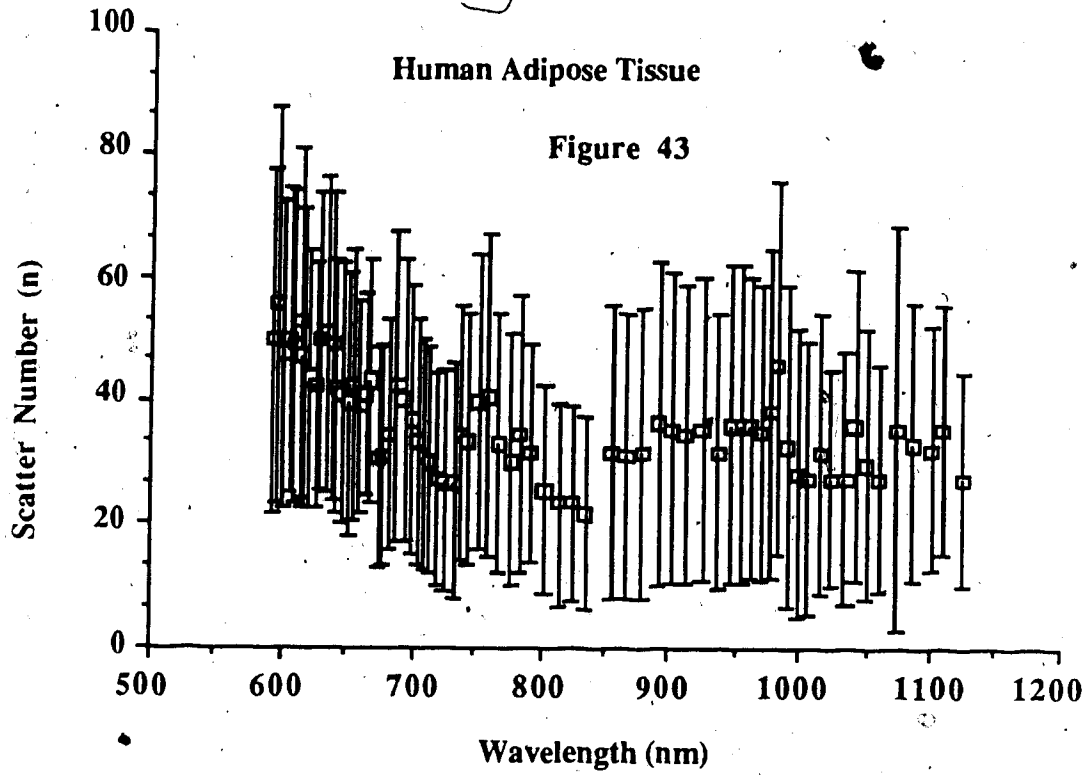


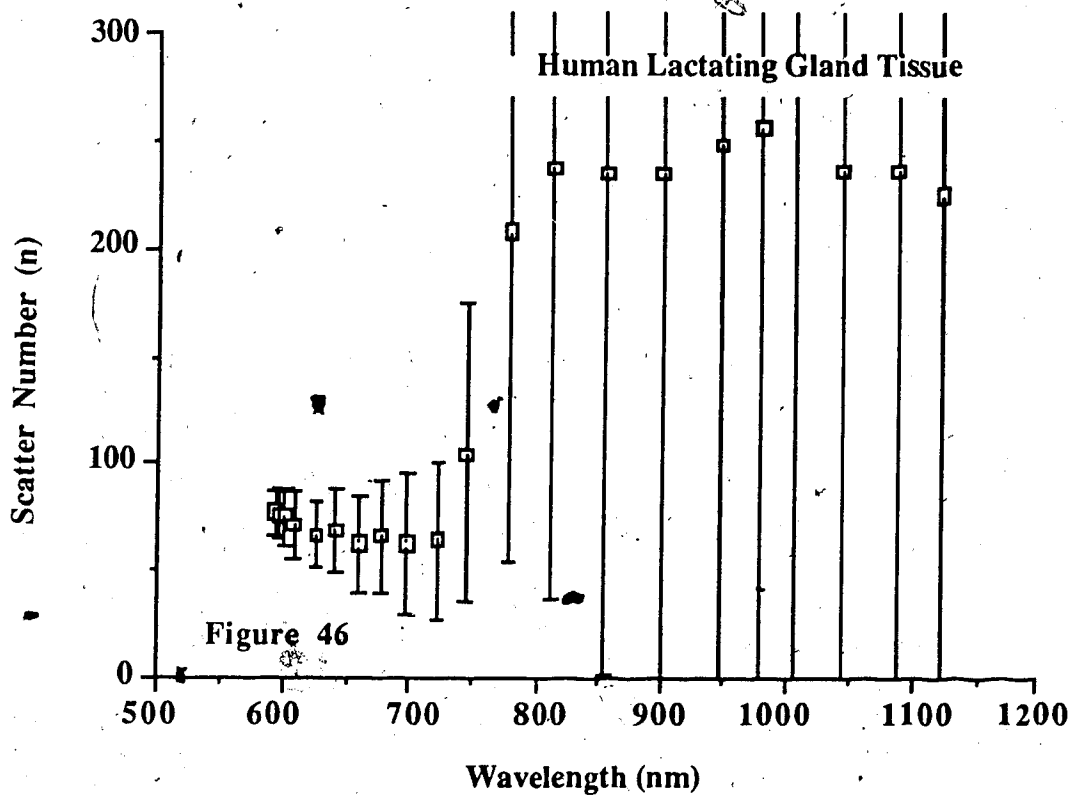
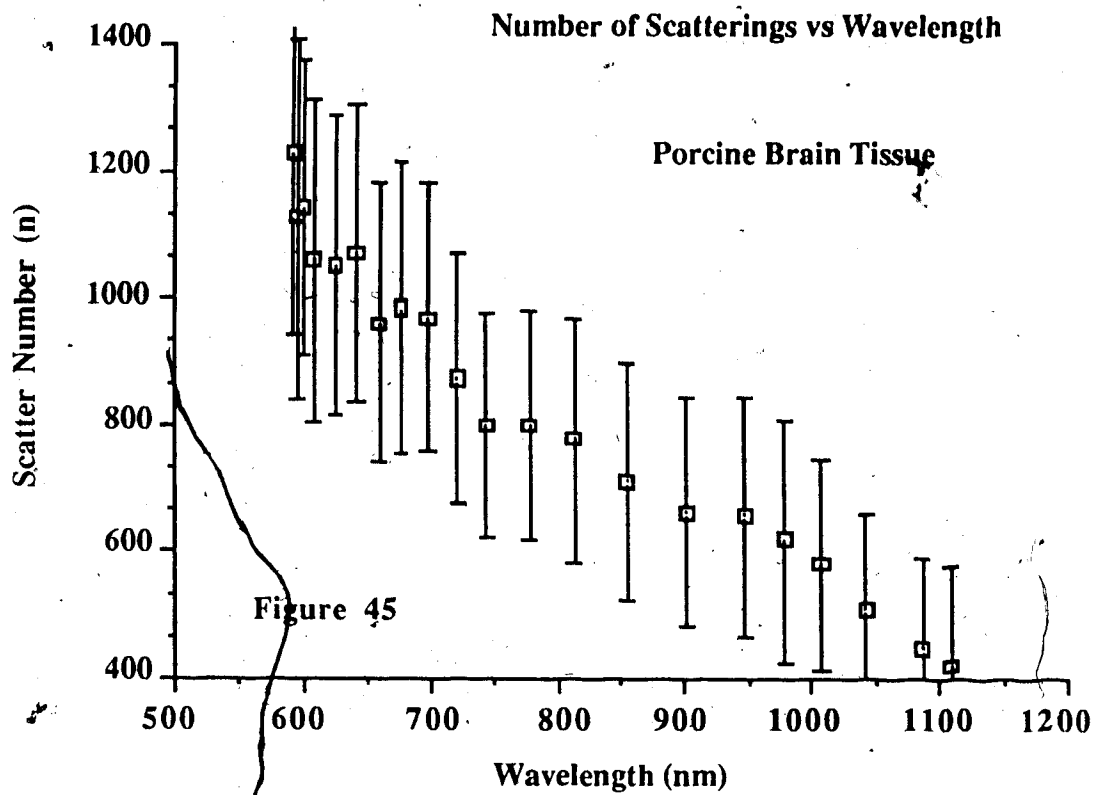


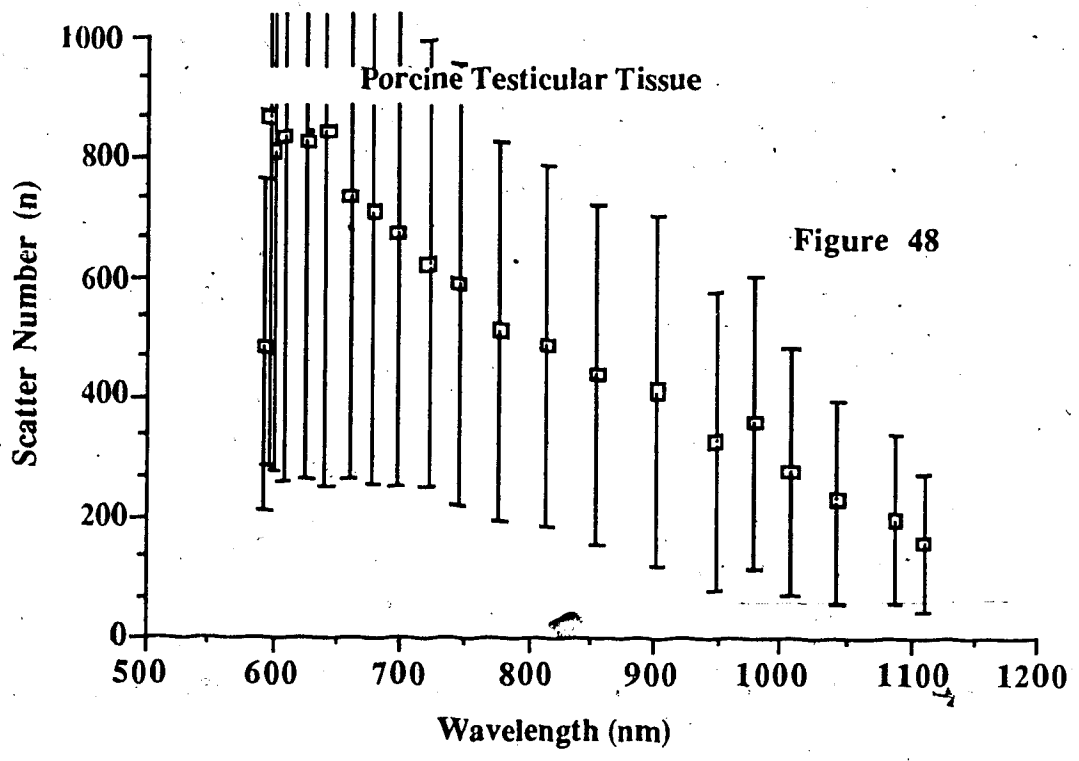
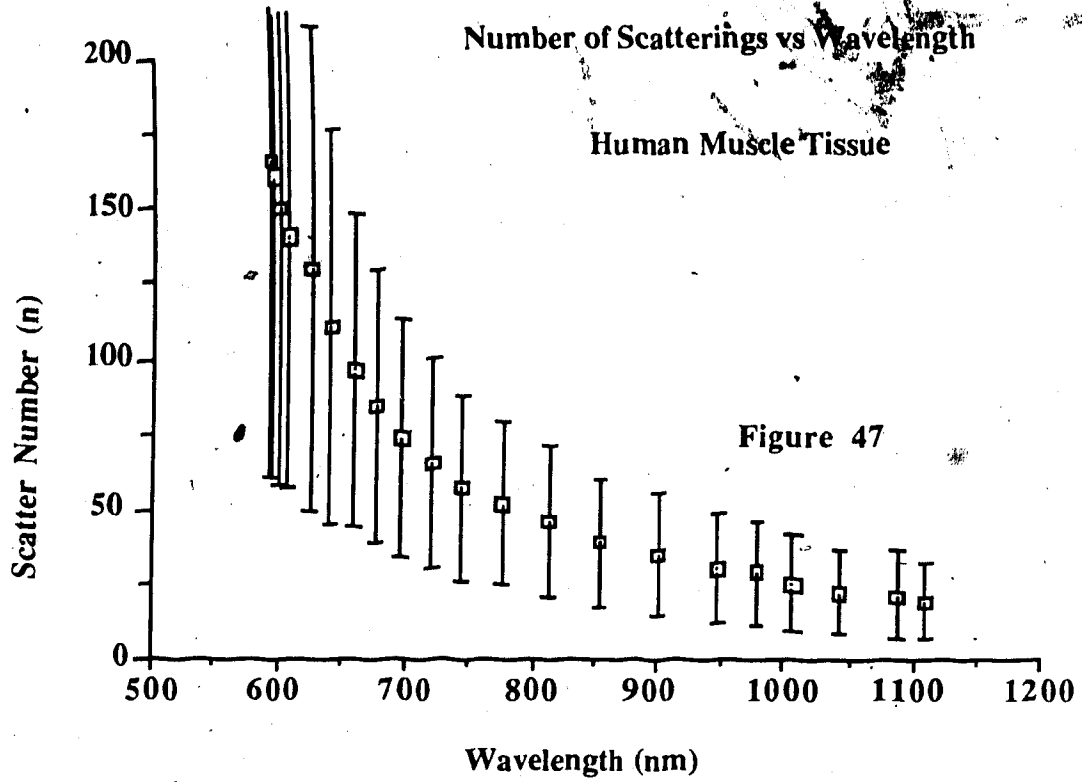




Number of Scatterings vs Wavelength







Scatter Number vs Wavelength

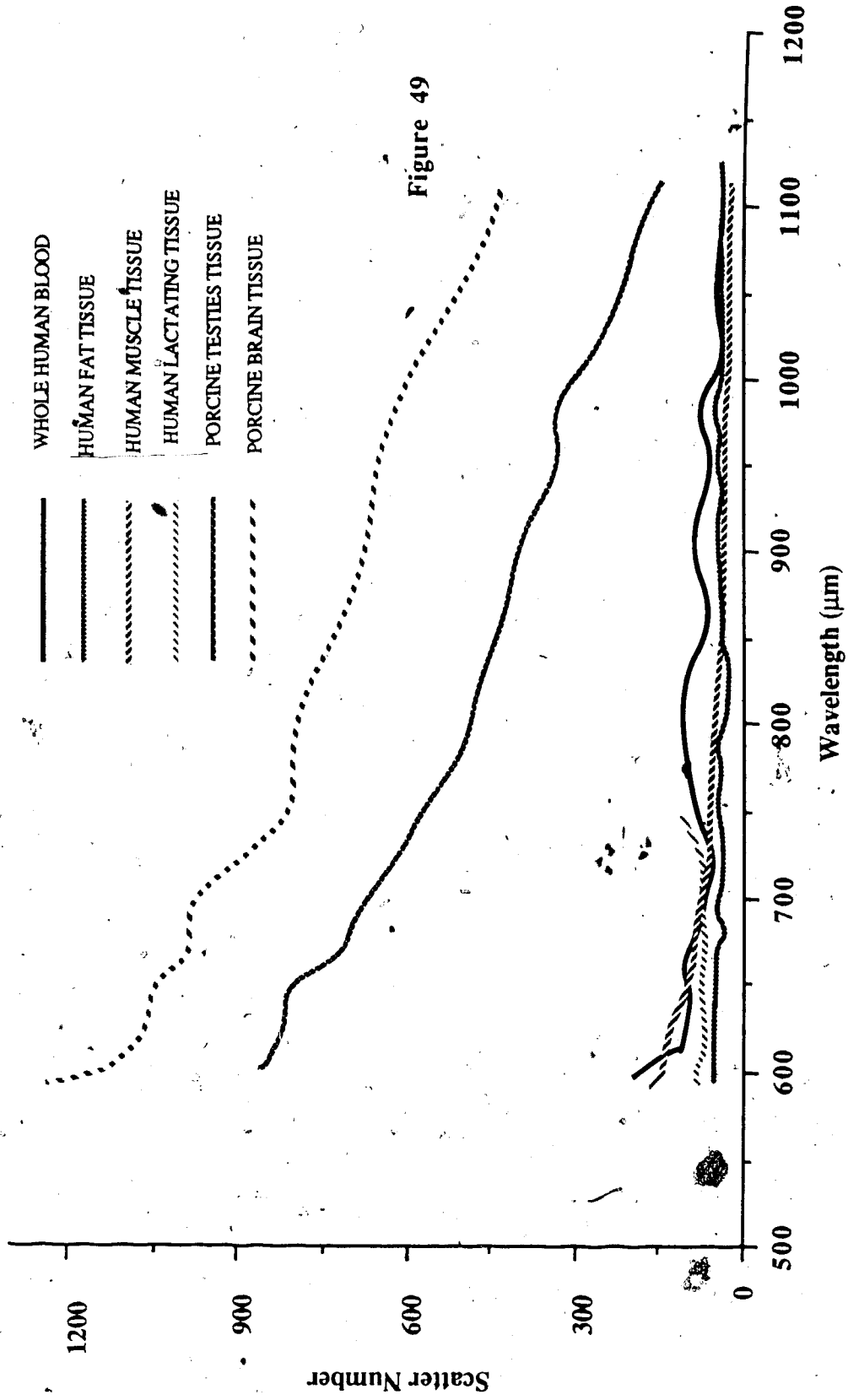


Figure 49

CHAPTER FIVE CONCLUSIONS

EXPERIMENTAL OBSERVATIONS

In the course of performing the transmission experiment it was found that the optical properties of the tissue samples varied greatly depending on the specimen and mounting procedure. As this variation overshadowed the structure of the transmission vs sample thickness relationship as defined by equation 23, a number of constraints were imposed to minimize this. The necessity of these constraints gives evidence not only of the variation in optical properties from specimen to specimen but show the dependence of the optics on tissue structure and temperature.

The rules that must be followed in order that self consistent results are to be achieved are:

- 1) All samples of a particular tissue type must be from the same specimen. The structural properties of a particular tissue can vary greatly depending on the contributor's age, health and fitness.
- 2) Freezing of the samples should be done to minimize the formation and size of ice crystals. Large crystals disrupt the tissue cells and thus change it's optical nature.
- 3) Spacers must be used to define the sample's thickness. Surface tension from the fluids involved in mounting the sample will pull the glass slides together changing the actual thickness spreading the tissue fiber.
- 4) The optical properties of tissues are temperature dependent. The samples must be kept at a common temperature during testing.
- 5) Blood has a tendency to settle out and must be agitated during testing.
- 6) The tissue must be examined microscopically before being used to assure that it is optically intact. The tissue also must not be torn or folded. There must be no air bubbles, blood stains or other foreign matter that may influence the results.

The specimen-dependence of the optical properties point out the limited value of very exact measurements of individual tissue samples. It may be a more suitable goal at

present to find the range of the coefficients for particular tissues in order that future applications and experiments could be knowingly conceived and designed. Though there potentially are medical applications that require a high degree of precision in a limited time, such as laser microsurgery, knowledge of the range of possibilities is paramount in developing the required quick measuring techniques.

Experimental Model

In reviewing the data from this work it was found that a straight line fit to a $\ln(1/T)$ vs sample thickness plot did not extrapolate to zero as predicted by Beer's Law. The probable cause of this was due to a significant amount of scattered radiation in the transmitted beam. In order to deal with this problem two methods were developed, one empirical in nature and the other of a more mathematical basis.

The first method, referred to as the zero thickness extrapolation used the 'apparent' mean free path (δ_a) as defined by;

$$\delta_a = \frac{x}{\ln(1/T)} \quad (13)$$

where δ_a is the apparent-mean free path length

T is the transmission ratio

x is the sample thickness

The result of fitting the apparent mean free path vs sample thickness with a straight line is an empirical equation;

$$\delta_a = \delta_o + f_s x \quad (14)$$

where δ_a is the apparent mean-free path [μm]

δ_o is the real or actual mean free path [μm]

f_s is the 'scatter factor'

and x is the sample thickness in μm .

Being empirical this equation offers little for direct quantitative physical interpretation. The method does provide a simple means of analysis that does not require long computer time in complicated numerical fitting methods. This potentially might be applicable as a 'quick' means of determining the optical properties of a particular tissue in a limited amount of time.

The extrapolation method does assume that the fractional buildup of scatter increases constantly in accordance to the empirical relationship (14). This assumption, while obviously false at thicknesses where diffusion conditions exist, appears to hold in thicknesses where light is still in the early transition region. Whether this linear relationship is still valid for very thin tissue thicknesses of a couple mean free path lengths is questionable and a point that should be explored before depending heavily on the method.

The mathematical method developed in chapter four gives a relationship for the transmission ratio of;

$$T(x) = \frac{(n-1-\phi_{Col})}{(n-1)} e^{-\mu_o x} + \frac{\phi_{Col}}{(n-1)} e^{-\mu_{Scat} x} \quad (23)$$

This relationship pivots on the small angle assumption that of the photons detected the component of photon motion perpendicular to the collimation axis is negligible compared to the parallel component. This assumption fails if the collimation angle is too large. The degree of failure and the associated error in measurement should be tested. This could be accomplished using a phantom of microspheres of a size and concentration that follow Mie scattering theory. This phantom design has been used extensively by Flock in his work and the preparation methods for developing the phantom can be found in his paper referenced in the bibliography.

Between five and seven data points were taken during experimentation for the extraction of one parameter, the attenuation coefficient, using Beer's law. It was found that this experiment, performed with an angle of collimation of 2.7° , gave results that showed evidence of a large component of scattered radiation in the transmitted beam. As Beer's law does not take this scatter into account the above model (equation 23) was developed which requires four separate variables to define the situation. The number of variables greatly decreases the statistical accuracy with which they can be numerically fitted to the data. In order to make use of this small number of points the forward scatter source function (ϕ_{Col}) was set to 1. This makes the assumption that all the first scatter is still in a direction that would be seen by the detector. This assumption allows the results of the analysis to provide an extreme benchmark to compare with those experiments based on Beer's law that presuppose no scatter in the transmitted beam.

Flock's work at 633 nm with a much narrower collimation angle of 0.17° based on Beer's law gives a mean free path of $14.5 \mu\text{m}$ which compares very favorably with the results of this experiment which measure the mean free path at $15 \mu\text{m}$. Unfortunately both experiments use assumptions which may prove inaccurate and decrease the reliability of the measurement. In using Beer's law Flock's analysis presupposes that no scatter exists in the transmitted beam, an assumption that may be contested by the size of the non-zero intercepts of his $\ln(I_0/I)$ vs sample thickness plots. The analysis used in this paper assumes that all the first scatter S_1 is in the transmitted beam. As no measurements have been made of extremely small angle scatter ($<2.5^\circ$) there is no way of discerning how poor the assumption of $\phi_{Col}=1$ is. Nonetheless, considering the presently accepted values for the mean cosine (g) the results should be viewed with this possible fallacy in mind. An important point to note is that in both cases if corrections were made to relax the assumptions the analysis would lead to even smaller values of the mean free path lengths.

In order to alleviate any doubt in the experimental results of either experiments it would be advantageous to repeat the experiment undertaken here for a couple of tissues at a

single wavelength with the aim of obtaining enough data points to fit all four theory related factors. Once the possible statistical error in the measurement of the coefficients has been established the constraints of sample preparation could be relaxed so that multiple specimens could be used to develop a given tissue's data base. The resulting statistical deviation of fitting this data would be interpreted as the range of possible values of the coefficients once the afore measured experimental error has been taken into account.

In the process of defining the 'real and actual' values of the transport coefficients there may be a tendency to forget the actual point of taking these measurements. In most cases all that is needed at this point is a reasonable idea as to their values so that better use can be made of existing medical techniques. In the case of photodynamic therapy light scattered a fraction of a degree could easily be considered part of the primary beam without affecting the effectiveness of the resulting mode. If this path is taken it should be noted carefully, so that potential methods that may be effected by such minute indiscrepancies (i.e. cellular imaging) do not rely blindly on measurements made with coarser needs in mind.

APPLICATION OF RESULTS

In spite of the possible error in the actual value of the measured coefficients the analysis does provide a means of comparing the relative values of various tissues at a number of wavelengths. The scatter number (n) can be considered as a constant that depends on the collimation involved in the experimental set up and on the degree of anisotropy in the scatter phase function. For any given collimation angle, the higher the scatter number (n), the larger the mean cosine (g). The values of the other coefficients can be interpreted in terms of their definition according to transport theory.

The tissues studied have increasing mean free path lengths and decreasing scatter numbers at longer wavelengths. As photodynamic therapy would be enhanced by deeper penetration of light, providing a suitable photoactivated drug is available, longer

wavelengths than those now in use would be desirable. While tissue related differences in the attenuation coefficient and scatter phase function diminish with longer wavelengths, no matter what wavelength is chosen for treatment, the presence of pockets of fat or brain-like tissue will greatly affect the treatment fields. Any situation where these tissues are involved must take into account their unique optical properties (see figure 50). Such a situation already exists in radiotherapy with inhomogeneity corrections for bone and lung tissue, but with a much simpler dependence on density and atomic number only.

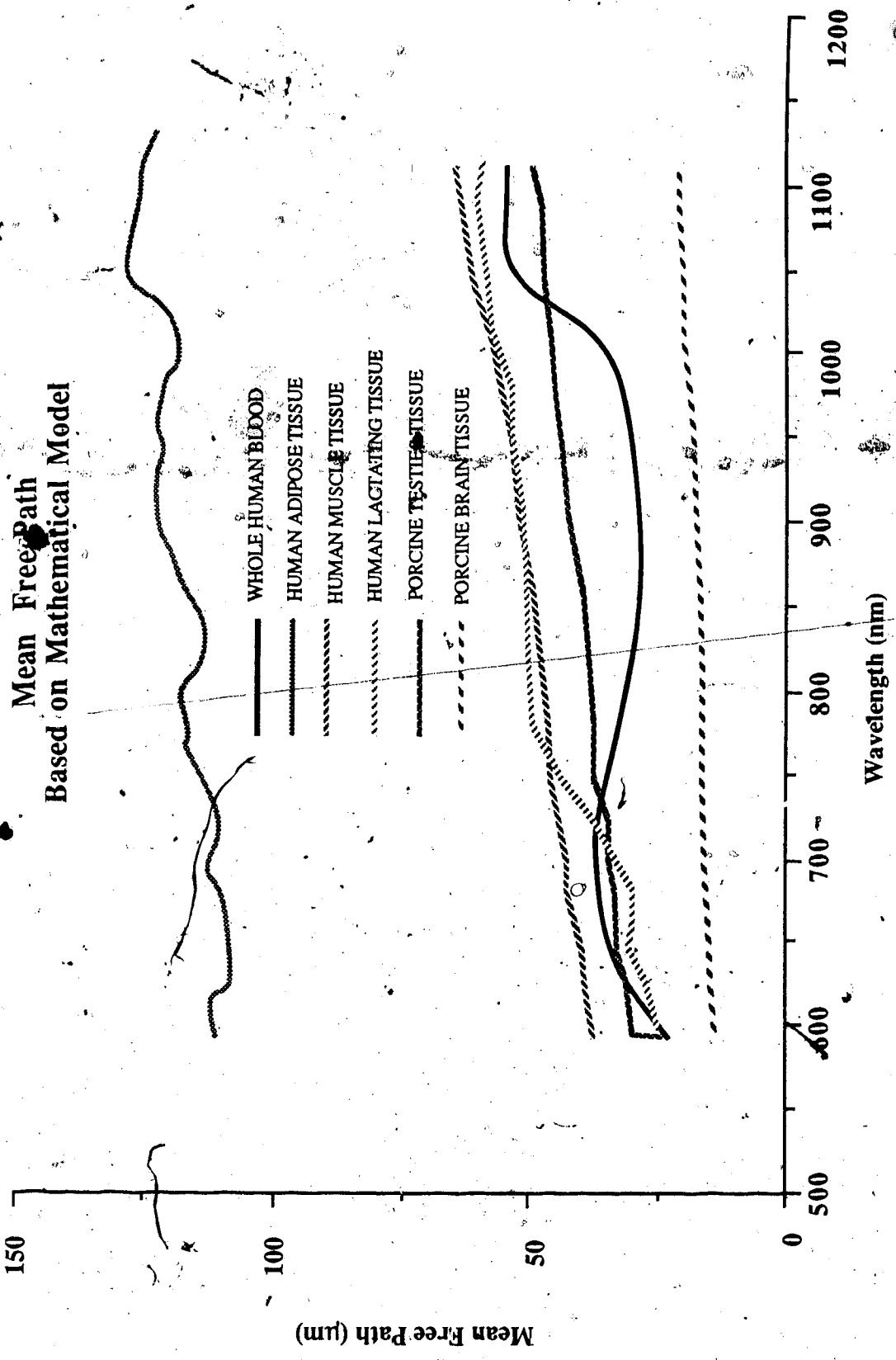
The mean free path seems to increase with increase in number of cell walls the beam must transverse. [198] supports this view with his observation that for the three cell types tested he found the extinction ($\ln(T)$) for a given concentration, is almost proportional to the cross-section area of each type of cell." If the cell walls are the optical elements in the interaction then one would expect the scatter to become more forward directed as the cells of the tissues become more extended and elongated. While this does seem to be obvious in extreme cases of cell structure such as brain and adipose tissues, cells with less discriminate variations such as muscle and testicular tissue do not appear to follow this rule rigidly. In these latter cases it could be that the intercellular structures are dense and large enough to have a significant influence on the scattering.

A comparison of the muscle spectrum with testes, lactating gland, skin etc. does not reveal any irregularities in the spectrum. This observation does not support the suggestion made by Jacka and Wilksh that the myofibrils in striated muscle act as diffraction gratings increasing the anisotropic nature of the scattering.

The presence of a large scatter component in the transmitted beam raises doubts that diaphanography will ever develop into a method capable of producing clear well defined images at depth. Images achieved using present methods appear to be due to the highly

anisotropic nature of the scattering events transferring the information of inhomogeneities to the surface via the extremely long transmission zone.

The size of the mean free path suggests that images could be made of objects on the order of a few cells thick. This sort of application requires a much more detailed study of the actual scattering mechanism than those presently done. Mathematical models such as the one developed in this work may benefit this situation but presently technical problems such



BIBLIOGRAPHY

- Anderson R.R., Optical radiation Transfer in the Human Skin and Applications in *in vivo* Remittance Spectroscopy, **J. Invest. Dermatol.**, 77:13, (1981)
- Bevington P.R., **Data Reduction and Error Analysis for the Physical Sciences**, McGraw-Hill Book Co., N.Y., (1969)
- Boulinois J., Photophysical Process in Recent Medical Laser Developments: A Review, **Lasers in Medical Science** 1#1:47, (1984)
- Bolin F.P. et al. A comparison of Spectral Transmittance for Several Mammalian Tissues: Effects at PRT Frequencies in: **PORPHYRIN LOCALIZATION AND TREATMENT OF TUMORS**, (1986), Edited by D.R. Doirin and C.J. Gomer, Alan R. Liss Inc., New York, p. 211-225
- Bruls W.A.G. and van der Leun J.C., Forward Scattering Properties of Human Epidermal Layers, **Photochem. and Photobio.**, 40#2:231, (1984)
- BIOMEDICAL LASER (THE)**, Edited by L. Goldman, Springer-Verlay, New York, (1981)
- Bustad L.K., McClellan R.O., and Burns M.P. (Ed.), **SWINE IN BIOMEDICAL RESEARCH**, Battella Memorial Institute Pacific-Northwest Laboratory, Richland Wash., (1966)
- Caster W., Breast Imaging: A Review Course, (1986), Meeting of the Canadian Assosiation of Radiologists in Halifax
- Case K.M. ,and Zweifel , **LINEAR TRANSPORT THEORY**, (1967), Addison-Westey Publishing Company
- Chandrasekhar S., **RADIATIVE TRANSPORT**, (1950), London: Oxford University Press

- Coltman J.W., Ebbighausen E.G., and Altar W., Physical Properties of Calcium Tungstate X-ray Screens, **Journal of Applied Physics**, **18**:530, (1947)
- Crilly R.J., A Study of the Optical Properties of Soft Tissues in the Near Infrared, **Medical Physics**, **13**:603, (Abstract), (1986)
- Cutter M., Transillumination as an Aid in the Diagnosis of Breast Lesions, **Surg.Gyne.and Obstet.**, **48**#6:721, (1929)
- Davison B., **NEUTRON TRANSPORT THEORY**, (1957), London: Oxford University Press
- Doiron D.R., Svaasand L.O. and Profio A.E., Light Dosimetry in Tissue: Application to Photoradiation Therapy in: **PORPHYRIN PHOTSENSITIZATION**, (1983), ed. Kessel D. and Dougherty T.J., Plenum Press, New York, pp 63-76
- Doiron D.R., Photophysics of and Instrumentation for Porphyrin Detection and Activation in: **PORPHYRIN LOCALIZATION AND TREATMENT OF TUMOURS**, (1984), ed. Doiron D.R. and Gomer C.J.A., (New York: Liss), pp 41-74
- Duderstadt J.J. and Martin W.R., **TRANSPORT THEORY**, (1979), John Wiley & Sons Inc.
- Eichler J., Knof J., and Lenz H., Measurements on the Depth of Penetration of Light (0.35-1.0 μm) in Tissue, **Rad. and Envio. Biophys.**, **14**:239, (1977)
- Ertefia S. and Profio, Spectral Transmission and Contrast in Breast Diaphanography, **Med. Phys.**, **12**#4:393, (1985)
- Fante R.F., Relationship between Radiative-Transport and Maxwell's Equations in Dielectric Media, **J.Opt.Soc.Am.**, **71**#4:460, (1981)
- Flock S.T., Wilson B.C., and Paterson M.S., Total Attenuation Coefficients and Scattering Phase Functions of Tissues and Phantom Materials at 633 Nanometers, **Medical Physics** (1987), Publication accepted and pending.

Fuller T.A., **The Physics of Surgical Lasers, Lasers in Surgery and Medicine**
1:5, (1980)

Hardy J.D., Hammel H.T. and Murgatroyd D., Spectral Transmittance and Reflectance of
Excised Human Skin, **Journal of Applied Physiology**, 9:257, (1956)

Hardy J.D. and, Muschenhein C., The Radiation of Heat from the Human Body, IV.
The Emission, Reflection and Transmission of Infra-red Radiation by the
Human Skin, **Journal of Clinical Investigation**, 13: 817, (1934)

Hecht E. & Zajac A., **OPTICS**, (1976), Addison - Westley Pub. Co., Reading Mass.

Hetzl F.W., Photodynamic Therapy SSIII(2), **Med. Phys.**, 13#4: 622, (1986)

Johnson C.C., Optical Diffusion in Blood, **IEEE Transactions on Bio-Medical
Engineering**, BME-17#2:129-133, (1970)

Katsuo Aizawa et al. A New Diagnostic System for Malignant Tumors using
Hematoporphyrin Derivative Laser Photoradiation and a Spectroscope
in: **PORPHYRIN LOCALIZATION AND TREATMENT OF
TUMORS**, (1984), Edited by D.R. Doirin and C.J. Gomer, Alan R.
Liss Inc., New York, pp. 227-238

Kiefhaber P. et al., Endoscopical Control of Massive GI Hemorrhage by Irradiation
with a High-Powered Neodymium Yag Laser, **Prog. Surg.**, 15:144, (1977)

Kubelka P., New Contributions to the Optics of Intensely Light Scattering Materials :
Part I, **J. of the Opt. Soc. of Amer.**, 38#5:448, (1948)

Kubelka P., New Contributions to the Optics of Intensely Light Scattering Materials .
Part II: Nonhomogeneous Layers, **J. of the Opt. Soc. of Amer.**,
44#4:330, (1954)

Longini R.L. A Note on the Theory of Backscattering of Light by Living Tissue,
IEEE Transactions on Bio-Medical Engineering, BME-15#1,
(1968)

LASER APPLICATIONS IN MEDICINE AND BIOLOGY, Edited by

M.L. Wolbarsht, Plenum Press, New York, (1971)

Lasers in Medicine, **Health Devices (ECRI)**, June (1984), **13** #8:151

Muller P.J. and Wilson B.C., An Update on the Penetration Depth of 630 nm Light in

Normal and Malignant Brain Tissue in vivo (Preliminary Communication),

Phys. Med. & Bio., **31**#11:1295, (1986)

Norris K.H. and Butler W.L., Techniques for Obtaining Absorption Spectra on Intact

Biological Samples, **IRE Transactions on Bio-Medical Electronics**,

p153,(1961)

Pedersen G.D., McCormick N.J., and Reynolds L.O., Transport Calculations for Light

Scattering in Blood, **Biophysical Journal**, **16**:199, (1976)

Polyani T.G., Physics of the Surgical Laser, **International Advances in Surgical**

Oncology, **1**: 205-215, (1978)

Preuss L.E., Bolin F.P., and Cain B.W., A Comment on Spectral Transmittance in

Mammalian Muscle, **Photochemistry and Photobiology**, **37** #1:113, (1982)

Profio A.E. and J. Sarnaik, Fluorescence of HpD for Tumour Detection and Dosimetry in

Photoradiation Therapy in: **PORPHYRIN LOCALIZATION AND**

TREATMENT OF TUMORS, (1984), Edited by D.R. Doirin and

C.J. Gomer, Alan R. Liss Inc., New York, pp. 163-175

Profio A.E. and Doiron D.R., Dosimetry Considerations in Phototherapy, **Med. Phys.**,

8 #2:190, (1981)

Marynissen J.P.A. and Star W.M., Phantom Measurements for Light Dosimetry using

Isotropic and Small Aperture Detectors in: **PORPHYRIN LOCALIZATION**

AND TREATMENT OF TUMORS, 1984

Edited by D.R. Doirin and C.J. Gomer, Alan R.

New York, pp. 133-148

- McPhee M.S. et al., Surgical Lasers: Machines in Search of a Disease in:
MODERN MEDICINE IN CANADA, (1982), **7**:1445
- Shalev S. et al., The Physical Basis fo Diaphanography, **W555 Medical
 Imaging and Instrumentation '85**, (1985)
- Shuster A., Radiation Through a Foggy Atmoshere, **Physical Journal** **21**#1:1,
 (1909)
- Svaasand L.O. and Ellingsen R., Optical Properties of the Brain, **Photochemistry
 and Photobiology**, **38** #3:293-299, (1983)
- Svaasand L.O. and Ellingsen R., Optical Penetration of Human Intracrainial Tumors,
Photochemistry and Photobiology, **41** #1:73, (1985)
- Rogers D.W.O., Analytic and graphic Methods for Assigning Reors to Parameters in
 Non-Linear Least Squares Fitting, **Nuclear Instruments and
 Methods**, **127**:253-260 (1975)
- Takatani S. and Graham M.D., Theoretical Analysis of Diffuse Reflectance from a Two-
 Layer Tissue Model, **IEEE Transactions on Biomedical Engineering**,
BME-26 #12:656, (1979)
- Wan S., Parrish J.A., Anderson R.R., and Madden M., Transmittance of Nonionizing
 Radiation in Human Tissues, (1981), **Photochemistry and Photobiology**,
34: 697
- Wilksch P.A. and Jacka F., Studies of Light Propropagation Through Tissue in:
PORPHYRIN LOCALIZATION AND TREATMENT OF TUMORS,
 (1984), Edited by D.R. Doirin and C.J. Gomer, Alan R. Ljss Inc., New York,
 pp.149-161
- Wilson B.C. et al., Instrumentation and Light Dosimetry for Intra-operative Photodynamic
 Therapy (PDT) of Malignant Brain Tumours , **Phys. Med. Bio.**,
31#2:125, (1986-1)

- Wilson B.C. and M.S. Patterson The Physics of Photodynamic Therapy,
Phys. Med. Biol., 31#4:327, (1986-2)
- Wilson B.C., Patterson M.S. and Burns D.M., The Effect of Photosensitizer
concentration in Tissue on the Penetration Depth of Photactivating Light,
Lasers in Medical Science, 1: 235-244, (1986-3)
- Wilson B.C., Jeeves W.P. and Lowe D.M., *In vivo* and *post mortem*
Measurements of the Attenuation Spectra of Light in Mammalian Tissues,
Photochemistry and Photobiology, 42 #2:153, (1985)
- Wolf E., New Theory of Radiative Energy Transfer in Free Electromagnetic Fields,
Physical Review D, 13#4:869, (1975)
- van der Putten W.J.M., and van Gernert M.J., A Modelling Approach to the Detection of
Subcutaneous Tumours by Hematoporphyrin-Derivative Fluorescence,
Phys. Med. Bio., 28 #6:639, (1983)
- Zdrojkowski R.J. and Pisharoty N.R., Optical Transmission and Reflection by
Blood, **IEEE Transactions on Bio-Medical Engineering**,
BME-17:122, (1970)
- Zdrojkowski R.J. & Longini R.L., Transmission of Light Through Blood,
J. Opt. Soc. Amer., 58:898, (1969)

Appendix E: Derivation of the Diffusion Approximation

In the case of radiative transport through tissue all scattering events are elastic, thus photon energy is conserved. This in general is not essential for the diffusion approximation but greatly simplifies the derivation in this case. This aspect of photon conservation can be written as;

$$\int d\hat{\Omega} \cdot I \left[\frac{\mu_s}{4\pi} \int d\hat{\Omega}' S(\hat{\Omega} \cdot \hat{\Omega}') I(\hat{\Omega}') - \mu_s I(\hat{\Omega}) \right] = 0 \quad (A1)$$

Given this relation the basic equation for radiative transport through tissue,

$$\hat{\Omega} \cdot \nabla I = -\mu_o I + \frac{\mu_s}{4\pi} \int S(\hat{\Omega}', \hat{\Omega}) I(\hat{\Omega}') d\hat{\Omega}' \quad (A2)$$

can be integrated over all movement angles (Ω) to get;

$$\nabla \cdot \mathbf{r}(x) + \mu_a \psi(x) = 0 \quad (A3)$$

where ψ is the energy fluence rate [W/m^2] and is the zeroth angular moment of the specific intensity as defined by the equation ;

$$\psi(x) = \int d\hat{\Omega} I(x, \hat{\Omega}) \quad (A4)$$

Similarly \mathbf{r} is the first angular moment as defined by the equation,

$$\mathbf{r}(x) = \int d\hat{\Omega} \hat{\Omega} I(x, \hat{\Omega}) \quad (A5)$$

and is related to the Poynting vector of the photons in a vacuum (Wolf (1976)). This use of the Poynting vector assumes that photons undergo discrete interactions and do not interact in a continuous manner with the molecule's electromagnetic fields. As this is not necessarily true, care should be exercised when interpreting this definition of the second moment of photon energy flow. For a more in depth treatment of this point review Wolf (1976), Zubairy (1977), and Fante (1981).

Equation (A3) contains the zeroth and first moment of the photon direction vector (Ω) with respect to the intensity. By multiplying the transport equation by Ω^n and

integrating over all space the result would be an equation involving the n^{th} and $(n+1)^{\text{th}}$ moments of photon direction vector with respect to intensity. Thus the basic transport equation could be expanded into an infinite set of equations of the various moments. In the diffusion derivation only the first two such generated equations are used.

In order to make use of the second generated equation it must be noted that;

$$\int d\hat{\Omega} \int d\hat{\Omega}' S(\hat{\Omega}, \hat{\Omega}') I(\mathbf{x}, \hat{\Omega}') = g r(\mathbf{x}) \quad (\text{A6})$$

where g , called the mean cosine of the scatter, is defined earlier as;

$$g = \frac{1}{4\pi} \int_{4\pi} S(\hat{\Omega}, \hat{\Omega}') (\hat{\Omega} \cdot \hat{\Omega}') d\hat{\Omega} \quad (\text{A7})$$

Also in order to avoid the introduction of the second order moment the approximation is made that

$$I(\mathbf{x}, \hat{\Omega}) \cong \frac{1}{4\pi} \psi(\mathbf{x}) + \frac{3}{4\pi} r(\mathbf{x}) \quad (\text{A8})$$

reducing the second moment term into

$$\int_{4\pi} \hat{\Omega} [\hat{\Omega} \cdot \nabla I(\mathbf{x}, \hat{\Omega})] d\hat{\Omega} = \frac{\nabla \psi(\mathbf{x})}{3} \quad (\text{A9})$$

It is this substitution that assumes that the amount of photons moving in any given direction is nearly constant and makes the diffusion approximation what it is.

Now by defining the transport coefficient as;

$$\mu_{tr} = \mu_o - g \mu_a \quad (\text{A10})$$

and multiplying the transport equation by $-\hat{\Omega}$, the resultant product can be integrated over $d\hat{\Omega}$ to give;

$$\frac{\nabla \psi(\mathbf{x})}{3} + \mu_{tr} r(\mathbf{x}) = 0 \quad (\text{A11})$$

This solution is more commonly shown using the diffusion coefficient which is defined as $D = 1/[3\mu_{tr}]$ to give

$$r(x) = -D \nabla \psi(x) \quad (A12)$$

which is commonly known as Fick's law.

Using (1) and (2) the solution for ψ is found to be

$$\psi(x) = \psi_0 e^{-\sqrt{\mu_a/D} x} \quad (A13)$$

for a plane source against a semi infinite phantom with no internal sources. ψ_0 is usually defined by the boundary conditions.

Note that the coefficient in the exponential is related to the diffusion length, L_0 ,

$$L_0 = \sqrt{\frac{D}{\mu_a}} = \frac{1}{\mu_0 (3(1-\alpha)(1-\alpha g))^{1/2}} \quad (A14)$$

which is also the apparent mean free path when diffusion conditions exist. α is the albedo, defined as the ratio μ_s/μ_0 .

Using the obvious variations on this solution for different source types this basis offers the easiest method of extracting tissue properties applicable to transport theory. As long as light is collected from well within the diffusion region the problem of scatter can be taken into account. Unfortunately the extracted result is an inseparable combination of the very constants needed for more detailed modeling using the exact form of the transport equation. This means that additional experiments are required to determine these individual components. The basis of the experiment reported in this work is to find some of these basic components, the attenuation coefficient and the scatter coefficient.

The majority of optical experiments with tissue applicable to transport theory have used this model. The main body of this work was done with photodynamic therapy in mind and most of the conclusions drawn from the work reflect this view point.

APPENDIX II DIFFUSION APPROXIMATION

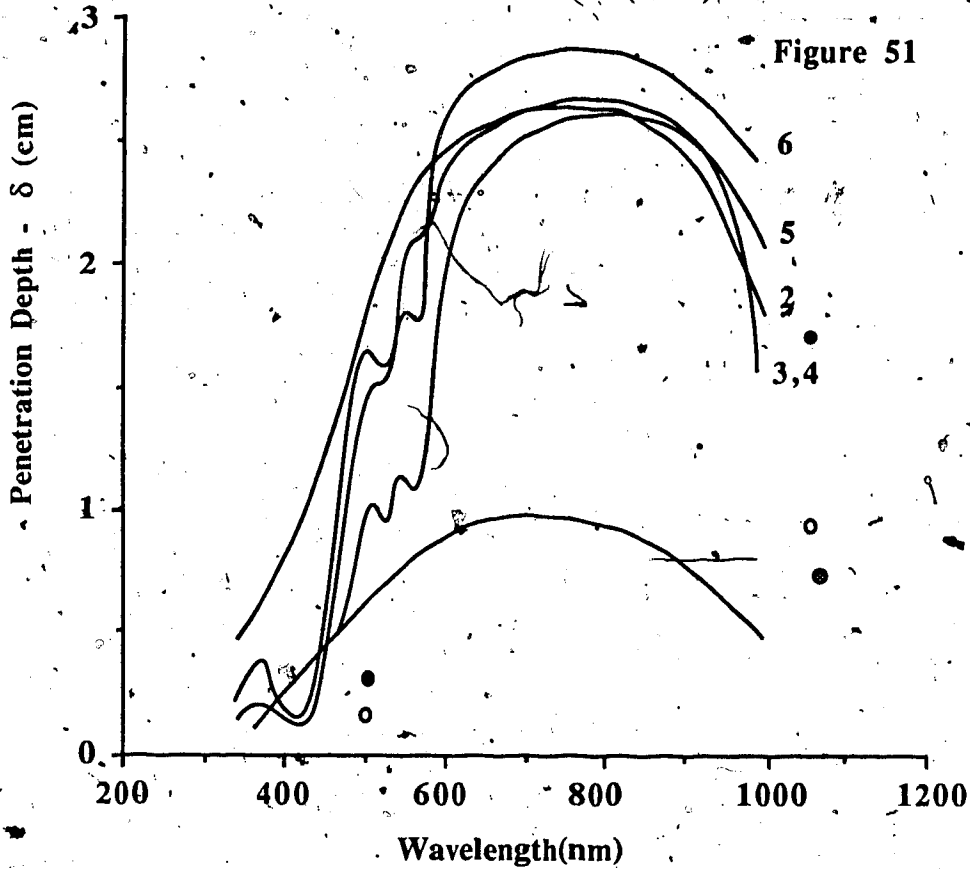
SUMMARY OF PAST RESULTS

The most popular method used by experimentalists in the field is based on the diffusion approximation to the transport equation. This approximation allows for a fairly easy experimental determination of associated constants but has a number of problems when applied to a practical situation. The most important of these is that it is valid only for the region well away from any boundaries or light sources that might upset the directional balance, or equilibrium that defines the diffusion zone. (see figure 1)

Using the obvious variations on this solution for different geometric situations this basis offers the easiest method of extracting tissue properties applicable to transport theory. As long as light is collected from well within the diffusion region the problem of scatter can be taken into account. Unfortunately the extracted result is an inseparable combination of the very constants needed for more detailed modeling using the exact form of the transport equation. This means that additional experiments are required to determine these individual components. In spite of this shortcoming the majority of optical experiments with tissue applicable to transport theory have used this model and extracted valuable information of the light tissue interaction. In the following summary the some of the data and conclusions from this work are listed.

Penetration Depth vs Wavelength for Diffuse Radiation

Modified from Eichler (1977)

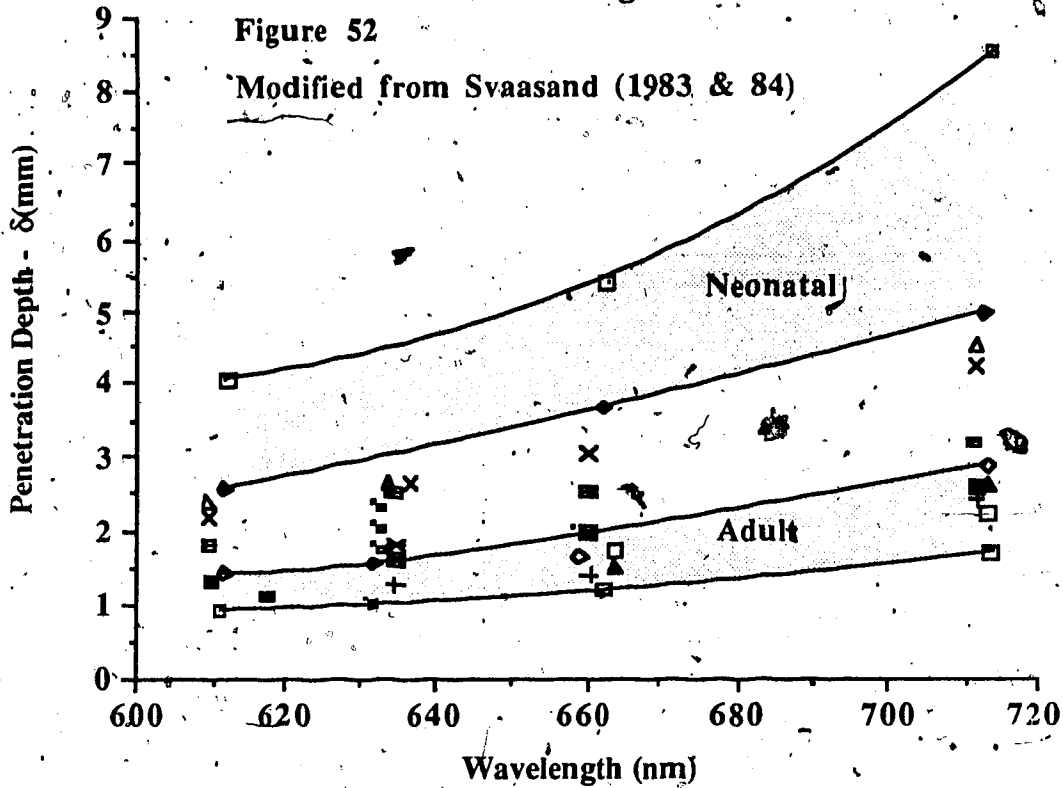


- 1 - Human Liver (no blood)
 - 2 - Human Kidney (no blood)
 - 3&4 Porcine Liver and Kidney (nearly no blood)
 - 5 - Porcine Kidney (some blood)
 - 6 - Porcine Liver (some blood)
-
- Rat Liver (in vivo) Ref. Kiefhaber (1977)
 - Rat Stomach (in vivo) Ref. Kiefhaber (1977)
 - Rat Kidney and Liver Ref. Bodecker (1974)

Penetration Depth for Various Brain Tissues : Normal and Malignant

Figure 52

Modified from Svaasand (1983 & 84)



- Male: Newborn
- Male: 2 Months Premature
- Cat Brain (ref. Doiron (1981))
- ◇ Female: 84 years (F 84)
- F 67
- M 81 White Matter
- ▲ M 81 Gray Matter
- △ M 40 Glioblastoma
- M 51 Astrocytoma I - II
- + Metastasis from Lung (OAT-c)
- M 68 Astrocytoma III
- × M 59 Astrocytoma III
- × F 67, Meningioma

It can be seen that while hemoglobin, melanin and related pigments (see Figure 51) are important absorbing compounds in visible wavelengths, the near infrared does not show this influence. The resulting clear zone or 'therapeutic window' (as referred to by Bolin (1984), Wilson (1986)) can be used for techniques such as photodynamic therapy which require a deep penetration of light into the tissue. Unfortunately the photoactivated drugs in use presently absorb just on the edge of this window and as such can be still influenced by high concentrations of melanin (Hardy (1956)). If this is the case, techniques that use external light sources to irradiate skin tumors will have to take into account skin pigmentation levels when calculating treatment values.

This problem of light being strongly absorbed by organs with high concentrations of pigment such as the kidneys and liver could be alleviated if a photo-drug was found that worked farther into the optimal clear zone. (Pruess (1982), Eichler (1977))

The actual mechanism of interaction of light in the clear zone is scatter. The how and what that interacts with the light to cause the scatter is presently under study. One such study, noted in the figure 52 is by Svaadsand (1983), pointed out a decrease in penetration depth in adult brain tissue compared to neonate brain tissue. This effect was suspected to be related to the increased amount of myelin in the nerve sheaths of mature brains. Myelin being double refractive would act as a unique scattering mechanism in the situation. As this scatter is dependent on the structural arrangement of the myelin it can be assumed that any tissue studied must preserve its *in vivo* structure as well as its substance. This dependence on structure may be so important that structurally unique tissues may have their own unique optical properties. This view can be supported by Pruess (1982), who noted that bovine adipose tissue has a half value layer twice that of bovine muscle.

The diffusion theory has proven highly successful for the initial exploration into the optical properties of tissue but unfortunately is too limited for general problems. In order to do this the actual values of the basic transport coefficients must be found. These

can then be applied to techniques such as Monte Carlo to understand the complex situations around sources and boundaries.

Geometric dependent theories used in other fields have been adopted by some investigators in an effort to circumvent the physical problems involved with measuring the actual transport defined coefficients (ie μ_0). Unfortunately these models lack flexibility when applied to real situations and the constants derived are not readily applicable to transport theory (although this has been attempted). Of these theories the two most popular are the invariant embedding technique and the Kubelka-Munk theory. For a derivation and explanation of these methods see reference Klier (1972) and Kubelka (1948).

